Development of a Commercial Manufacturing Process of 9-[(*R*)-2-(phosphonomethoxy)propyl] adenine (PMPA): A Key Intermediate for the Production of Tenofovir-based HIV Medicines

by

Banele Mbutho

A dissertation submitted to the Faculty of Science,

University of the Witwatersrand,

In partial fulfilment of the requirements for the degree of Master of Science

Johannesburg, 2023

DECLARATION

I declare that the dissertation is my own, unaided work. It is being submitted for the Degree of Master of Science at the University of the Witwatersrand, Johannesburg. It has not been submitted before for any degree or examination at any other University.

22nd day of August 2023

ABSTRACT

South Africa runs the largest antiretroviral (ARV) program in the world and yet 99% of the active pharmaceutical ingredients (APIs) used to make ARVs are imported from China. Dependence on imported APIs has major cost implications and influences the medication's security of supply. This project was concerned with making it possible to produce the APIs tenofovir, a precursor for tenofovir disoproxil fumarate and tenofovir alafenamide locally and at a lower cost.

A new synthetic route recently introduced by Medicines 4 All (M4ALL) was studied and used in this dissertation. The four-step process that produces an adenine derivative was optimized and scaled into a commercial industrial process producing tenofovir intermediates in repeatable yield and purity. This route was determined to be the most cost-effective since it utilized low-cost and commercially available diaminomaleonitrile and triethyl orthoformate as starting materials—contrary to the synthetic routes currently used by the 17 largest tenofovir manufacturers. Key process improvements included a decrease in the number of solvents used and the minimization of by-product formation. Results showed that high yields of tenofovir intermediates were successfully synthesized using this new route.

As such, the chemical company we conducted this research in, Chemical Process Technology Pharma will be able to employ this synthetic methodology to affordably produce the APIs used in the manufacturing of ARVs locally improving access to affordable medication.

ACKNOWLEDGEMENTS

I am grateful to my supervisor, Prof Charles De Koning for his continuous support, guidance, and encouragement throughout this project.

I am also grateful to my co-supervisor, Dr Mukut Gohain, for all the insightful discussions and lab skills transfer. Without your active guidance and ideas, I would not have made progress in the project. I am eternally grateful to the CPT management for the collaboration with the university and for equipping me with invaluable skills that are relevant and specific to the pharmaceutical industry. To the CPT colleagues thank you for all the patience and willingness to help and teach.

I extend my gratitude to the API cluster for giving me this opportunity and for financial support.

Special thanks to my family and friends, I am eternally grateful for all the sacrifices you have made for me. To my loving partner, I thank you for always supporting me and being my cornerstone. Without your continuous support, I would have not made it this far.

And thank you, God, for the gift of life and guidance.

TABLE OF CONTENTS

ABBREVIATIONS

AcOH	Acetic acid
AZT	Zidovudine
AICA	Amino-1-(2-hydroxypropyl)-1-H-imidazole-4-carboxamide
δ	Chemical shift
$CDCl_3$	Deuterated chloroform
COSY	Correlated spectroscopy
°C	Degrees Celsius
DAMN	Diaminomaleonitrile
D_2O	Deuterated water
DMAP	4-Dimethylaminopyridine
DCM	Dichloromethane
DMF	*N*,*N*-dimethylformamide
DMSO-d_6	Deuterated dimethyl sulfoxide
EADI	Ethyl N(2-amino-1,2-dicyanovinyl) formimidate
EtOAc	Ethyl acetate
Et_3N	Triethylamine
HPI	5-Amino-1-(2-hydroxypropyl)-1H-imidazole-4-carbonitrile
HPA	9-[(RS)-2-hydroxy propyl] adenine
HPLC	High-performance liquid chromatography
HRMS	High resolution mass spectrometry
h	Hour
HMBC	Heteronuclear multiple bond correlation
HSQC	Heteronuclear single quantum coherence
Hz	Hertz
IR	Infrared
MADI	Methyl N-(2-amino-1,2-dicyanovinyl) formimidate
MeCN	Acetonitrile
MeOH	Methanol
m/z	Mass/charge ratio
min	Minutes
MeMgCl	Methyl magnesium chloride
NMR	Nuclear magnetic resonance

K_2CO_3	Potassium carbonate
PMPA	9-(2-Phosphonyl-methoxypropyly) adenine
$(CH_2O)_n$	Paraformaldehyde
rt	Room temperature
NaO-*t*Bu	Sodium *tert*-butoxide
TMSCl	Trimethylsilyl chloride
TLC	Thin layer chromatography
TsCl	4-Toluenesulfonyl chloride

CHAPTER 1: BACKGROUND AND PROJECT OVERVIEW

1.1 Introduction

In the early 1970s, India and China focused on generic medication manufacturing.[1] China was the global leader in chemicals and Active Pharmaceutical Ingredients (API) supply, whereas India supplied formulations/finished products.[1,2] These countries formed a partnership with pharmaceutical research and development companies in the developed world—Europe and the USA. This partnership allowed the developed world to cut production costs on account of China and India's low-cost manufacturing and distribution, skilled labour, and low-cost clinical trials.[3] On the other hand, this increase in the production of generic drugs by China and India led to a considerable decrease in the South African pharmaceutical manufacturing industry.[1]

The South African pharmaceutical industry was well established in the late 1990s and was reported to be the largest pharmaceutical industry in Africa.[4] This was mainly because it was isolated from the international market and the provision of medicine was not distributed equally among the members of the population.[1] Between 1995 and 2010 over 30 companies ceased operations—mainly pharmaceutical facilities and R & D companies—due to increased imports of pharmaceuticals, policies that were introduced to address the inequality in the distribution of medicines, and the high cost of running the manufacturing facilities.[1,4]

APIs are compounds that exert therapeutic effects in medicines. Almost all APIs are prepared by chemical synthesis of simple raw materials through various processing steps.[5] For patient administration, APIs are formulated with additional ingredients (excipients) to afford finished product drugs that are available as tablets, capsules, liquid and/or injectables.[4] These additional ingredients are inactive and less expensive than the API and are added on the formulations production to ensure APIs stability, increase shelf-life, and intestinal absorption.[5,6] The South African pharmaceutical industry currently focuses on the formulation stage of finished product,[4] as they import about 90% of the active pharmaceutical ingredients (APIs) they use—including antiretrovirals (ARVs) and antibiotic APIs.[1,2] Importing APIs affects the cost of producing medicines locally because APIs represent a substantial amount (55-99%) of the overall manufacturing cost of drugs.[5] Relying on imports from other countries for pharmaceutical products is detrimental to the healthcare sector in South Africa, especially since China has been reported to have shut down about a thousand factories in 2018, due to the pollution these factories were causing.[7]

In 2015, the Chinese government introduced strict environmental laws to curb industrial pollution. All the factories that did not comply with the environmental standards were shut down, including 150 API manufacturers.[8,9] The consequence was the shortage of supply for key starting materials in the pharma industry since China's API production and chemicals account for 20% of the globally exported volume—thus leaving a substantial gap in the international supply chain.[2,10] India was expected to fill the sudden gap since they are the second largest supplier of APIs; however, the Indian pharmaceutical industry is dependent on China for imports of key intermediates, and key starting materials for the APIs.[11] This dependence on China for critical APIs and raw materials affected the cost of API manufacturing in India.[11] For instance, the price of tenofovir disoproxil fumarate (TDF), a crucial API used to treat HIV/AIDS, was $120/kg in China and $130-134/kg in India.[11]

Efavirenz, another API used to treat HIV/AIDS, was listed at $95-99/kg in China but at $115/kg in India.[11] The cost of production was cheaper in China as compared to India because the Chinese government supported the Chinese manufacturing industry in the form of financial incentives and favourable regulatory policies—a feature that was not as prominent in India. For instance, the economic environment in China generally permits lower capital expenditure requirements, lower cost of capital, cheaper logistics, and cheaper—electricity all of which the government plays a role in subsidising.[11]

The recent (COVID-19) pandemic outbreak disrupted the export of essential medicines from China, further affecting dependent nations globally.[11] The consequences of the outbreak in 2020 were price volatility, shutdown of medicine manufactures, increased healthcare burden, and ultimately shortage of medicines—especially in developing countries.[12]

1.2 HIV Epidemic

AIDS, also known as acquired immune deficiency syndrome, is among the leading causes of death around the globe. It destroys the human body's immune system and makes it vulnerable to all kinds of infections and diseases.[13] In 1981, the first case of AIDS was reported in the USA among homosexual males. The infected individuals displayed symptoms of pneumonia and Kaposi's sarcoma, a cancer that mainly affects older males.[13] In 1983, a scientist determined that the cause of the deadly AIDS is the human immunodeficiency virus (HIV), which can be transmitted by transfer of fluids from an infected person, mainly through the sexual route.[13] HIV targets a type of white blood cells, specifically CD4 cells, which acts as the body's first line of defence against intruders. Once the CD4 cells are destroyed, the body

is left defenceless then the virus makes copies of itself and multiplies and causes a lifelong infection—AIDS—that without treatment could lead to death. [13]

1.3 Breakthrough in HIV treatment

The failed cancer drug from the early 1960 zidovudine (AZT) was discovered to be effective against HIV. AZT blocks the HIV replication cycle, by targeting the HIV-1 reverse transcriptase and stops the virus from multiplying.[13,14] In 1987, AZT (Figure 1) was approved to be used against the virus by the US Food and Drug Administration (FDA). As successful as AZT was in stopping HIV from multiplying, when used alone it displayed severe side effects such as liver problems and low blood cell count.[13] Over the years the FDA approved numerous synthetic drugs that worked well against HIV and belong to the same drug class as AZT called the nucleoside reverse transcriptase inhibitors (NRTIs).[14]

1.4 New Classes of antiretroviral drugs

In the early 1990s, HIV outbreaks were detected across multiple nations when AZT was the only drug class used to treat HIV. It was discovered that over time the AZT treatment was no longer effective as the death toll started rising due to HIV infections rising.[13] The virus evolved, mutated, and developed drug resistance against AZT treatment.[13] In 1995, the FDA approved saquinavir, which belongs to a drug class called protease inhibitors (PIs). Saquinavir suppresses HIV replication by inhibiting a viral enzyme called the HIV-1 protease.[15] This prevents the virus from copying itself and infecting other cells. Protease inhibitors are best used in combination with reverse transcriptase inhibitors to prevent drug-resistant strains of HIV.[13,14] A year later, nevirapine (viramune) which belonged to the non-nucleoside reverse transcriptase inhibitors (NNRTIs) drug class was approved. Just like the NRTIs (AZT), the NNRTIs target the viral enzyme HIV-1 reverse transcriptase, by binding to the hydrophobic site away from the catalytic site, this changes the viral enzyme's shape and inhibits its activity.[13,15]

Scientists discovered that the available drug classes were more effective in the treatment of HIV when used in combination.[13,16] This is because the combined drugs target different sites of the virus, which makes it difficult for the virus to become resistant to all drugs simultaneously.[16] In 2001, US FDA approved a new antiretroviral drug tenofovir disoproxil fumarate (TDF),[15] which was used in combination with other antiretroviral agents.[16] Tenofovir disoproxil fumarate (TDF) was a prodrug that was synthesized to increase tenofovir oral bioavailability.[15,17] Tenofovir is structurally distinct as it is a nucleotide analogue as opposed

to the pre-existing nucleoside drug class. TDF, similar to NRTIs and NNRTI, results in viral DNA chain termination by means of HIV-1 reverse transcriptase enzyme inhibition.[15]

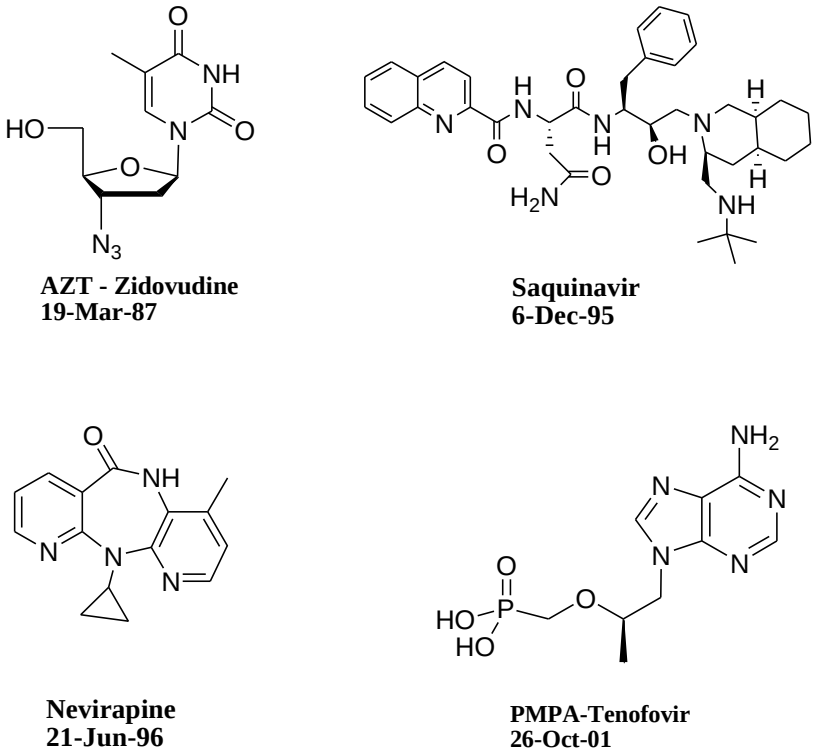

Figure 1. First antiretroviral drugs approved for HIV infection.

Over the years the USA FDA has approved numerous antiretroviral drugs, and combination of highly active antiretroviral therapy (HAART) become the new standard form of treatment for HIV for the past two decades.[13] The HAART regime was successful in fighting and controlling the virus, preserving the immune system, and lengthening the life span of the infected individuals.[13,16] The HAART regime also had drawbacks such as a high pill burden which made it difficult for patients to adhere to medication and led to frequent discontinuations of prescribed antiretroviral drugs.[18,19] This is because the early HAART regime required the administration of more than 25 different drugs and patients were required to at least take 3 pills a day, which had severe side effects due to the extreme dosing frequency.[19] Over the years, the administration of antiretroviral drugs has improved—reducing pill burden—leading to an increase in drug adherence. In 2006, the first single-tablet regime, with includes tenofovir (TDF) as well as emtricitabine (FTC) and efavirenz (EFV), which became available as the first line treatment for HIV.[18] The simplified single-tablet regime of all three APIs showed excellent efficacy, safety, higher adherence, increased viral suppression rates, and lower health costs; furthermore, it could be administrated once daily.[19] More single-tablet regimes administrated

as triple drug therapy have been approved since then and they are the current standard care for HIV treatment.[18]

1.5 HIV treatment in SA

South Africa (SA) has the largest concentration of people living with HIV, estimated at 8.45 million.[17] The first AIDS death was reported in SA in 1981, and during that time the rate of HIV infection and mortality was relatively low compared to the rest of Africa. Whereas countries like Uganda were faced with the AIDS epidemic.[13,20] The rate of HIV infections started to rise drastically in the 1990s, as they were estimated to be between 74000 – 120 000 people living with HIV.[20,21] Still, the HIV epidemic received little to no attention for over a decade. Given the limited knowledge about HIV/AIDS, prevention and treatment responses were implemented involving the Sarafina play and Virodene scandal in 1996.[20] The department of health awarded a contract worth over a million to produce the musical theatre: Sarafina, which was used as an AIDS communication strategy, to reach young people. The locally developed drug, Virodene was introduced as new antiretroviral therapy and was said to be less expensive in comparison to the triple-drug therapy (HAART). Virodene was rejected by the scientific community, as the drug was declared unfit for human consumption and poses severe hazards. [20]

Since detection of the first case, the South African government was in denial of the existence of HIV and AIDS—which resulted in the estimated death of 330, 000 people who were denied lifesaving antiretroviral drugs.[20,21] In 2003, the South African cabinet approved the HIV treatment plan and developed the ART programme, which was followed by delays and only began in 2005, enrolling approximately 85 000 people living with HIV.[20,21] The change in leadership transition from the former AIDS denialist Thabo Mbeki to former President Jacob Zuma led to the unpreceded expansion of HIV treatment programme since 2008.[20,22] As a result South Africa is home to the biggest antiretroviral (ARV) program in the world, yet for the support of its ART program, South Africa still solely depends on API imports.[21,22]

Over 90% of the people living with HIV receive free antiretroviral therapy from the public health sector in South Africa; the current spending of the government on the HIV programme is estimated to be ZAR1 billion annually.[21] In 2021 there was an estimated 200 000- 300 000 new infections.[21] The continued rise in HIV infections means that people will continue to enter the anti-retroviral therapy (ART) programme for decades to come and the government will continue to spend billions of Rands in importing ARV APIs.[21] As the global demand for ART

APIs continues to rise, it is probable that it might exceed the capacity of the generic producers to manufacture these APIs.[5] This would lead to drug shortages as generic producers like India prefer to supply the more lucrative and high-priced markets like Europe and the USA.[1,17]

In South Africa, stock-outs of ARVs have been reported throughout the years.[12,23] Stock-out is defined as the absence of essential medicine at the health facility required by a patient until the next order is received.[23] The stock-outs were reported to be a challenge worldwide, with ART stock-outs higher in Africa than in any other continent.[23,24] Patients suffer the most from the effects of these stock-outs because they frequently result in the interruption or discontinuation of ARV treatment, which results in increased drug resistance, lowered immunity, the risk of opportunistic infections, HIV transmission, and eventually more deaths.[12,21] Some of the reasons for the prevalence of stock-outs nationwide were due to production delays, quality problems, shortage of raw materials and key APIs, and poor logistics infrastructure.[23,25]

As a result, the key challenge facing sub-Saharan Africa is proving sustainable access to HIV treatment, especially as it is home to 70% of the world's HIV/AIDS infected people.[17] ARV APIs are the most costly component of the HIV and AIDS treatment.[1,5] Generic manufactures supply APIs at a 20% markup on the cost of production.[5,6] As a result, many nations cannot afford to provide access to all people living with HIV/AIDS.[2,26] In South Africa, nearly 1000 people die of AIDS every day[17] and this situation would likely worsen because of the frequent power outages (loadshedding), high unemployment rate which weaken the South African Rand and thus drives prices of imported ART APIs and finished products upwards. Therefore, there is an urgent need for the development of local ARV API manufacturing in the African continent.[2,17] This MSc project is concerned with making it possible to produce ART APIs (TDF) locally and at a lower cost than what is offered by generic producers.

CHAPTER 2: LITERATURE REVIEW

2.1 Tenofovir

Tenofovir is a nucleotide reverse transcriptase inhibitor used as the first-line treatment against HIV in South Africa in combination with other antiretroviral drugs which is considered superior to treatments involving the nucleoside analogue class: AZT and stavudine.[15,27] This is due to the lower rate of resistance development and lower incidence of toxicity for tenofovir combinantions.[28] Both AZT and stavudine were eventually phased out because of the severe side effects that were reported such as liver problems, and low blood cell count.[24,29] One study reported that 20% of patients that commenced with the stavudine based regime asked to be switched to alternative ARVs within 3 years, due to the toxicity that the patients experienced such as peripheral neuropathy, lactic acidosis, and lipoatrophy.[24]

Tenofovir is unique in that it is an acyclic nucleoside phosphate that experiences two intracellular phosphorylation steps to form its active metabolite, tenofovir diphosphate—a competitive inhibitor of HIV-1 reverse transcriptase that terminates the growing viral DNA chain.[15,30] Unlike NRTIs drugs that require 3 phosphorylation steps to confer activity the decreased phosphorylation requirement for tenofovir diphosphate allows it to inhibit a variety of dividing and non-dividing cell types.[15,31] This unique and important property is not found in the existing nucleoside analogue classes, particularly AZT and stavudine.[15] Studies showed that tenofovir was a useful antiviral agent with an extended intracellularly half-life: however, its polar character prevented the effective entry of the analogue into the cells—limiting its activity.[15,31] Consequently, improvements were made to the tenofovir drug such as the addition of the two alkyl methyl carbonate esters to produce the prodrug, Tenofovir Disoproxil fumarate (TDF) **2** (Figure 2.1).[32] The synthesized prodrug TDF improved the stability, intestinal absorption, and cell permeability of tenofovir.[28,32] Years later, another prodrug tenofovir alafenamide (TAF) **3** (Figure 2.1) with improved properties was launched.[33,34] Both the prodrugs TDF and TAF are synthesized from adenine **4** (Scheme 2.1).[35]

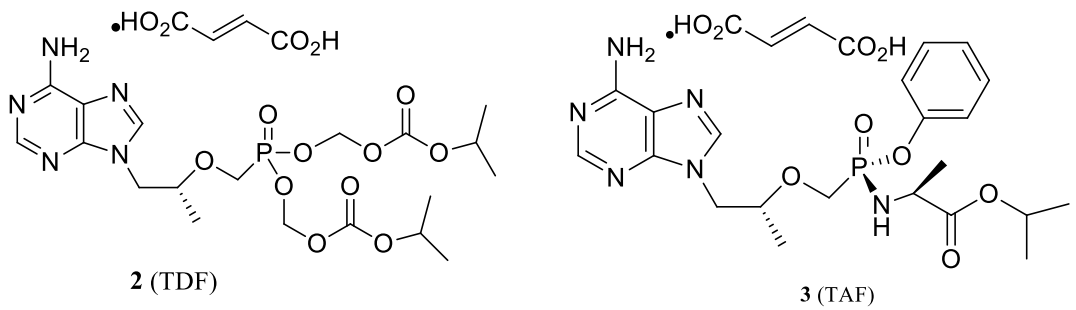

Figure 2.1. Pro-drugs of Tenofovir, TDF and TAF.

2.2 TDF and TAF

Both the prodrugs TDF and TAF are used for first-line therapies for chronic HIV and (Hepatitis B virus (HBV) infections.[33,36] Hepatitis B is the irritation and inflammation of the liver due to infection with the hepatitis B virus.[37] For HIV infection, these drugs are used in combination with emtricitabine and lamivudine.[5] After oral administration, TDF undergoes esterase hydrolysis and yields tenofovir.[32] TAF is intracellularly metabolized by lysosomal carboxypeptidase cathepsin A (cat A) to tenofovir.[33] Then tenofovir is intracellularly converted to its active form tenofovir diphosphate which targets the RNA-dependent DNA (reverse transcriptase) of either HIV or Hepatitis B virus— causing termination of the viral DNA's growth, due to lack of the ribose ring.[31,36] Both TDF and TAF, are used in pre-exposure prophylaxis (PrEP) for HIV infection.[38] PrEP involves the administering of antiretroviral agents by uninfected individuals, to lower the risk of sexual HIV acquisition.[36,38]

Both the prodrugs demonstrated excellent efficacy and tolerability,[39] however, concerns remained over TDF causing acute renal failure, bone loss, and Fancomi syndrome, especially in the older HIV-infected population.[24,40] This is due to TDF having high circulating plasma levels of tenofovir, which is eliminated through the body renally.[24,32] Whereas TAF showed higher intracellular concentration and lower plasma concentration of tenofovir.[39] This means that TAF is quickly absorbed by cells compared to TDF and produces higher levels of intracellular tenofovir diphosphate at substantially lower doses of tenofovir meaning reduced exposure to the kidneys and bones.[24,34]

Switching from TDF- regime to the TAF regime, provided better clinal outcomes and reduced toxicity by 30-fold factor.[33] But the high cost of TAF limits the replacement of TDF with TAF, especially in developing countries.[5,24] TDF is an old prodrug that was approved in 2001 by the FDA. Initially, TDF was marketed as the stand-alone medication Viread, later sold in combination with other antiretroviral drugs under the following brand names: Emtrivia,

Truvada, Atripla, Complera, and Stribild.[33] In 2008, Gilead sciences the originator of TDF entered into a voluntary license agreement with 11 Indian generic manufacturers to limit generic competition, the voluntary license restricted the Indian generic manufacturers from exporting the API TDF to certain countries.[24,41] Years later the voluntary license became void, which allowed the generic producers to freely manufacture and export TDF without restrictions.[41] Today, they are close to 17 generic versions of TDF, the market competition has driven down the prices of TDF.[42] Gilead sciences were approved for TAF in 2015 by the FDA and were sold as a stand-alone tablet under the brand name Vemlidy and as a component in combination tablets: Genvoya, and Descovy.[34] Currently, they are no generic versions of TAF available because it was a patented drug until 2022. So TAF is relatively expensive compared to TDF.[40]

2.3 Tenofovir Efficacy against SARS-CoV-2

In 2019, the Coronavirus caused by the severe acute respiratory syndrome virus (SARS-CoV2) was categorised as a global crisis by the World Health Organisation (WHO), as millions of people were infected, and the mortality rate of patients was at 5-10%.[30,36] Scientists discovered that SARS-CoV-2 has a similar RNA sequence to the coronavirus family members such as SARS-CoV and MERS-CoV.[36] Since vaccine production takes time and the was an urgent need for prevention or treatment for COVID-19 infections,[43] long discovered drugs that were used to target viral RNA-dependent RNA polymerase (RdRp) or coronavirus were repurposed to treat the new member: SARS-CoV-2.[36] Among those drugs was remdesivir (adenosine analogue in Figure.2.2) which had an established safety profile as it was already in use for its antiviral therapy of a wide range of retroviruses like Ebola, SARS-CoV, and MERS-CoV.[43]

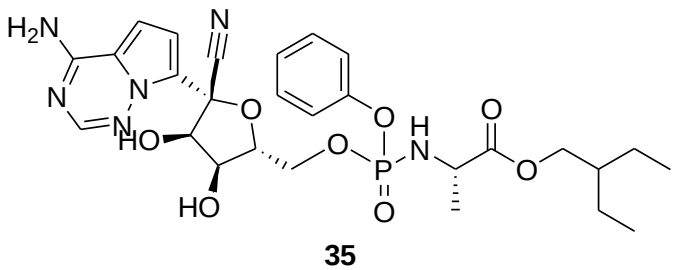

35

Figure 2.2. Structure of remdesivir.

At the beginning of the pandemic, HIV-infected people were considered at high risk for severe COVID-19, since their immune systems were compromised, and were thus susceptible to infections and diseases.[36] However, studies show that HIV-infected patients that were regularly

taking TDF-based ART were less compromised than patients on other antiretroviral agents.[36] Coincidentally, tenofovir, the acyclic nucleotide analogue, which inhibits the viral reverse transcriptase, has been hypothesized to be active against COVID-19.[44] This is because tenofovir has a similar structure to remdesivir which has been approved as the antiviral medication for COVID-19.[36] In Spain, a study was done to investigate the incidence and severity of COVID-19 from 77 590 HIV-infected people.[44] The patients that were taking TDF-based ART, had a lower risk of COVID-19 incidences, less hospitalization, and no mortality.[44] On the other hand, patients who took other antiretroviral agents (abacavir and lamivudine), showed no significant difference in COVID-19 incidence, risk of hospitalization, and mortality among the infected people. Another study was done on HIV-negative people from PrEP users.[36] As mentioned before, both TDF and TAF are used as PrEP against HIV infection in people at risk of acquiring this infection. Observation shows a high prevalence of SARS-CoV-2 antibodies from PrEP users than those who did not take PrEP. Lower prevalence of SARS-CoV-2 from TDF-based PrEP was observed as compared to TAF users.[36] Therefore, the clinical data shows TDF as a potential medication for SARS-CoV-2.[30,44] Thus, the demand for TDF could rise in the future.

2.4 Synthesis of Tenofovir Disoproxil fumarate

The manufacturing of TDF was originally patented by Gilead Sciences,[17] where the key starting material adenine is transformed into TDF in three stages and four reaction processes.[35] In the first step, adenine (**4**) is condensed with *R*-propylene carbonate (RPC, **5**) to yield the secondary alcohol 9-(2-hydroxyl) propyladenine (HPA, **6**). The second stage involves the alkylation of HPA (**6**) with diethyl(tosyloxy)methylphosphonate (DESMP,**8**) in the presence of a lithium alkoxide base. Thereafter, tenofovir diethyl phosphate ester **9** undergoes hydrolysis which is mediated by bromotrimethylsilane (TMSBr) affording tenofovir (**1**). In stage 3, tenofovir (**1**) is converted into the free base tenofovir disoproxil **11** through alkylation esterification with chloromethyl isopropyl carbonate (CMIC, **10**) and this undergoes salt formation with fumaric acid to complete the synthesis of TDF (**2**), with an overall yield of 13%.[8,17,28]

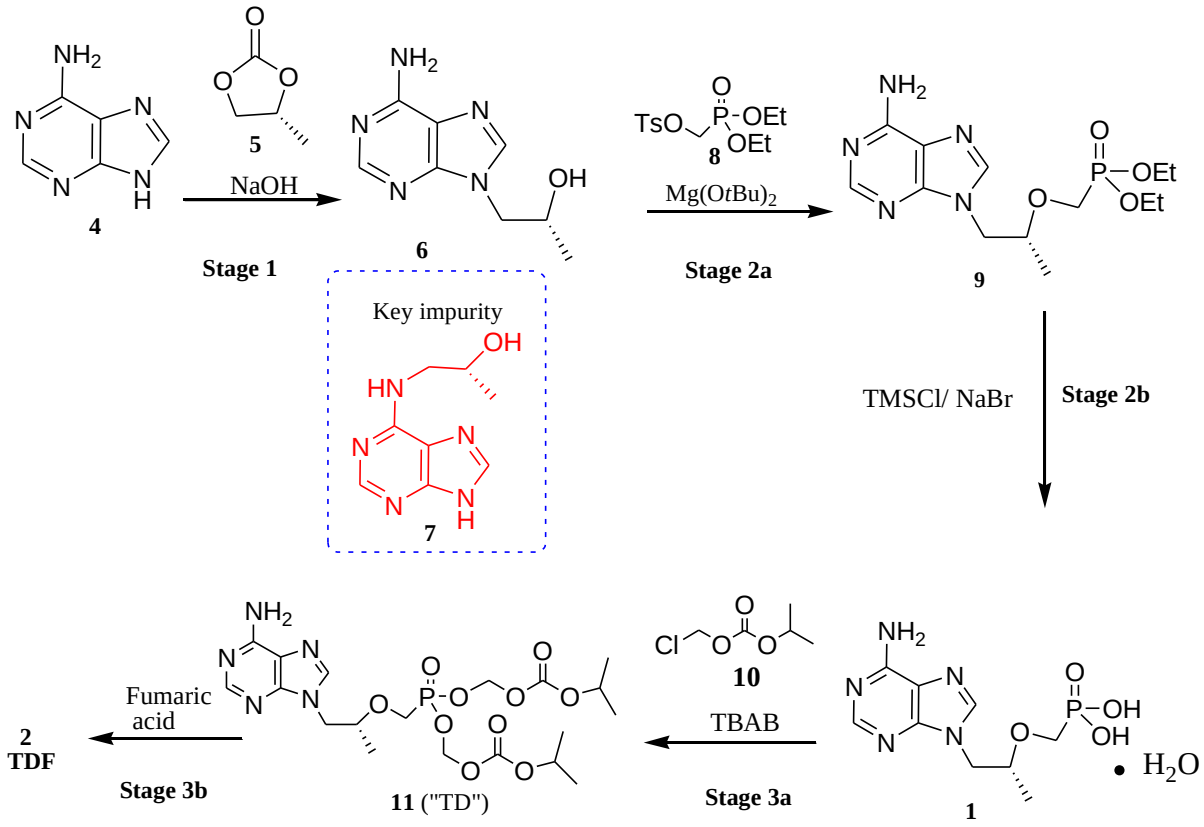

Scheme 2. 1. Industrial process for tenofovir disoproxil fumarate.

In 2010, Clinton Health Access Initiative (CHAI) reported a few process improvements to TDF manufacturing (Scheme 2.1).[28] Key improvements include the telescoping of the stage 2 process, which include the alkylation of HPA **6** with tosylate **8** followed by hydrolysis. Even though the magnesium *tert*-butoxide (MTB) was identified as the optimum base to promote the alkylation of **6** with **8**, and it afforded excellent conversions (> 90%), the hydroscopic nature of the base is a limitation. For the hydrolysis process, low-cost trimethylsilyl chloride (TMSCl) and NaBr in N-Methyl-2-pyrrolidone (NMP) were introduced in place of TMSBr.[14,17] These two reactions were telescoped because compound **9** is water soluble, prone to hydrolysis, and difficult to crystallize, therefore leading to loss of material.[28]

In stage 3, tert-butyl ammonia bromide (TBAB) was introduced for the alkylative esterification of PMPA **1** with chloromethyl isopropyl carbonate (CMIC, **10**). The level of product decomposition during the workup and isolation was greatly reduced by the invention of cyclohexane extraction to remove surplus reagents in the absence of water. The mentioned process improvements increase the isolation of tenofovir from 35% to 59%, and the overall yield of the desired API, TDF (**2**) was improved to 24%.[28]

In 2016, Riley and co-workers[35] made further process improvements in the synthesis of TDF, especially in the first two stages. In the previously published methods, including both the Gilead and CHIA routes (Scheme 2.1), the first stage that yields HPA (**6**), is commonly prepared by reacting the commercially available adenine (**4**) and suitable carbonate **5** at 120 ^{0}C in DMF, with a catalytic amount of sodium hydroxide (NaOH).[28] The key impurity observed in this stage was a formation of the regioisomer **7**, where the site of addition for the aliphatic side chain was on the exocyclic NH_2 group.[35] When toluene was used to isolate pure HPA (**6**) from DMF, the crude yield was reported at 84 % with the key impurity **7** formed in a 8 % yield. The product was recrystallized further with the solvent mixture of MeOH/IPA (1:1) to give a final yield of 66% with 1.7% traces of the regioisomer. The improvements that were made involved a change of catalyst, where the potassium bases showed greater success than any other bases.[17] Potassium hydroxide being the most promising base in dry DMF, as it improved the reaction rate (2.5 h vs. 22h) and afforded pure HPA in 65%, with no unwanted regioisomer.[17]

Riley also suggested an alternative base to the use of MTB in the coupling of HPA (**6**) and DESMP (**8**). Not only was the MTB reagent expensive but the conversion or variation of results of stage 2 was dependent upon the quality of the MTB.[42] The magnesium tert butoxide by-product magnesium salts led to the loss of product and made the reaction work up and purification difficult.[42] This is because the magnesium salts are hygroscopic, it absorbs water and makes it hard to recover the intermediate **9** because it is water-soluble.[35] The presence of the unwanted by-product also complicates the next step in the telescoped process: hydrolysis, this is because TMSBr or TMSCl/NaBr are moisture-sensitive reagent.[35,44] Therefore, the published method replaced MTB and solvents used with Grignard and tert-butanol in cyclohexane and provided an efficient workup and purification process that could isolate pure tenofovir diethyl phosphate ester **7**, which was not possible with the pre-existing routes (CHIA and Gilead).[35] The alternative base used was the low-cost methyl magnesium chloride in combination with tert-butanol the conversion was done in a solvent-free condition, and **7** was recovered in 85% yield with >94 % HPLC purity using the liquid-liquid extraction (involving chloroform and dichloromethane) protocol. Pure PMPA (**1**) was isolated in a 73% yield using the TMSCl/NaBr and was further treated in 33% HBr/acetic acid.[35]

The process improvements made in the synthesis of TDF (**2**), include the use of cheap reagents, reduced E factor, telescoping and process optimization, which increased the overall yield from 13% to 69%. [17] As a result imports and exports prices of the TDF API decreased over time. During this time 2010-2016, reports show that the was a price drop in PMPA (**1**)**,** which

decreased by 33% from the original $300/kg to under $100/kg.[8] These improvements enabled lower-income countries to have access to HIV/AIDS treatment and save more lives in developing countries.[26]

TDF API pricing has changed dramatically over time. Volume demand, higher yields, more effective and simplified processing steps, and better raw material pricing are significant factors that contributed to the cost reduction for TDF over time.[5] High-volume demands decrease the cost contribution of raw materials, labour, cost of energy, waste disposal, shipping, and manufacturing equipment, such that it is cheaper to produce per ton.[6] The efficiency of the process or synthesis is also based on the amount of waste generated per kilogram of product manufacture. This is because managing waste is very expensive in chemical manufacturing, therefore increasing the overall yield of the API synthesis, reduces the manufacturing cost of the API.[3,5]

Over time the increased volume of demand for TDF resulted in more competition from multiple suppliers, which improved the chemistry and changed the routes of synthesis this resulted in a reduction of cost on raw materials and APIs pricing.[5] About 50-70 % of the overall cost of API manufacturing is accounted for by raw material, in most process.[2] For instance, the earlier published TDF manufacturing routes, show that the use of MTB was a huge success in stage 2a alkylation of **6** with **8** (Scheme 2.1). During this time 2008-2009, MTB was very expensive as it was single-sourced from an Indian supplier who synthesized it from reacting dimethyl(magnesium) with tert-butanol in anhydrous ether.[3,45] As more chemical companies entered the API industry over time, MTB production became more affordable. Other researchers opted to use less MTB or lower-cost alternative bases such as NaOtBu or even MeMgCl/ tert-butanol. This lowered the demand for MTB and impacted its pricing which decreased drastically over time.[3] Certainly, a lot of study and development has gone into lowering the production cost of TDF as an API, including using inexpensive raw materials, reaction optimization, improving yield, decreasing processing times, and reducing the amount of waste generated. However, all the current 17 manufacturers of TDF are still using the same chemistry steps and raw materials, from when it was first launched in 2001.[42] The key materials include adenine, R-propylene carbonate, DESMP, chloromethyl isopropyl carbonate (CMIC), and fumaric acid (Figure 2.3). The lack of new synthetic routes for the synthesis of TDF has led to raw materials dependency, which will result in unsteady prices and shortages. For instance, key starting material adenine **4** is a critical cost component for TDF and is still single sourced from a Chinese supplier, due to the high cost of infrastructure used to manufacture

adenine.[11] As a result, the adenine price has fluctuated over the years making it difficult to further minimize the TDF cost production. [42]

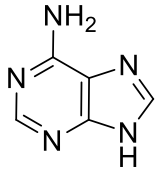

Adenine

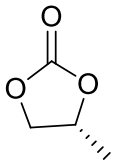

R-propylene carbonate

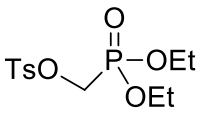

DESMP

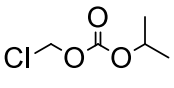

CMIC

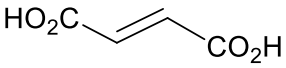

Fumaric Acid

Figure 2.3. Critical raw material used in the manufacturing of TDF.

In 2020, Derstine *et al* published an alternative strategy for PMPA synthesis.[42] The newly published route is the subject of this MSc dissertation, it utilizes inexpensive and different raw materials that can be used for multiple processes. For instance, the starting material for the new process, diaminomaleonitrile (DAMN, **12**) is easily obtained by polymerization of HCN, DAMN (**12**) is also used in the synthesis of various heterocyclic compounds.[46] The key starting materials for the new routes' simple building blocks can be obtained readily from high-volume raw materials like hydrogen cyanide, phosphorus trichloride, *L*-threonine, ammonia, and formaldehyde (Figure 2.4).[42]

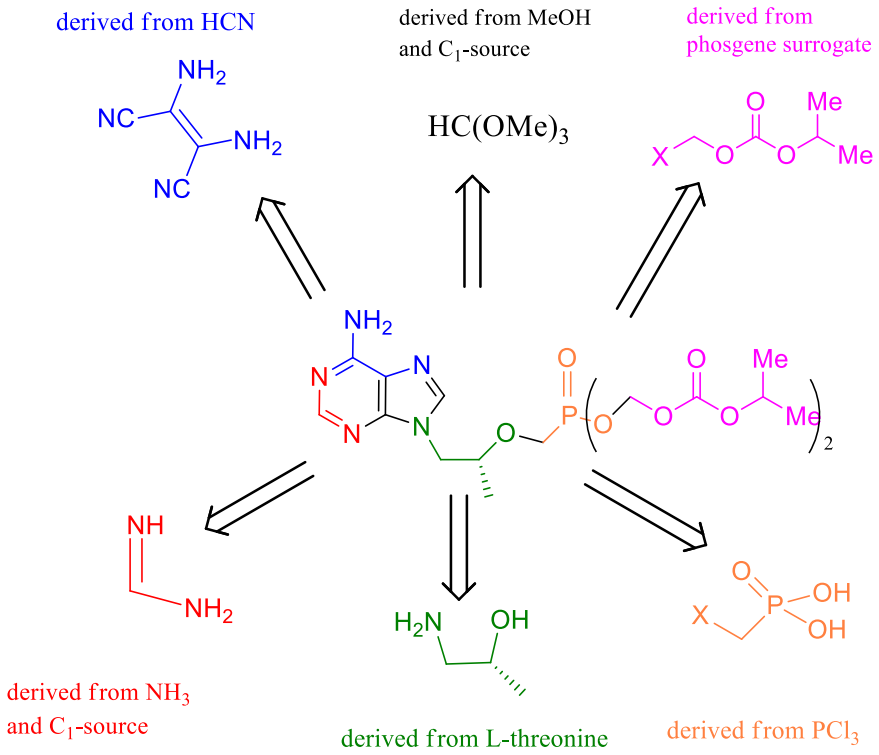

Figure 2.4. Tenofovir disoproxil fragments sourced from inexpensive, commodity raw materials.

Using DAMN (**12**) as the starting material, the open-access technology supplied by Medicines-4-All (M4ALL) and funded by the Gates Foundation have made substantial improvements in the TDF process. They have increased the overall yield of PMPA from 59% to approximately 70%. The commercially available and low-cost diaminomaleonitrile (DAMN, **12**), which exists as a HCN tetramer, is reacted with trimethyl orthoformate (**13**) to produce methyl *N*(2-amino-1,2-dicyanovinyl) formimidate (**14**) in good yield. The imidate **14**, is condensed with (R)-1-aminopropan-2-ol (**15**), which introduces the stereogenic centre, to form the amino-alcohol intermediate, followed by cyclization in presence of barium hydroxide monohydrate ($Ba(OH)_2$) to give the chiral (*R*)-5-amino-1-(2-hydroxypropyl)-1*H*-imidazole-4-carbonitrile (HPI, **17**). To form the adenine core, the HPI intermediate is condensed with formamidium acetate in DMF to yield HPA (**6**), in good yield. This is followed by a sodium *tert*-butoxide (NaOtBu) promoted alkylation of HPA with the ((tosyloxy)methyl) phosphoric acid, this efficient process produces PMPA (**1**) in 70% overall yield.

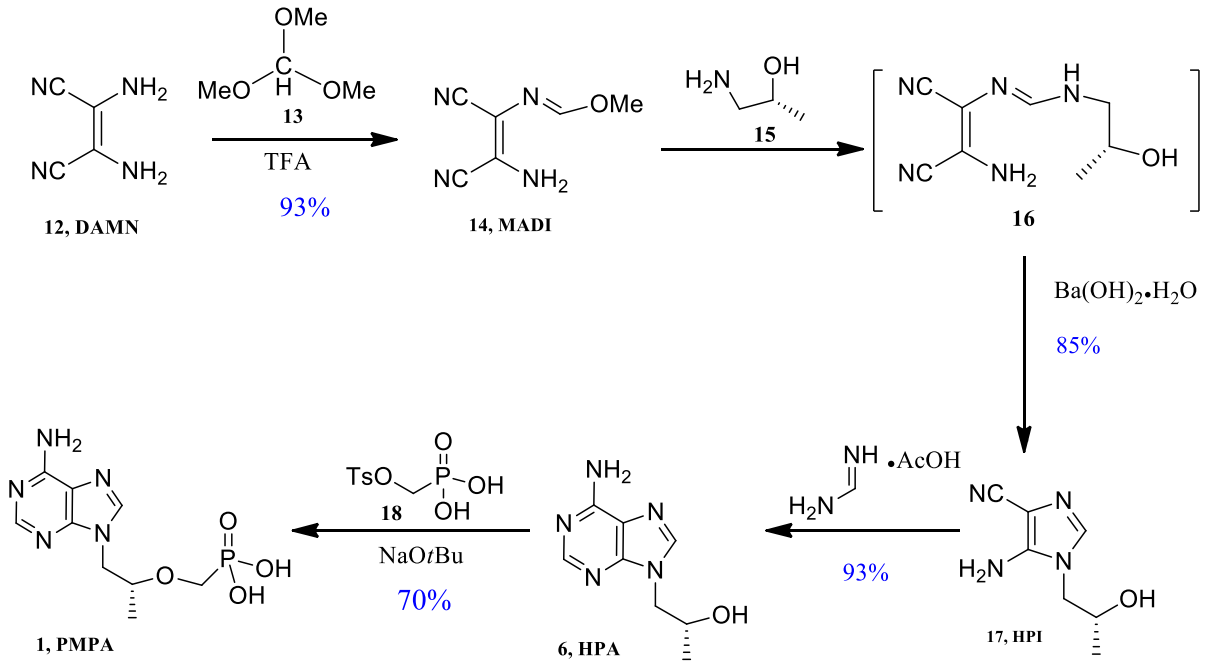

Scheme 2 2. Proposed M4ALL process for Tenofovir.

The challenge with the M4ALL technology is in the last two steps in the synthesis of PMPA (**1**). The biggest issue with this route is that it uses tosyloxy methyl phosphonic acid as the alkylating agent with HPA.[47] This is synthesized from the deprotection of the diethyl ester of DESMP (**8**). All TDF manufacturers use DESMP (**8**) as a key material to produce PMPA (**1**) because it is derived from low-commodity material and has a well-developed process.[47] However, the deprotection of diethyl ester of DESMP (**8**) is problematic, as it is difficult and often requires the use of the expensive and toxic TMSBr in dichloromethane, and with a tedious work-up process.[47]

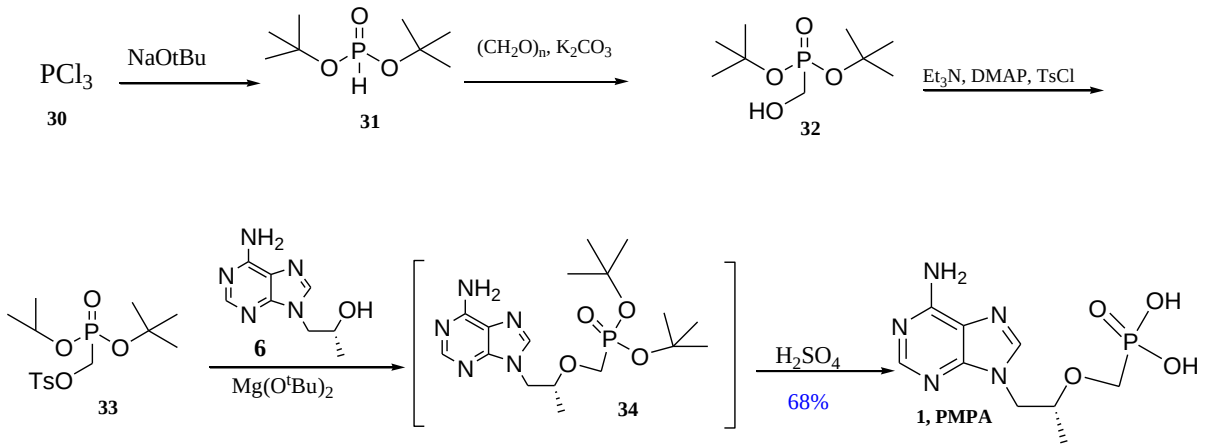

Scheme 2.3. Alternative synthesis of PMPA.

In 2021, a new synthetic strategy for PMPA was published.[48] The new route uses di-*tert* butyl phosphite instead of the problematic diethyl phosphite as the phosphonic acid precursor (scheme 2.3). The di-*tert* butyl phosphite is synthesized from phosphorus trichloride (**30**) and NaO*t*Bu. Followed by hydroxymethylation using paraformaldehyde with catalytic K_2CO_3 in acetonitrile. The tosylate group is then installed and the resulting (di-*tert*-butoxy phosphoryl) methyl 4-methylbenzenesulfonate (**33**) is reacted with HPA (**6**). To generate pure PMPA (**1**) in 68% yield, the tert-butyl group were cleaved off in presence of cheaper acids such as sulfuric acid or by applying heat.[47]

The prices of TDF (**2**) have decreased over time due to improved chemistry, decreased processing time, competition from multiple suppliers for procurement of critical raw materials, and reduced waste generated. Further reduction for the manufacturing cost of TDF cannot continue indefinitely unless new changed routes for the synthesis of TDF that uses low-cost materials are introduced. As a result, this MSc dissertation focuses on developing and optimizing an industrially feasible process for the first four steps that produce the adenine core (HPA,**6**), using new M4ALL technology for the synthesis of PMPA (**1**). According to the published manuscript, the yields for the first four steps are high and use inexpensive raw materials.[42] However, it was observed that each step uses multiple additional solvents and reagents that are omitted from this proposed Scheme 2.2. This MSc project aims to improve the yield and the chemistry of the new routes; reduce waste generation by employing one solvent system for each proposed step and reduce processing time. In addition, the process development of HPA (**6**) will focus also on scale-up and optimization of the synthetic routes which include: solvent choice, recycling, telescoping, and reagent choice, which will lead to a safe, reproducible, economical, and environmental friendlier manufacturing process.

CHAPTER 3: RESULTS AND DISCUSSION

3.1 Method Development for Step 1

3.1.1 Synthesis of MADI (14)

The most common route for TDF manufacturing is a three-stage, four-reaction step process (Scheme 2.1) that has not changed since the drug was FDA approved in 2001.[2] All 17 current manufacturers of TDF use the same synthesis steps and raw materials, utilizing adenine **4** and propylene carbonate **5** as starting materials. As a result, HCN pentamer adenine prices have fluctuated in recent years, further contributing to the high cost of TDF in the marketplace.[42]

This MSc project is concerned with the reduction of the cost of tenofovir using new and improved routes with alternative starting materials such as diaminomaleonitrile (DAMN) and trimethyl orthoformate (TMOF). DAMN (**12**)—an HCN tetramer—has received significant attention due to its application in diverse areas such as heterocyclic synthesis, material science, and prebiotic chemistry.[49] DAMN (**12**) is formed through HCN polymerization and is used as an anticancer agent; insecticide; and precursor in the manufacturing of the antiviral agent TDF that is effective against HIV and HBV.[50] The growing interest in this versatile synthon has resulted in the development of various synthetic procedures for its synthesis using hydrogen cyanide—thus making it cheap and readily accessible.[49,50]

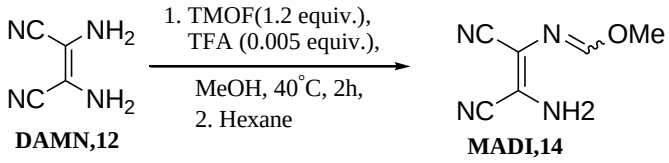

Scheme 3.1. Published synthesis route for MADI.

The above reaction (Scheme 3.1) was performed at a small scale where DAMN (**12**) was charged with methanol (MeOH) in a reaction flask. TMOF (**13**) was charged into the reaction mixture with 1 drop of trifluoroacetic acid (TFA). The slurry obtained became difficult to stir, resulting in poor mixing of the reaction. The reaction flask was heated from 25 ℃ (room temperature) to 40 ℃ for 2 h. After heating and stirring for 2 h, the reaction was charged with hexane, cooled to room temperature, and further cooled down to 0 ℃. The reaction did not yield the anticipated product: methyl *N*-(2-amino-1,2-dicyanovinyl) formimidate (MADI), as a pale-yellow solid[42]; instead a brown semi-solid mixture was obtained. The reaction progress was monitored using TLC and GC-MS analysis. TLC indicated a significant presence of impurities (see Figure 3.1, plate A).

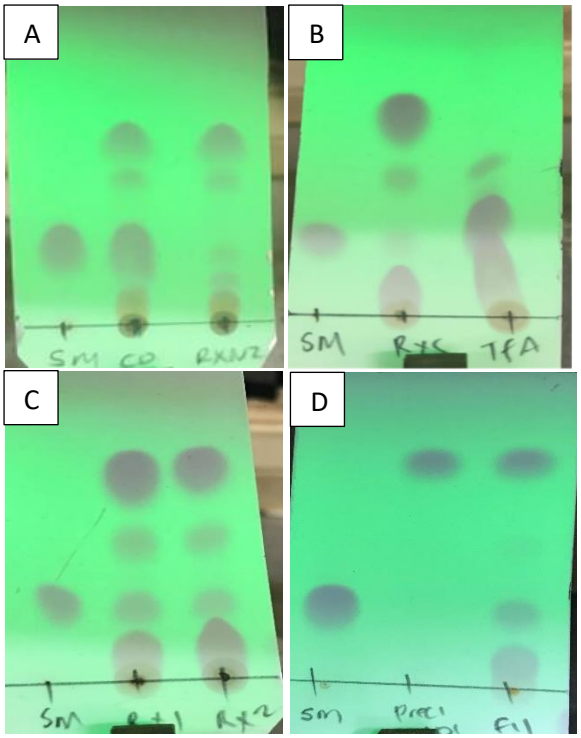

Figure 3.1. TLC plate (A) shows the starting material (sm), co-spot, and rxn2 spot after heating and stirring for 2 h at 40 ℃**.** TLC plate (B) shows the effects of excess catalyst (TFA). TLC plate (C) reveals the synthesis of MADI after 1 h(RX1) and 2h(RX2) at 60 ℃, and TLC plate (D) shows the stating material (sm), precipitate (MADI) and filtrate (fil); it also reveals the results of the optimized process for the synthesis of MADI.

3.1.2 Parameters that affect synthesis of MADI, 14

The failure to synthesize MADI (**14**) compelled the investigation of parameters that could possibly affect its synthesis. By studying the reaction under different conditions, it was then observed that the amount of acid catalyst, temperature, and reaction time affect the purity of the product.[48] When the amount of acid catalyst (TFA) was increased, the amount of by-products increased see (TLC plate B, Figure 3.1.). On TLC plate B, the RX5 spot shows the reaction after stirring and heating for 2 hrs at 40 ℃ and the TFA spot shows what occurs when we add one drop of acid to the existing reaction (RX5). Addition of TFA resulted in the consumption of product and the subsequent increase in the amount of impurities. Furthermore, the effect of temperature was tested as the reaction was conducted at 60 ℃. TLC plate C in Figure 3.1. shows that at high temperatures, the number and amount of by-products increased. These findings are consistent with literature in that increased temperature, reaction period, and excess use of catalyst lead to an increase in the number of by-products formed.[48]

3.1.3 Optimised synthesis of MADI

After studying and understanding the parameters that affect the synthesis of MADI (**14**), the published method was optimized in the laboratory. DAMN (**12**) was charged with MeOH into a reaction flask and stirred for 5 min at room temperature (25 ℃), followed by the addition of TMOF (**13**) and diluted (MeOH) TFA were added. Diluting the strong catalyst TFA with reaction solvent MeOH was done to make sure that no slurry mixture formed as previously seen. TLC analysis showed that most of the starting material DAMN (**12**) was consumed after heating and stirring at 40 ℃ for 2 h. Hexane was then added and the desired MADI (**14**) precipitated out of solution. The reaction was cooled to room temperature and then to 0 ℃. The precipitate was collected through vacuum filtration and the product was obtained as a pale-yellow solid with 80% yield (see Figure 3.2, image A).

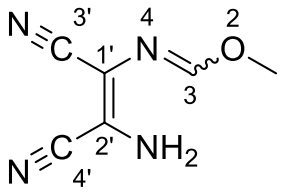

The pale-yellow solid was characterized with TLC, GC-MS, IR, ^{1}H NMR, and ^{13}C NMR spectroscopy. TLC analysis plate D in Figure 3.1 shows three spots: starting material **12**, precipitate (MADI **14**), and filtrate. The middle spot (MADI) had only one spot which indicates there were no observed impurities (confirmed with GC-MS); the filtrate spot shows that the filtrate still has some starting material, MADI (**14**), a by-product (bottom spot).

The ^{1}H NMR spectrum displayed a new singlet resonating downfield at δ 7.99 ppm for HC=N proton (C3-H). The primary amine protons (-NH_2-) appeared as a singlet at δ 7.04 ppm, and three methyl protons also appeared as a singlet at δ 3.82 ppm. The ^{13}C NMR spectrum displayed six carbon signals, with the newly formed bond HC=N (C3) appearing downfield at δ 157.3 ppm, and the methoxy group (-OCH_3-) resonating at δ 55.1 ppm. The infrared spectrum shows the presence of NH at 3466 and 3354 cm^{-1} and C=N stretching vibrations at 1632 and 1602 cm^{-1}. Two strong stretching vibration bands appear at 2236 and 2195 cm^{-1} due to the presence of the two nitrile groups (C≡N) present in methyl *N*-(2-amino-1,2-dicyanovinyl) formimidate **14**.

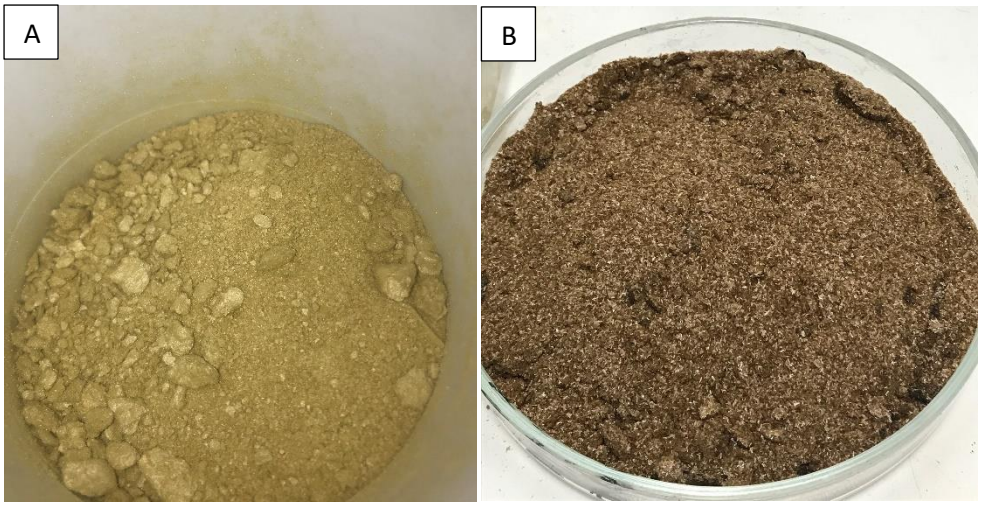

Figure 3.2. Shows imidate derivate products isolated through filtration. (A) shows pale-yellow solid MADI, (B) shows brown-crystalline solid EADI.

3.1.4 Process challenges

The published method for the synthesis of MADI (**14**) (Scheme 3.1) uses a two-solvent system: methanol and hexane.[42] The reaction commences by using MeOH as a reaction solvent followed by hexane which is used as an insolvent for the crystallization of MADI. The issue with this method is the amount of waste produced as it uses two solvents MeOH:hexane in 1:6 ratio. The waste solvent is not recoverable and waste management is thus quite expensive. In addition, industrial use of the solvent hexane is not ideal because hexane has been classified as a threat to human health and the environment.[51] According to the Centers for Disease Control (CDC) hexane poses a danger to workers as it is classified as a neurotoxin and is a highly explosive substance.[51]

As previously noted, at high temperatures we observe an increase in impurities (Figure 3.1, plate C). This is because DAMN (**12**) is known to decompose or undergo polymerization at high temperatures (<45 °C).[48] *N*-(2-amino-1,2-dicyanovinyl) formimidate derivatives are also easily decomposed; therefore they need to be synthesized within a short period[48]—if the reaction is set to be two hours it must be done exactly in two hours. Bearing this in mind, it is not practical to accurately control the temperature (i.e., instantly cool reaction vessel down to room temperature at the end of the reaction) and reaction period in the industrial plant.

3.1.5 Key Process Improvements

3.1.5.1 Solvent change

As previously mentioned, *N*-(2-amino-1,2-dicyanovinyl) formimidate derivatives are easily decomposed;[48] therefore, the method developed had to be simple, feasible, safe, and scalable. The first step was to change from a two-solvent system (MeOH:hexane) to a one solvent system (toluene). The solvent toluene is favoured because it is the most recycled and reused solvent at Chemical Process Technology (Pty) Ltd, thus readily available. Toluene was ideal because it was used as both the reaction solvent and the crystallization solvent. In addition, toluene is not as flammable as hexane,[51] and is easier to handle. A key benefit of using toluene is that it was recoverable by distillation. It can therefore be treated and reused for other processes at CPT.

3.1.5.2 Change of trialkyl orthoformate

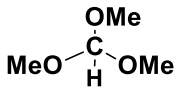

TMOF, 13

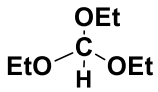

TEOF, 19

For the newly improved method, TEOF (**19**) was used instead of TMOF (**13**). This change was due to how well the reaction progressed when toluene was used as illustrated in TLC plate F (in Figure.3.3) showing the reaction after 2 h [isolated product EADI (**20**) spot marked as (fp) and the filtrate spot]. When TMOF (**13**) was initially reacted with DAMN (**12**) under the same condition as **19**, the reaction was not as successful (see Figure.3.3, TLC plate E) because the starting material was not fully consumed after heating and stirring for 2 h at 40 °C. The switch between TMOF and TEOF was cost motivated as well. At a commercial scale, triethyl orthoformate is less expensive compared to trimethyl orthoformate and as such, the cost of producing EADI (**20**) is less than the cost of producing MADI (**14**).

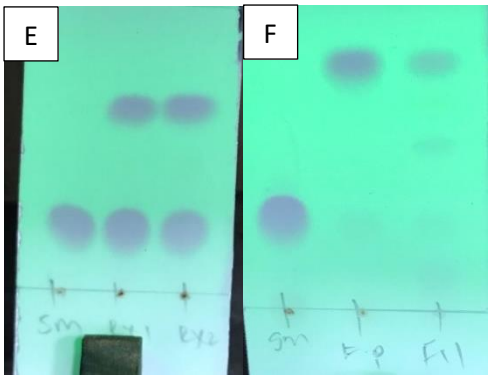

Figure 3.3. TLC plates (E) synthesis of MADI in toluene after 1(RX1) and 2(RX2) hrs at 40 ℃. TLC plate (F) shows synthesis of EADI in toluene after 2 hours at 40°C , spots represented in the TLC are the stating material (sm), finished product (EADI) after filtration and filtrate spot (FP).

3.1.5.3 Amount of acid catalyst

As previously mentioned, the published method used an excess of the catalyst TFA which led to an increase in by-products (Scheme 3.1). This is because an excessive amount of TFA makes the reaction difficult to stir, thus resulting in poor mixing and an increase in impurities. This is not ideal for the commercial production of **20** because the whole point of this research project was to lower the overall production cost of tenofovir. This is only possible if we produce a high yield while not compromising the quality of the product. The patent literature reported that the ideal amount of catalyst needed to condense DAMN and trialkyl orthoformate must be between 0.2–0.5% by mol with respect to DAMN (**12**).[48] Different amounts of TFA were used in multiple attempts within the suggested range. The optimal amount was found to be 0.003 equiv., which was then used to synthesize EADI **20** (see in Scheme 3.2).

The key benefit observed from the mentioned process changes was that the reaction done in toluene (Scheme 3.2) was far more stable in terms of temperature and reaction time since it was stable for a longer reaction period (> 3 h) and the was minimal waste produced. The optimum temperature range to produce EADI was discovered to be between 40–45 ℃.

The published method uses more acid catalyst (0.005 equiv.). When this amount of catalyst was added into the reaction it resulted in a thick slurry mixture which made it challenging to stir the reaction—resulting in poor mixing of the reagents and consequently low isolated yield. Patent literature reported that *N*-(2-amino-1,2-dicyanovinyl) formimidate can be produced by condensing DAMN and a trialkyl orthoformate in methanol/dioxane with heating and refluxing.[48] Mitsuru *et al* demonstrated that trimethyl orthoformate (TMOF) or triethyl orthoformate (TEOF) can be used interchangeably.[48]

In summary, to overcome the previously mentioned challenges of increased impurities and low yield, the reagents were changed such that EADI was synthesised rather than MADI; trimethyl orthoformate (TMOF), methanol as a solvent, and excess quantities of TFA catalyst were replaced with triethyl orthoformate (TEOF), toluene as a solvent, and low quantities of TFA catalyst, respectively. The reaction was initially performed at a small scale in the laboratory where it was successful and was then moved to a pilot scale using Radleys reactor.

3.1.6 Larger Scale Synthesis of EADI (20) in a Radleys Reactor

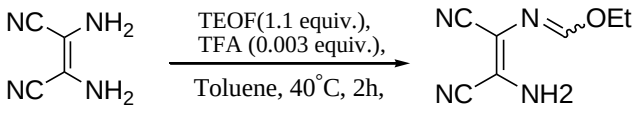

DAMN,12 **EADI,20**

Scheme 3.2. Optimized industrial process for synthesis of EADI.

DAMN (**12**) and toluene were charged to the reactor and were stirred for 5 minutes at room temperature. Triethyl orthoformate (**19)** and trifluoroacetic acid (TFA) were charged into the reactor. The internal temperature of the reactor was increased to 40 ℃ and was stirred for 2 h. TLC and GC-MS analysis were used to monitor the consumption of the starting material (**12**). The suspension was allowed to slowly cool down to room temperature over 30 min and then to 0 ℃ for an additional hour. A 90% yield of a dark brown crystalline solid was collected using vacuum filtration. The reaction solvent (toluene) was recovered by distillation. Ethyl *N*-3-amino-2,3-dicyanovinyl) formimidate **(**EADI, **20**) was fully characterised with IR, HRMS ^{1}H, and ^{13}C spectroscopy. TLC plate F in Figure 3.3 shows three spots: starting material **12**, precipitate **20**, and a filtrate spot. The precipitate spot shows full conversion of DAMN (**12**), and the filtrate spot shows little to no product [EADI (**20**)] presence.

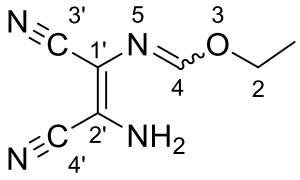

The ^{1}H NMR spectrum showed four proton signals with an appearance of a new quartet resonating at δ 4.29 ppm for the (C2-H) proton. The methylene signal of the ethyl enol ether was split by the adjacent methyl protons (C1-H) with a coupling constant of 7.0 Hz. The methyl group (protons) appeared upfield as a triplet resonating at δ 1.26 ppm. The C1-H peak was coupled with the adjacent -CH_2- protons with a coupling constant of 7.1Hz. The ^{13}C NMR spectrum showed seven carbon signals with the appearance of a new carbon signal for the ethyl group (C2) resonating at δ 63.8 ppm. The presence of the CH_2 group was also observed in the DEPT 135 spectra of the isolated product as this carbon signal appeared as a negative peak at 63.8 ppm.

3.1.7 Impurity profile

The *N*(-2-amino-1,2-dicyanovinyl) formimidate compounds are known to be easily decomposed when they are under higher temperature conditions and longer reaction periods.[48] Therefore, an optimized method was developed to increase the yield of EADI (**20**) and decrease the impurities. Despite the process improvements that were implemented in the synthesis of EADI, some of the EADI still decomposed, see filtrate spot in the TLC plate F in Figure 3.3 showing traces of unknown impurities. Therefore, the possible structures of the unknown impurities that form alongside MADI/EADI were investigated.

According to the patent literature when DAMN (**12**) is condensed with trimethyl orthoformate (**13**) in methanol under higher temperature conditions and increased reaction periods, MADI (**14**) cyclises and forms 4,5-dicyanoimidazole (**21**, Figure 3.4) as a by-product .[48]

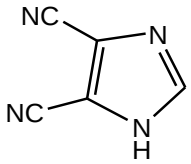

21

Figure 3.4. One of the reported by-products in the synthesis of MADI.

Attempts were made to synthesize and confirm the unknown impurity. As such, the published method for synthesis of MADI was used (Scheme 3.1). However, the reaction was performed

at slightly higher reaction temperature (50 ℃) and a longer reaction period. After 4 h passed, the reaction mixture was cooled down and concentrated using the rotavapor (under vacuum). The remaining dark-brown residue was purified using column chromatography (dry loading) which resulted in the isolation of the starting material DAMN (**12**) and the desired product MADI (**14**). The patent only mentioned one by-product **21**, but the TLC and GC-MS analysis shows other significant impurities; neither were identified as 4,5-dicyanoimidazole (**21**).

At this point we were satisfied that the changes we had made to the process would allow for a scalable synthesis of EADI and so we moved onto the next step.

3.2 Method Development for Step 2

3.2.1 Synthesis of HPI (17)

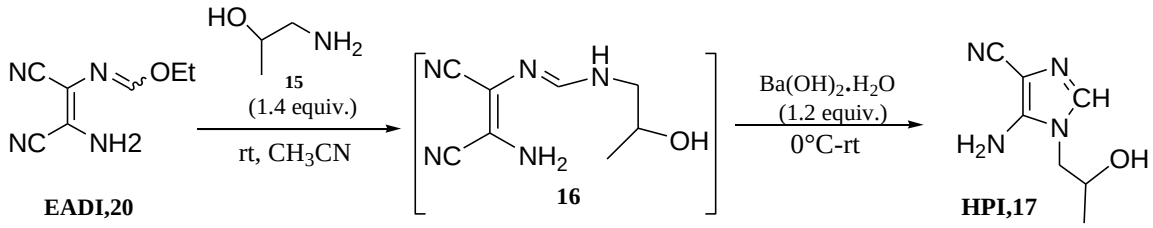

Scheme 3.3. Proposed route for HPI synthesis.

Having obtained EADI (**20**) in good yield (90%) from DAMN (**12**), it was now treated with 1.4 equiv of racemic amino-2-propanol (**15**) in acetonitrile (MeCN) at room temperature. After stirring at room temperature for 2.5 h, TLC analysis shows that **20** was fully consumed. The addition of amino-2-propanol **15** to imidate compound **20** was rapid; no significant decomposition was observed. According to the published method,[42] the reaction of **20** and **15** are supposed to yield amino-alcohol intermediate **16** only; however, two spots observed from the TLC analysis, one for the desired amino-alcohol intermediate **16** and the bottom spot for target compound, HPI (**17**). This is because compound **16** is unstable[52] and can readily cyclize to form HPI (**17**) in small quantities (see Figure 3.6,TLC plate G). To further induce cyclization of **16**, the reaction mixture was cooled down to a lower temperature of 0–5 ℃ and was treated with an aqueous barium hydroxide solution, this is because the addition of basic solution onto the amidine **16** was exothermic since a temperature increase was observed. The solid barium hydroxide monohydrate (1.2 equiv.) was charged with deionized water and the reaction was increased and maintained at room temperature.

As the reaction proceeded, colour change from light brown to red-brown was observed, an indication of induced cyclization.[42] Complete cyclization of amidine **16** under basic conditions was rapid since the complete conversion of **16** to imidazole **17** occurred after stirring for 1 h and 15 min at room temperature. After full conversion to imidazole **17**, the reaction mixture was filtered on a Büchner funnel to remove unreacted/excess $Ba(OH)_2$ and rinsed with reaction solvent MeCN. Fourty percent of the volume of the reaction solvent MeCN was distilled *in vacuo* at 40 °C. The reaction mixture was further heated to 50 °C; the aim was to heat the reaction until it changed colour to dark brown.[42] In this case however, there was no colour change observed. After stirring for 10 min at 50 °C, the reaction was cooled down to 40 °C, charged with dichloromethane (DCM) in a single rapid portion, and cooled down to room temperature for over an hour. The reaction was further cooled down to between 0–5 °C for an additional hour to precipitate imidazole **17**. However, when the reaction mixture was filtered on the Büchner funnel under vacuum, the desired product **17** as a pale-grey solid was not found. Instead, the filtrate had traces of black oil that was collected in a round bottom flask and later formed two phases: organic and aqueous (DCM:Water). The product was in the aqueous phase (top layer) which was dark brown, as shown in Figure 3.5 below.

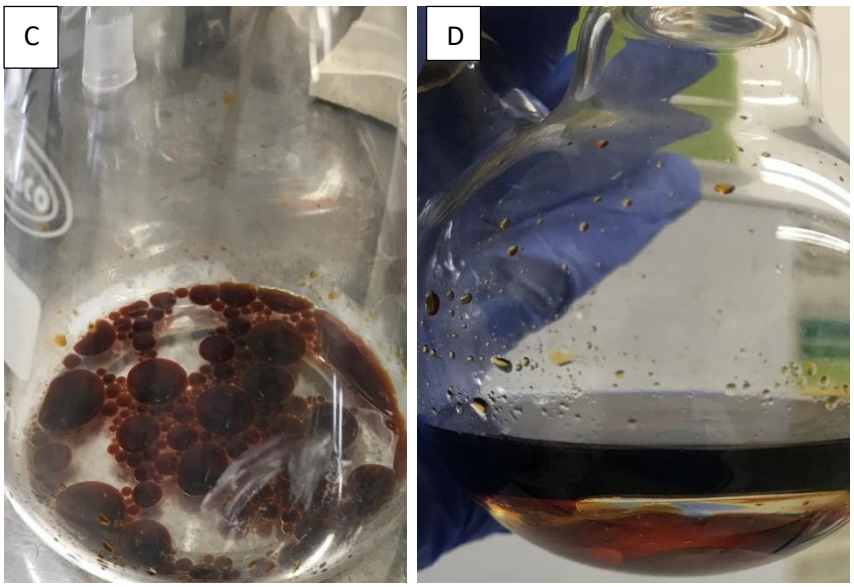

Figure 3.5. Filtrate collected from HPI synthesis.

3.2.2 Process challenges

3.2.2.1 Complete removal of $Ba(OH)_2$

Imidazole has long been synthesized in high yields through a reaction of amidines and a strong base.[48] To isolate imidazole in high yield and high purity, the choice of base used is critical.[52] Commonly used bases are made of alkali metal hydroxides such as potassium hydroxide, sodium hydroxide, and barium hydroxide.[48] Among these, monohydrate $Ba(OH)_2$ was the preferred base for inducing cyclization of **16** to imidazole **17**.[52] According to the patent, the amount of base used to provide a basic aqueous solution should range between 1 to 3 equiv. in relation to the staring material **20**.[48] The published method for the synthesis of HPI (**17**) uses 1.2 equiv. of $Ba(OH)_2$ which is charged with deionized water in the reaction. The cyclization of amidine **16** in the presence of basic media was rapid as the amidine **16** was completely consumed after stirring for 1 h and 15 min at room temperature as monitored using TLC (Figure 3.6). The reaction was filtered under vacuum to remove the excess $Ba(OH)_2$. It was observed that the published method does not effectively remove $Ba(OH)_2$. After filtration, the presence of $Ba(OH)_2$ in the reaction affects crystallization and isolation of HPI (**17**) as well as the colour and quality of the product **17**. This was observed in this reaction as crystallization of desired product **17** was not obtained. The reaction was thus performed at different equivalents of $Ba(OH)_2$. It was observed that irrespective of the equivalents used within this range (0.5 – 1.2 equiv.), the cyclization of amidine **16** to **17** was successful.

3.2.2.2 Product degradation

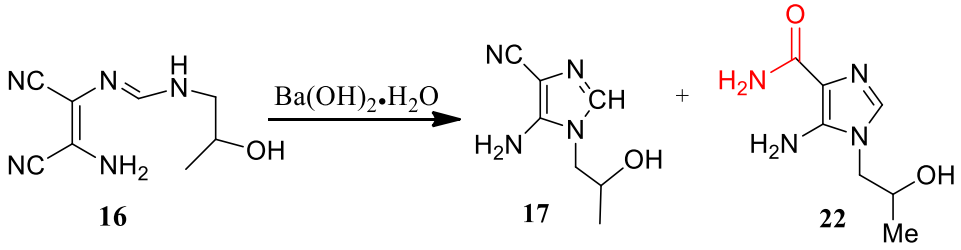

Scheme 3. 4. Synthesis of HPI 18 and HPI-amide 22.

The remaining $Ba(OH)_2$ after cyclization does not only affect the isolation of HPI (**17**) but also promotes the formation of the amide by-product **22** which lowers the yield of the desired product **17**. According to the patent, when reaction mixture temperature of **17** is raised above 30 ℃ and the reaction period is prolonged, the nitrile group of compound **17** is prone to hydrolysis to afford the amide in the presence of a basic medium.[48] This is an issue because the published method instructs that there must be distillation at 40 ℃ to remove 40% of the reaction

solvent MeCN after filtering and removing the excess Ba $(OH)_2$.[42] The issue is that $Ba(OH)_2$ is not removed completely even after filtering which then promotes the hydrolysis of **17** to amide **22**. This explains the observed second spot in TLC plate H after distilling the acetonitrile at 40 °C under vacuum, see Figure 3.6.

When the reaction mixture of **17** was left at room temperature overnight, a change in colour from dark brown to a black solution was observed. TLC analysis of the black solution showed the presence of the by-product. This means that HPI (**17**) solution in basic media is not stable[52] and that is an issue, especially for the scale up reaction in the pilot plant.

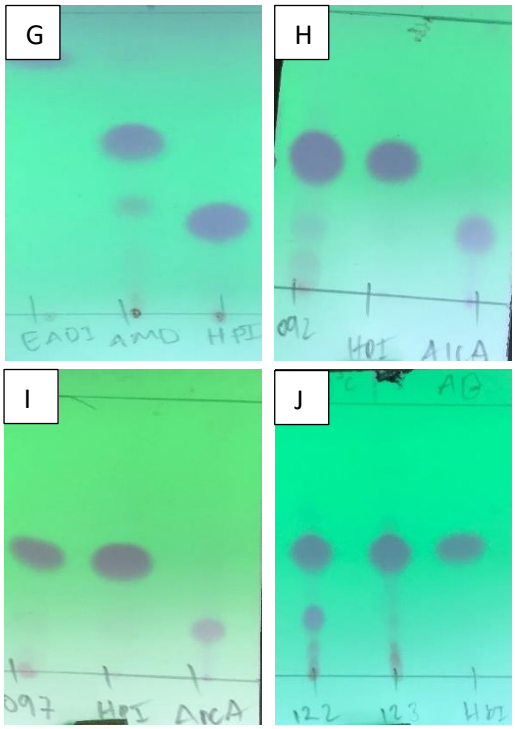

Figure 3.6. TLC analysis during the synthesis of HPI under different conditions. (a) TLC plate G shows the starting material with the intermidiate **16** (AMD) and finished product **17** spot (b) TLC plate H shows the degradation of HPI product after distilling acetonitrile at 40 °C (c) TLC plate I shows the product HPI with pH adjustment after distilling acetonitrile (d) TLC plate J show behaviour of HPI reaction at a higher temperature of 60 °C; 122 spot (no pH adjustment), 123 spot (pH adjusted).

3.2.2.3 Two solvent system

The published method uses a two-solvent system, acetonitrile and dichloromethane (1:1 ratio).[42] Acetonitrile is used as the reaction solvent and dichloromethane is used as the insolvent to promote product precipitation. The basic media that is used to induce cyclization of **16** to **17** involves $Ba(OH)_2$ partially dissolved in deionized water. When suspension **17** is filtered, it was observed that the collected filtrate forms two layers: aqueous and organic layers (dichloromethane), see Figure 3.5, image D. The use of the insolvent dichloromethane in the isolation of **17** did not play a significant role but rather added to the waste produced in step 2.

Part of developing a commercial manufacturing process for the tenofovir intermediate involves reducing the overall cost of production, including minimizing waste produced since waste management is expensive.

Another issue with the use of dichloromethane is that it is an acute inhalation hazard, classified as a neurotoxin, and has been proven to cause damage both to the brain and central nervous system. The use of dichloromethane in an industrial plant is not ideal as it is very volatile and therefore not safe for the environment and the plant workers.[53]

3.2.3 Process improvement

3.2.3.1 pH adjustment

The synthesis of imidazole **17** was achieved by reacting amidine **16** with a strong base $Ba(OH)_2$ at room temperature in MeCN. The cyclization of **16** was very rapid in the presence of basic media. After the addition of a basic aqueous solution, the reaction pH was confirmed to be 12.58 with a pH meter. Even after all the amidine **16** was consumed and cyclized, and the excess $Ba(OH)_2$ was removed by filtration, the pH of suspension **17** was still measured to be 12.58. The presence of basic media is what promoted the hydrolysis of the desired product **17** to HPI-amide **22**. It was reported that hydrolysis of the nitrile group is pH and temperature-dependent.[54] This explains the degradation of the product after distilling the MeCN and the degradation of the product when it was left for a longer period after the complete conversion of amidine **16**.

Both the pH and reaction temperature were adjusted to produce and isolate the desired product **17**. Initially, the pH of the reaction mixture **17** was adjusted and neutralized from 12.58 to 7.00 using an aqueous HCl solution at lower temperature conditions. The reaction changed colour from brown to a black suspension. The MeCN was distilled partially from the black suspension and left overnight. After 18h, it was observed with TLC analysis that HPI (**17**) did not degrade to **22**, it was stable but there was no precipitation of barium salts. So, the crystallization and isolation of **17** remained a challenge. After multiple pH adjustments, it was discovered that when the reaction pH is lowered to 9.60 with aqueous HCl solution, the formation of by-product **22** was minimized (see Figure.3.6, TLC plate I) and any remaining $Ba(OH)_2$ was neutralized and isolated as $BaCl_2$ (see Figure 3.7, image E). Therefore, pH adjustment does not only help with minimizing by-product formation but also removes the unwanted $Ba(OH)_2$ after cyclization.

3.2.3.2 Removal of $Ba(OH)_2$

Adjusting the pH of the reaction mixture from 12.58 to 9.60 helped to remove the remaining $Ba(OH)_2$ as it was neutralized to produce $BaCl_2$. Another technique that was used to ensure the complete removal of $Ba(OH)_2$ involves the addition of acetone after pH adjustment and concentration of the reaction mixture via distillation of MeCN. It was observed that $Ba(OH)_2$ is insoluble in non-polar solvents like acetone and ether. Therefore, acetone solvent was utilized because it is readily available at CPT. In addition, HPI (**17**) dissolves in acetone and did not form any products. The precipitated $Ba(OH)_2$ is removed through vacuum filtration and is rinsed with cold acetone.

3.2.3.3 Solvent system

The method for producing aminoimidazole derivatives involves mixing amidines and a basic aqueous solution in aprotic solvents such as ethers and acetonitrile.[48] When aprotic solvents are used as reaction solvents, there are fewer by-products produced. However, when solvents like alcohol are used (ethanol, methanol), by-products are easily produced.[48] The published method uses acetonitrile as a reaction solvent for the cyclization of **16** to **17**. After amidine is fully consumed, dichloromethane is used as an insolvent[42] to help with the precipitation of the desired product **17**, which in our case was not successful.

Part of developing an industrial process for tenofovir intermediate includes minimization of solvent waste. Therefore, the use of insolvents to isolate or precipitate the desired product must be avoided. Part of the process improvements implemented involved the use of reaction solvent acetonitrile and precipitating product **17** from water rather than the recommended dichloromethane.

3.2.4 Optimized process

After many attempts at optimizing the process, a new method was established. When the cyclization reaction of **16** was complete, the reaction temperature was lowered to 5 ℃ using an ice bath. A calculated amount of aqueous HCl solution was added and the reaction was left to stir for 30 min under cooler temperature conditions. The addition of aqueous HCl solution to the reaction (pH 9.60) triggered a colour change and the forming and accumulation of a solid at the bottom of the flask. The precipitated product was discovered to be $BaCl_2$. This means the HCl reacts with the remaining base $Ba(OH)_2$ to form $BaCl_2$ which precipitates and is removed via vacuum filtration. The reaction was filtered using the Büchner funnel with celite

to remove the black tars. After pH adjustment, the acetonitrile was distilled completely at 40 ℃ under reduced pressure. No degradation of desired product **17** was observed. As such, lowering the pH of the reaction from 12.58 to 9.60 made **17** more stable even when it was exposed to higher temperatures (50–60 ℃). Under the aforementioned conditions, the product **17** still did not undergo partial hydrolysis (see Figure 3.6, TLC plate I).

After removing the acetonitrile completely by distillation at reduced pressure and increased temperature, acetone was added to further remove any remaining $Ba(OH)_2$ in the reaction mixture. The reaction was stirred for 30 min, and the temperature was adjusted to cooler conditions to further decrease the solubility of $Ba(OH)_2$ in acetone. In a few instances there was a precipitate observed which was believed to be $Ba(OH)_2$. In other instances there was no precipitate, which means the pH adjustment did effectively remove the excess $Ba(OH)_2$. If a precipitate was present it was removed via vacuum filtration and TLC analysis was done to confirm that it was not the desired product **17**. The reaction was then distilled at 30 ℃ under reduced pressure. Acetone was removed completely, the reaction was transferred into the flask, and the flask was rinsed with a calculative amount of water. The reaction mixture mass temperature was increased to 40 ℃ and stirred for 10 min. The reaction mixture temperature was gradually decreased to cooler conditions (2–5 ℃) for approximately 2 h or until the HPI (**17**) precipitated. The slurry mixture was then filtered via vacuum filtration and was washed with a calculated amount of cold water to yield 82% of an off-white solid **17**. It was observed that yield and purity are inversely proportional. When more water was used to wash the solid precipitate **17**, the cleaner the product appeared. A wide range of colours for the isolated product **17** were obtained ranging from a purplish colour to an off-white solid as shown in Figure 3.7 (image F and G). The change in colours was also associated with the presence of the base and how much water was used to rinse the precipitate.

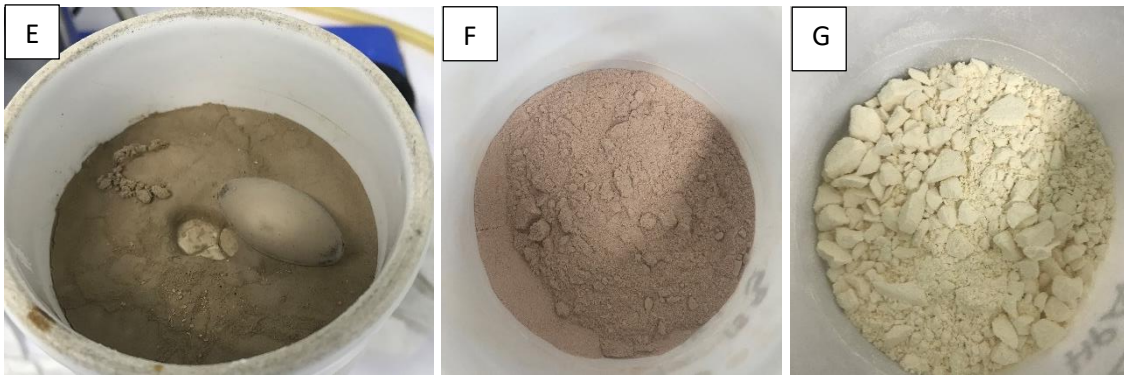

Figure 3.7. Shows the collected precipitate during the synthesis of HPI **17** (E) Collected $BaCl_2$ (F) and (G) collected HPI product.

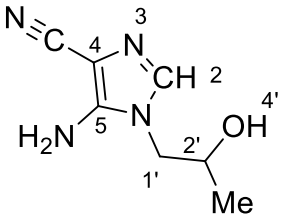

The isolated product **17** was found to be pure by TLC, IR, GC-MS, ^{1}H NMR, and ^{13}C NMR spectroscopy. The ^{1}H NMR spectrum showed the presence of imidazole proton (C2-H) which appeared as a sharp singlet at δ 7.12 ppm. The primary amine protons (NH_2) appeared as a singlet at δ 6.06 ppm. The asymmetric C2'-H proton appears as multiplet resonance at δ 3.85-3.82 ppm. The methylene protons C1'-H of the acyclic side chain bonded to N1 of the imidazole ring are diastereotopic as they are attached to the adjacent asymmetric carbon attached to the (-H, OH, and CH_3 groups). The methylene protons appeared as a doublet of the doublet, and each resonated at δ 3.80-3.77 ppm and δ 3.65-3.61 ppm. The hydroxy proton of the product **17** appeared as a doublet peak at δ 5.08 and 5.07ppm (H-4') because it is coupling with the C 2'-H proton with a coupling constant of 4.8 Hz. The COSY spectrum shows that the hydrogen at δ 5.07 ppm (H-4') is coupled by the hydrogen at δ 3.84 ppm (C2'-H), see appendix plate 3d, ^{1}H- ^{1}H *J* coupling. Three methyl protons attached to C3' appear as a doublet at δ 1.06 and 1.05 ppm because they are coupling with the adjacent C2'-H with a coupling constant of 6.2 Hz. New proton signals were derived from the reaction of EADI (**20**) with the amine **15** to give an amino-alcohol intermediate **16**, which is followed by cyclization in a basic aqueous solution. The ^{13}C NMR spectrum showed seven sharp peaks, with signals C-5 and C-2 around δ 148.4 and 134.0 ppm. The carbon signal for C-4 is the only aromatic carbon that is bonded to a single nitrogen atom and therefore resonates upfield at δ 90.7 ppm. In the HMBC spectrum, the C-4 shows a strong 3-bond correlation to the nearest protons C2-H (7.12 ppm) and NH_2 protons (6.06 ppm), and 4 bond correlation to the diastereotopic protons (C1'-H) at 3.77 and 3.62 ppm (appendix plate 3c, ^{1}H- ^{13}C correlations).

The IR spectrum of the product **17** showed the presence of a nitrile group as one intense band appearing at 2206 cm^{-1} for the stretching band. The IR spectrum also showed the NH stretching bands at this region 3160–3280 cm^{-1} and a strong band at around 1625 cm^{-1} assigned to C=N stretching vibration.

3.2.5 Impurity profile

The patent literature mentions that HPI (**17**) is prone to hydrolysis in the presence of a basic medium.[48] This was observed when the cyclization reaction of **16** was complete and the reaction was left overnight or exposed to temperature >30 ℃, the nitrile group undergoes partial hydrolysis in the basic aqueous solution to form a by-product amide **22** which was present in the crude product. The published method includes distilling about 80% of the acetonitrile under reduced pressure at 40 ℃.[42] The by-product formation was observed by TLC analysis where there was a second spot after distillation (see a Figure.3.6, TLC plate H). An extensive literature survey was done to reveal the impurity structure that was observed on the TLC analysis. The major impurity in the synthesis of HPI (**17**) was synthesized, characterized, and confirmed as 5-Amino-1-(2-hydroxypropyl-1-*H*-imidazole-4-carboxamide) **22**.

As the next step the synthesized AICA (**22**) was used as an impurity standard for the development of a selective analytical method in process development of HPI. In addition, this will help improve the quality control during manufacturing of TDF.

3.2.5.1 Synthesis of 5-Amino-1-(2-hydroxypropyl-1-*H*-imidazole-4-carboxamide)

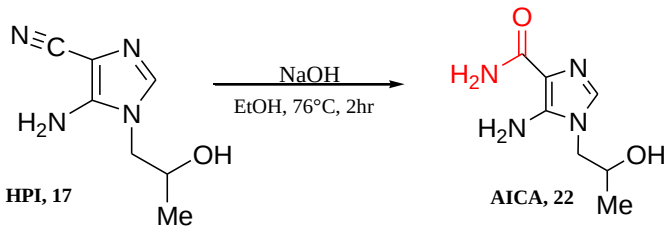

Scheme 3.5. Synthesis of the impurity **22**.

A flask was charged with HPI (**17**) along with NaOH and ethanol. The reaction was refluxed for 2 h while stirring. After 2 h, full conversion of **17** into **22** was confirmed with TLC analysis and the reaction was cooled down to room temperature. The reaction mixture was neutralized to a pH of 7 using an aqueous HCl solution. After neutralization, the reaction mixture was concentrated. The residue was poured into a flask and cooled down to lower temperatures of <10 ℃ until it precipitated. The milky slurry solution was filtered and washed with a cold mixture of water:ethanol (1:1). The precipitate yielded a white crystalline solid **22** and was fully characterized with TLC, IR, ^{1}H NMR, and ^{13}C NMR spectroscopy.

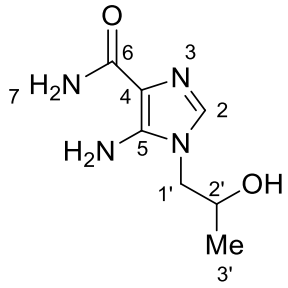

Compound **22** was found pure by TLC. The ^{1}H NMR spectrum showed a sharp singlet downfield at δ 7.05 ppm which was assigned to the imidazole proton (C2-H). The amide group experiences a partial double bond character due to resonance. The nitrogen lone pair can delocalize into the carbonyl group, forming the resonance structure where the carbon-nitrogen bond has a partial double bond character. The partial carbon-nitrogen double bond character restricts rotation around the carbon-nitrogen bond and results in the amide protons being chemically non-equivalent.[55] This explains the observation of the distinct two broad peaks downfield resonating at δ 6.77 and 6.63 ppm for the two different types of protons, the amide NH_a and the amide NH_b protons, respectively. The NH_2 group further from the amide group appeared as a sharp singlet at δ 5.70 ppm. The ^{13}C NMR spectrum also shows the presence of an amide group downfield at δ 167.3 ppm; the deshielded carbon was assigned to the carbonyl group (C6). The C4 signal was now more deshielded as it is the only carbon atom that is bonded to the nitrogen atom and carbonyl carbon and the C4 signal was assigned to the chemical shift 112.9 ppm. The IR spectrum showed that the nitrile group had undergone a hydrolysis reaction and converted to amide, we observed the presence of the carbonyl group (C=O) which overlaps with the N-H stretch at region 1606 cm^{-1}. The IR spectrum also showed the NH stretching bands at this region 3317–3093cm^{-1}.

3.3 HPA Process Development

3.3.1 Synthesis of HPA (6)

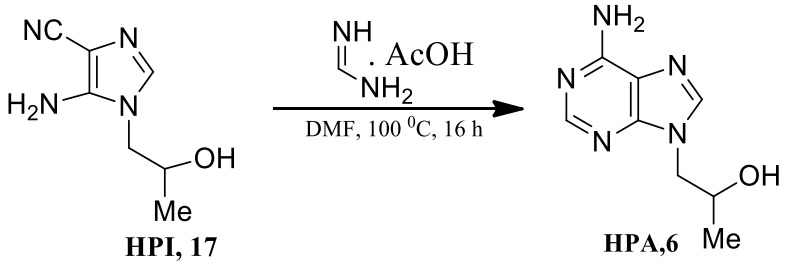

Scheme 3.6. Published method for HPA synthesis.

For the synthesis of HPA we initially followed the reported literature procedure.[42] The previously synthesized HPI (**17**) (1.0 equiv.) and formamidinium acetate (FAA) (1.7 equiv.) were charged with DMF at 25 ℃ in a flask. The mixture was heated and maintained at 110 ℃ for 16 h. TLC analysis showed that **17** was not completely consumed and thus the reaction was heated for an additional hour at 110 ℃. The reaction was cooled to 90 ℃, isopropyl alcohol (IPA) was added, and the reaction was cooled down to room temperature. The reaction was then further cooled down to the 0-5 ℃ range over 3 h under stirring. The suspension was filtered and washed with cold IPA. The isolated solid was dried in a vacuum oven at 65 ℃ for 2 h to afford HPA (**6**) as an off-white solid, unfortunately with the poor yield of 46%.

3.3.2 Thermal degradation of formamidinium

Formamidinium acetate is used as a condensing agent for the preparation of the adenine core **6**.[42] Formamidinium acetate is a salt of a strong base and weak acid which is used directly, i.e., without liberation of formamide.[56] The reaction temperature for Scheme 3.7 was done at 100 ℃ which resulted in the thermal degradation of formamidinium.[57] Formamidinium as a free base can undergo several thermal decomposition reactions including the formation of (a) *sym*-triazine and (b) hydrogen cyanide—both routes generating ammonia (NH_3) as a by-product.[57]

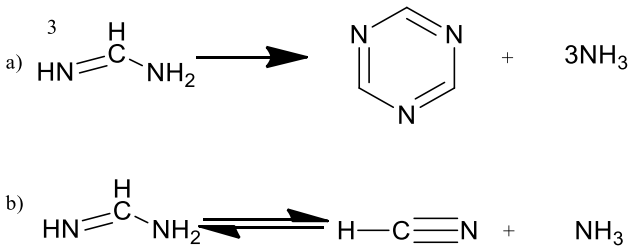

Scheme 3.7. Thermal decomposition of formamidinium generating (a) *sym*-triazine and (b) HCN.

For the synthesis of HPA, the nitrile route (b) was required as it possesses the additional carbon and nitrogen that are required to afford the adenine ring.[42,57] When the aminonitrile is condensed with FAA, ammonia was reported to be the nitrogenous group that was expelled from the amidine.[57]

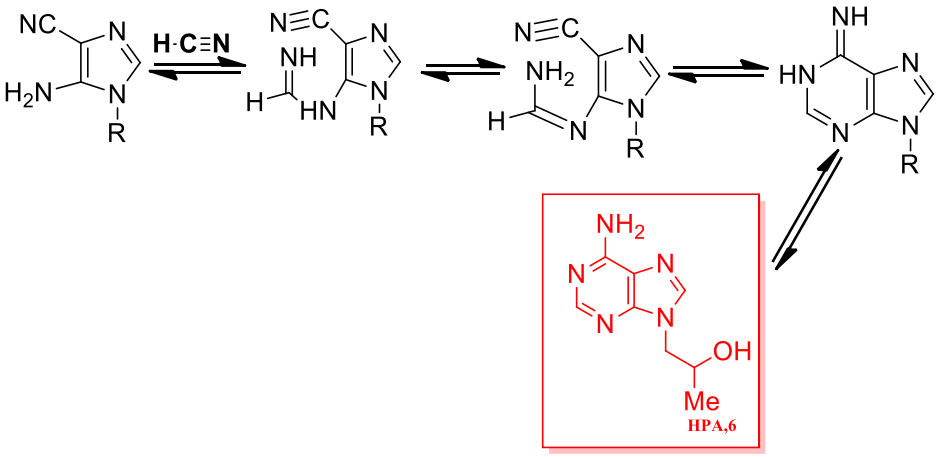

Scheme 3.8. Adenine ring formation from aminonitrile and HCN.

The main issue we found in conducting this step (Scheme 3.6) in the laboratory was that during thermal degradation of formamidinium, (a) *sym*-triazine was found to be the major product that was released at a higher temperatures (above 95 °C).[57] That was the reason why the yield was low, i.e., due to the side reaction and formation of the irreversible by-product (Scheme 3.7.a). Therefore, there is insufficient HCN released to react with aminonitrile (**17**), which explains the detection of residual HPI (**17**) after heating and stirring for 17-18 h at 100 °C.

3.3.3 Process improvement

To resolve the low isolated yield problem, two parameters were investigated: the amount of FAA used and the reaction temperature. The first attempt involved 1.4 equivalent of FAA mixed with 1 equiv. of HPI (**17**) in DMF; the reaction internal temperature was raised to 100 °C and the electric hot plate was set at 110°C. For the second reaction, HPI (**17**) 1.0 equiv. was charged with 1.4 equiv. of FAA in DMF; the reaction was heated to an internal temperature of 110 °C and the electric hot plate was set at 120°C. Both reactions were performed concurrently, and their set temperature was maintained for 4 h under stirring. The consumption of starting material **17** was monitored with TLC and HPLC. From the analysis, it was observed that the starting material (**17**) was partially consumed for both sets of reactions. TLC plate K (Figure 3.8) revealed the appearance of an impurity after stirring and heating the reaction at 120 °C for 4 h. On the other hand, the reaction done at 110 °C had no impurity forming.

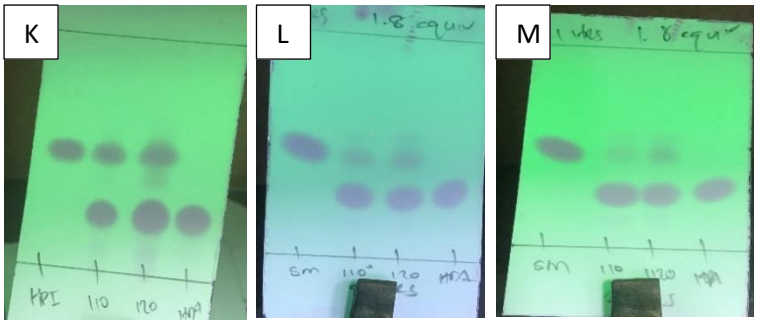

Figure 3.8. TLC plates for reactions done at 100 ℃ and 110 ℃ (K) 1.4 equiv. of FAA 4 h, (L) 1.8 equiv. of FAA at 8hrs, and (M) 1.8 equiv. of FAA at 21 h.

After 4 h passed, 0.4 equiv. of FAA was added into both reactions and stirred for an additional 4 h at 100 ℃ and 110 ℃. TLC analysis and HPLC were done for both samples. The reactions were then left overnight. The next day the crude material was collected and analysed with TLC and HPLC. The HPLC quantitative analysis showed that when FAA was added portion-wise every 4 h the consumption of HPI increased too. After stirring and heating at 100 ℃ for 4 h with 1.4 equiv. of FAA, HPA purity was measured to be 83.63%. After heating and stirring for 21 h at 100 ℃ with 1.8 equiv. FAA, HPA purity was 98.62%, which is in correlation with what is observed from the TLC plate M in Figure 3.8 where the bottom spot (**6**) in spot 110°C is becoming prominent, and the starting material (**17**) spot on the TLC is disappearing.

3.3.4 Optimized process

During process development, several reactions were conducted. It was discovered that excess use of FAA and high reaction temperatures resulted in a decrease in isolated yield of **6** as the impurities (*sym*-triazine) increased. Therefore, the best method developed thus far was the reaction done at 100 ℃ (electronic hot plate set at 110 ℃), with 1.8 equiv. FAA added portion-wise as mentioned above. Once the starting material is consumed, heat was turned off and the reaction mixture was concentrated in vacuo to half of the original volume. The distilled reaction mixture was allowed to cool down to 75 ℃, isopropanol was added to the reaction, and the reaction mixture was transferred into a Julabo reactor where it was further cooled down to room temperature and then to -15 ℃ over 3 h. The suspension was collected by filtration and washed with cold isopropanol. The solid was dried in a vacuum oven at 65 ℃ for over 2 h. The HPA (**6**) was obtained as an off-white solid with an 85% isolated yield, see Figure.3.9, image I. It must be noted that the isopropanol used as insolvent needs to be dry to allow for product crystallization.

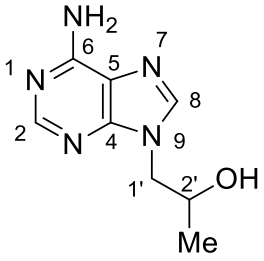

TLC indicated that the product was pure. Further characterizations including ^{1}H NMR, ^{13}C NMR spectroscopy, HPLC, and HRMS analysis were done on the off-white isolated HPA (**6**). The ^{1}H NMR spectrum showed two sharp singlets downfield that were assigned to the aromatic ring protons C2-H and C8-H resonating at δ 8.14 and 8.05 ppm. The assigned proton signals are in accordance with the theory of aromatic heterocyclic ring H-2 and H-8 proton signals that have been reported to be δ 8.46 and 7.95 ppm.[58] The spectrum showed a new proton signal at δ 7.18 ppm belonging to the NH_2 group. The single proton signal for the amino protons is due to their identical nature and they do not split with any neighbouring protons. The multiple resonance signals observed upfield at δ 4.02–3.98 ppm was assigned to the methylene protons C1'-H that are attached to N9 of the imidazole ring. The split patterns of the CH_2 group are due to the adjacent attachment to the asymmetric carbon that is bonded to H, CH_3, and OH groups. This makes CH_2 protons chemically inequivalent and each C1'-H proton gives a doublet due to *J* coupling with the C2'-H proton. The multiplet resonance that appears at δ 4.13–4.08 ppm was assigned to the C2'-H. The COSY spectrum shows that C2'-H (4.10 ppm) is coupled with hydroxy (-OH-), C1'-H, and C3'-H protons. The hydroxy group attached to the asymmetric carbon C2' was observed as broad singlet δ 5.03ppm; this was in accordance with literature as alcoholic proton signal resonance normally ranges between δ 0.5–5 ppm.[58] The three methyl protons C3'-H appear upfield as doublet δ 1.06 ppm due to scalar coupling with C2'-H with a coupling constant of 5.8 Hz. The condensation of FAA and HPI (**17**) is proven by the presence of the additional carbon signal C2 that comes from the formamidinium (Scheme 3.8). The new carbon signal C2 resonated at 152.73 ppm which in turn couples to C2-H (8.14 ppm, 1 bond, HSQC). The nitrile carbon C6 that was condensed with amino schiff base resonates downfield as aromatic carbon at 156.4 ppm. The other aromatic carbon atoms were assigned as follows C4>C8>C5 with chemical shift values resonating at 150.2, 141.9, and 119.9 ppm. C5 was assigned upfield in the ^{13}C NMR spectrum because it was the only purine ring carbon that was bonded to a single nitrogen atom out of all the purine ring carbons. Examination of the IR spectrum for the off-white product **6** showed that the nitrile stretch band was absent; this further proves that the condensation of FAA with

aminonitrile **17** took place as expected under optimized conditions. Isolated HPA (**6**) melting point was between 191.5–193.4 ℃ which is aligned with literature (191–195 ℃).[59]

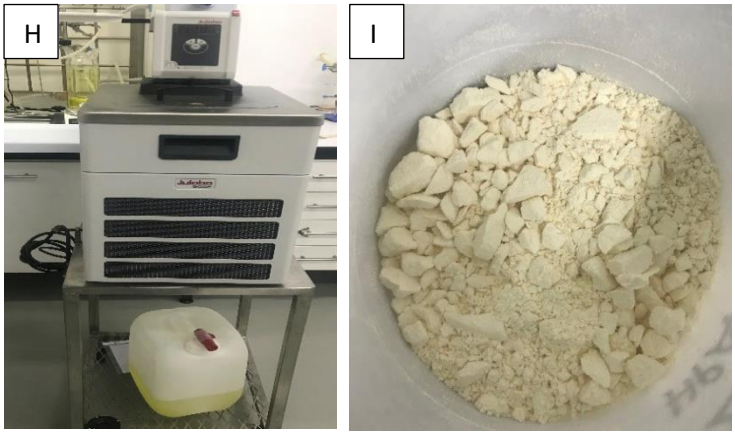

Figure 3.9. (H) Julabo used to maintain the reaction under cooler conditions and (I) shows the isolated HPA (**6**).

3.3.5 Impurity profile

Upon crystallization and drying of the solid product **6**, the isolated material gave off an acetic acid smell. The sample was submitted for GC-MS, IR, and NMR analysis. The ^{1}H NMR and ^{13}C NMR spectrum showed an additional peak resonating at δ_H 1.9 ppm and δ_C 172.6 ppm which was assigned to acetic acid.[60] However, the acetic peak was not visible or concentrated enough to appear in the chromatogram. The same sample was left in a vacuum oven set at 100 ℃ for over an hour. The sample was then analysed using GC-MS and NMR. The ^{1}H NMR showed that the acetic acid peak was no longer present (Figure 3.10, spectrum a) as the acetic acid had been removed through evaporation. In addition, the sample no longer gave off the acetic acid smell.

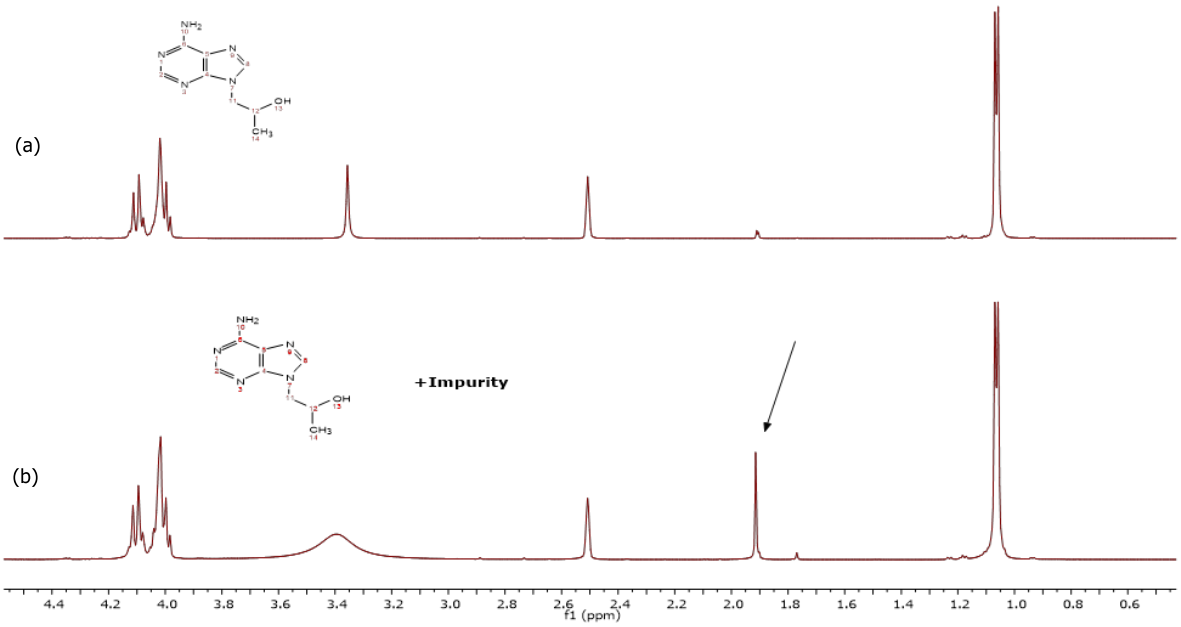

Figure 3.10. ^{1}H NMR analysis of the isolated product showing acetic acid as a major impurity.

3.4 (R)-1-aminopropan-2-ol Process Development

3.4.1 Introduction

According to the M4ALL published method for synthesis of HPI (**17**) in Scheme 2.2, (R)-1-aminopropan-2-ol is condensed with the synthesized MADI (**14**) to further produce the chiral HPI.[42] However, the prices of the (R)-1-aminopropan-2-ol are prohibitive for a cost effective process which will result in an increase in the cost of producing the HPI intermediate. To decrease the overall cost of production of tenofovir, the direction of this study was steered towards the development of a method for the synthesis of *R*-1-aminopropan-2-ol (**15**) at CPT instead of purchasing the starting material.

Decarboxylation of α-amino acids is a long-known reaction that leads to the production of free amines with a range of applications for the synthesis of biologically active compounds.[61] After conducting a thorough literature survey on the decarboxylation of α-amino acid, several potential routes were discovered. For a very long time, non-enzymatic decarboxylation of α-amino acids was done at very high temperatures greater than 200 °C.[62] This was because the reactions were exothermic and therefore needed to reach higher activation energy.[62] As seen in pyruvoyl-dependent histidine decarboxylase, nature lowers the activation energy using enzymatic reactions.[62,63] In these reactions the α-amino acid first condenses with pyridoxal phosphate to form a Schiff base which allows for easier decarboxylation.[62] This approach

underpins the commonly used methods: catalytic decarboxylation of α-amino acids with aromatic aldehyde/ketones in high boiling solvents.[62]

Other non-enzymatic methods involve irradiation with UV light[61] or heating the amino acids in high-boiling solvents such as diphenylmethane.[64] Another promising method was published by Laval and Golding where the decarboxylation of the α-amino acid was performed in a one-pot synthesis that involves sequential reactions starting with oxidative decarboxylation of α-amino acid to nitriles induced by *N*-bromo succinimide.[61] This is then followed by reduction of the nitrile to an amide using sodium borohydride-nickel chloride. This reaction seemed promising especially since it was carried out in water at room temperature. However, it involved the use of toxic NBS which poses a challenge for industrial waste disposal as metal-bromide and boron-containing by-products will have to be catered for.[61] Therefore, to produce the desired free amine (R)-1-aminopropan-2-ol, an industrially-friendly method was developed.

3.4.2 Decarboxylation of α-amino acid mechanism

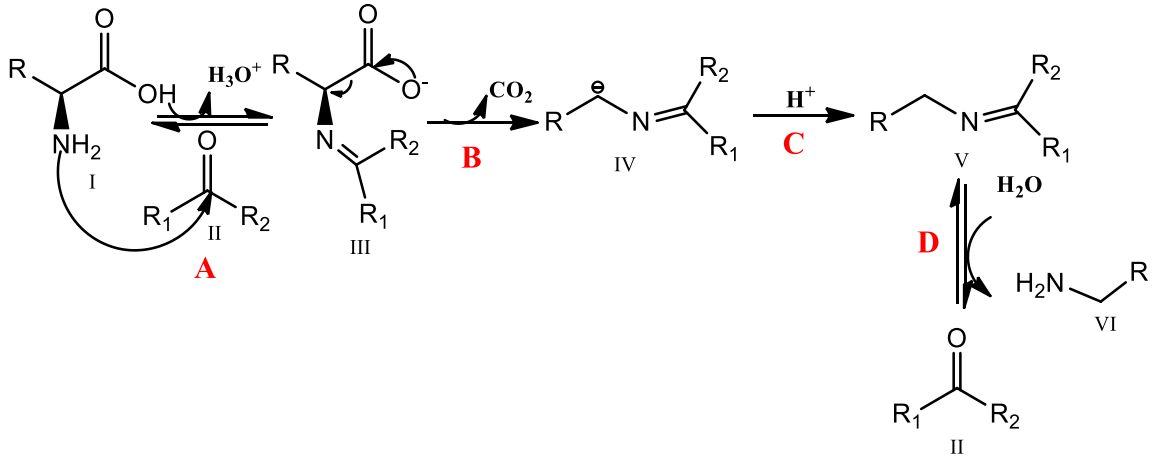

Scheme 3.8. Decarboxylation of α-amino acid.

Mechanisms of the α-amino acid decarboxylation are divided into four parts (Scheme 3.8), which start by condensing the α-amino acid (I) with the ketone catalyst (II) to form the Schiff base (III) where the substrate nitrogen is double bonded to the carbonyl group of the ketone catalyst.[63,65] The carbonyl group of the α-amino acid is removed and its negative charge is transferred to the α-carbon of the substrate creating a carbanion (IV).[63] After CO_2 is released, the α-carbon undergoes protonation and the amine product (VI) is then ready to be released through hydrolysis of the Schiff base(V).[65] Both the formation and the hydrolysis of the Schiff base are reversible reactions.[61]

3.4.3 Decarboxylation of L-threonine

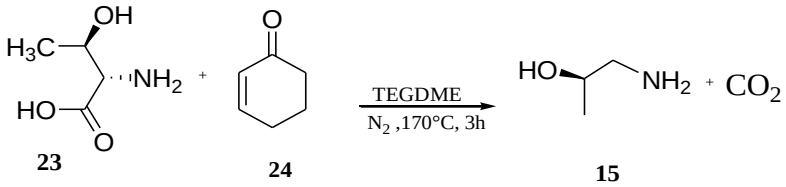

23 **24** **15**

Scheme 3.9. Decarboxylation of L-threonine.

L-threonine (**23**), 2-cyclohex-1-one (**24**), and tetra ethylene glycol dimethyl ether (TEGDME) were charged into a reactor flask. The reactor was heated from room temperature to 170 ℃ with active stirring immersed in an oil bath. The reaction internal temperature was maintained at 170 ℃ for 3 h under nitrogen atmosphere. The progress of the reaction was followed by observing carbon dioxide evolution. After 3 h, there was no CO_2 evolution, instead, the slurry solution became a homogenous red-brown solution. The reaction was cooled down and the free amine base **15** was collected via distillation under a vacuum. A colourless liquid, the desired product **15**, only started distilling around 71–90 ℃ under reduced pressure (21 mbar). The distilled sample of (R)-1-aminopropan-2-ol (**15**) was collected with a yield of 76% and was analysed with GC-MS.

3.4.4 Impurity profile

GC-MS analysis confirmed that the desired product (R)-1-amino-2-propanol **15** was formed but with a substantial number of impurities present such as dimer (**25**) and Schiff base (**26**). The literature survey done on the potential route for the decarboxylation of amino acids **23** did not have information about the formation of any by-products/impurities. The decarboxylation of α-amino acid in Scheme 3.8 is coordinated by the formation of the Schiff base where the α-amino acid is temporarily trapped and double bonded to the carbonyl carbon which allows for the elimination of CO_2. The Schiff base (**26**) in Scheme 3.10 was observed as one of the by-products in the synthesis of **15** since the observed chromatogram shows a peak with m/z of 153.12 for the distilled colourless product. This could be because the reaction was incomplete, i.e., the Schiff base did not undergo hydrolysis because had it done so it would have released the desired free amine. Alternatively, this could be because the free amine was very reactive such that it reacted again with the recovered carbonyl catalyst resulting in the observed Schiff base (**26**) as shown in Scheme 3.10.

Another by-product that was observed from the chromatogram analysis was the presence of the peak with m/z of 133.14 which was identified as the dimer (**25**) (Scheme 3.10). The free base (R)-1-amino-2-propanol has presence of both the amino (NH_2) and hydroxyl group (OH).

Both groups can act as H-bond donors and acceptors and can participate in hydrogen bonding leading to dimerization. It was reported that chances of dimerization of free base of amine **15** could depend on several factors such as temperature, solvent and the concentration of the compound.[66] It could be possible that the formation of dimer (**25**) was due to the factors mentioned earlier.

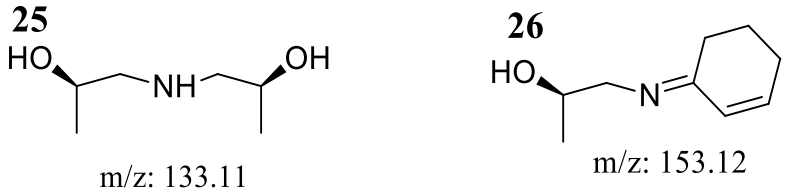

Scheme 3.10. By-products observed in the chromatogram of the distilled product.

Given the aforementioned, the method for decarboxylation of *L*-threonine (**23**) was changed by conducting the reaction in high boiling point solvents with both diphenyl ether and diphenylmethane at an elevated temperature of 200 ℃ and under a nitrogen atmosphere. After heating and stirring the reaction at 200 ℃ for 2–3 h, the suspension was distilled under a vacuum starting at 70 ℃. The distilled sample had a low yield (32%), and GC-MS analysis of the isolated yield shows the presence of solvents in the chromatogram. This is because both diphenyl ether and diphenylmethane are volatile; hence, the solvents are also distilled along with desired product **15** under vacuum. From observation, the decarboxylation of *L*-threonine **23** without a catalyst requires a substantial amount of energy and produces low isolated yield. As a result, different ketone catalysts were explored.

3.4.5 Catalyst optimization

The catalytic decarboxylation of α-amino acids was first discovered by Dose who introduced aromatic aldehydes as catalysts that can be used to drive decarboxylation reactions.[62] In 1886, Curtis and Lederer performed decarboxylation of glycerine with benzaldehyde heated to 130 ℃ and the product was reported to be benzylamine and not the desired methylamine.[62] This was attributed to the lack of resonance stabilisation of the Schiff base.[62,65] To avoid the transamination of the Schiff base, an aryl aliphatic ketone catalyst with an electron-donating substituent at the *o*- or *p*-position of the aromatic ring is needed to produce amine in high yield.[62,65] In 1986, Hashimoto and co-workers reported the use of cyclohex-2-en-1-one (**24**) as a catalyst in a wide range of amino acid decarboxylations.[64,67] This catalyst **24** increased the amine yield drastically as compared to the thermal reaction.[65] The challenge with the cyclohex-2-en-1-one **24** catalyst was that it must be applied at high temperatures, is generally expensive, and causes acute human toxicity.[65,67] Therefore, we opted to use the cyclohex-2-en-1-one

derivative: isophorone (**27**) because it is reported to perform well under mild temperature conditions and at a low catalyst loading. Isophorone is also a cheap and industrially available material.[65] Isophorone can also be synthesized in-house by base-catalysed aldol condensation of acetone.[65] In addition to the aforementioned challenges with cyclohex-2-en-1-one (**24**), it has a boiling point of 166 ℃ and the amine **15** also has a boiling point of 160 ℃. When distilling the desired product **15** under vacuum, small traces of the catalyst cyclohex-2-en-1-one were observed in the NMR spectrum of the isolated product **15**. Comparatively, isophorone has a higher boiling point of 215 ℃ and is not distilled together with the desired amino alcohol **15**.

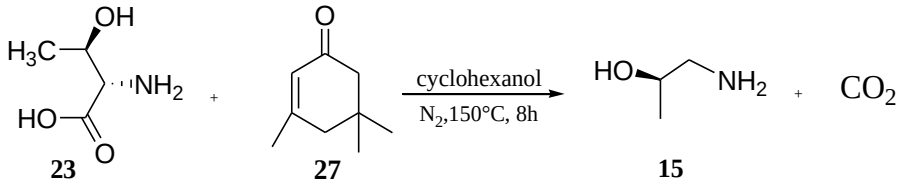

23 **27** **15**

Scheme 3.11. Improved synthesis of *R*-1-Amino-2-propanol.

L-threonine (**23**), isophorone (**27**), and cyclohexanol were charged into a reactor under a nitrogen atmosphere. The reaction was heated at 150 ℃ until gas evolution stopped (8h). The reaction was cooled down and the free amine **15** was collected *via* distillation under a vacuum. GC-MS was used to monitor the synthesis of *R*-1-amino-2-propanol (**15**) which showed that the desired product **15** was formed together with other impurities such as Schiff base (**29**) as shown in Scheme 3.12 along with the reaction solvent cyclohexanol.

29

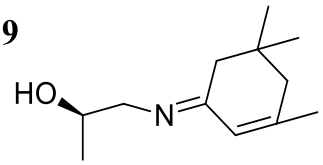

m/z: 195.16

Scheme 3.12. Schiff base by-product for Scheme 3.11.

Most of the reported methods for the decarboxylation of *L*-threonine (**23**) yield the desired product as a hydrochloride salt owing to the difficulty of removing the reaction solvent cyclohexanol.

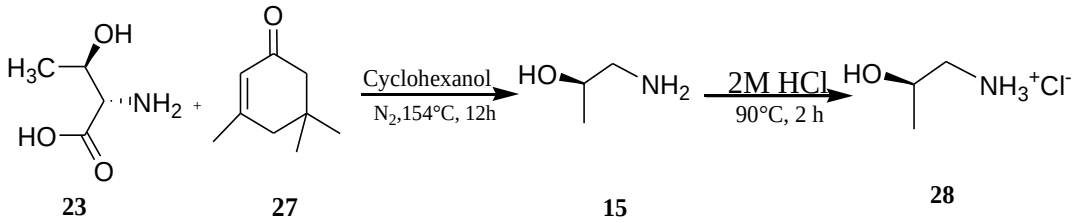

23 **27** **15** **28**

Scheme 3.13. Synthesis of amine hydrochloride salt.

Isophorone (**27**), *L*-threonine (**23**), and cyclohexanol were heated under a nitrogen atmosphere with a stirrer bar to a temperature ranging between 150–160 ℃. After 12 h, the reaction was homogenous, and the reactor was cooled to room temperature. Aqueous hydrochloric acid solution (2M) was added in a one-pot fashion and the reaction mixture was heated to 90 °C while stirring for 2 h. Thereafter, the reaction had two phases: the organic and the aqueous phase. The aqueous phase was collected and concentrated in a vacuum. The resultant hydrochloride salt was first vacuum- then freeze-dried overnight, weighed, and was analysed using NMR spectroscopy. The product **28** was obtained as a brown solid (see the image J, Figure 3.11) with a 94% yield.

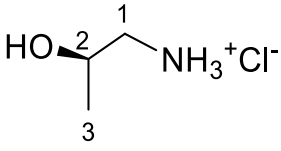

The isolated product **28** was found to be pure by ^{1}H NMR and ^{13}C NMR spectroscopy. The ^{1}H NMR spectrum shows new multiplet proton peaks resonating at δ 4.00-3.95 ppm for the C2-H proton. This multiplet signal of C2-H protons is due to the attachment of this unit (-H-C-OH-) to the adjacent methyl protons (C3-H) and methylenic protons (C1-H). The diastereotopic protons (-C1-H) resonated at different chemical shift as each proton (H_a/H_b) appeared as a doublet of a doublet at a chemical shift of δ 3.05-3.01 and δ_H 2.84-2.80 ppm. Three methyl protons C3-H appeared as a doublet at δ 1.18 ppm; this is because they are coupling with adjacent protons attached to C2 with the coupling constant of 64 Hz. The hydrochloride salt **28** was dissolved in D_2O and as such underwent deuterium exchange with both the OH and NH protons; hence, the signal peaks from the hydroxyl group and ammonium ion protons are absent. The ^{13}C NMR spectrum showed three carbon signals resonating at δ 64.2, 45.6, and 19.6 ppm. The above spectral data is in alignment with literature values.[67] Both IR and ^{13}C NMR spectrum showed the absence of the carbonyl group which further proved that the *L*-threonine (**23**) substrate had undergone decarboxylation and the amine salt **28** was successfully produced.

J

Figure 3.11. Image (J) shows the isolated amine salt from Scheme 3.13.

Amine hydrochloride salt **28** was isolated and characterized. After conducting a thorough literature survey, we could not find a practical method for the neutralization of the salt and isolation of the amine into a free base. The amine salt **28** was then treated with 3 saturated basic solution including NaOH, K_2CO_3 and $Ca(OH)_2$ each having a pH of 10 and stirred at room temperature for an hour. The free base amine was then extracted into dichloromethane 3 times. The combined organic phase was dried with Na_2SO_4, filtered, and then concentrated under vacuum to obtain **15**. The isolated product was obtained in small amounts and the chromatogram revealed the presence of a free base **15** and an unidentified by-product. The extraction of **15** with other organic solvents such as THF, 2-butanol, and ethyl acetate was attempted but was not successful. This is because amine **15** is hydrophilic;[68] hence the separation of the free base from the aqueous basic solution was laborious.

3.4.6 Solvent optimization

L-threonine (**23**) and other α-amino acids have been reported to undergo decarboxylation upon reflux in high boiling point solvents and in the presence of a ketone catalyst.[68,69] Commonly reported high boiling point solvents are cyclohexanol and tetraethylene glycol dimethyether (TEGME). The advantage of these solvents is the amine product solubility and the insolubility of *L*-threonine.[67,68] The solubility of amine products in both cyclohexanol and TEGME allows for the visual indication of reaction completion.[67] Initially, TEGME was used as a solvent in the reaction (Scheme 3.9); the issue with this solvent was that a rise in impurities was observed with its use. The impurity profile of the distilled products indicated the presence of Schiff base (**26**), dimer (**25**), and traces of reaction solvent (TEGME). The assumption is that the TEGME promotes the formation of the dimer. The reaction solvent was then replaced with cyclohexanol instead. The main issue with cyclohexanol as the reaction solvent was that it has the same boiling point as the desired product (R)-1-aminopropan-2-ol (**15**) at 160 °C. The chromatogram

of the distilled product showed presence of impurities such as Schiff base adduct and cyclohexanol. In addition, removal of the high boiling point solvent and purification was a challenge. Nonetheless, the amine product dissolved in the cyclohexanol and was subsequently isolated as amine hydrochloride salt in high yield (see Figure.3.11, image J). Separation of the amine **15** as a free base remained a challenge. This is because (R)-1-aminopropan-2-ol is hydrophilic[68] and as such, extraction of the free base from the aqueous solution was laborious and resulted in low yields of the product **15**. Consequently, an inert high boiling point solvent 1,3-dimethyl-3,4,5,6-tetrahydro-2(1*H*)-pyrimidinone (DMPU) was used as the reaction solvent. The reaction solvent DMPU and ketone catalyst isophorone (**27**) were used to develop the scalable method for the decarboxylation of **23** because the difference in boiling point between DMPU and isophorone mixture was 240 °C. The boiling point of the desired product **15** is 160 °C; therefore, this reaction allowed for simple distillation of (R)-1-aminopropan-2-ol (**15**) under vacuum.[69]

3.4.7 Optimized method

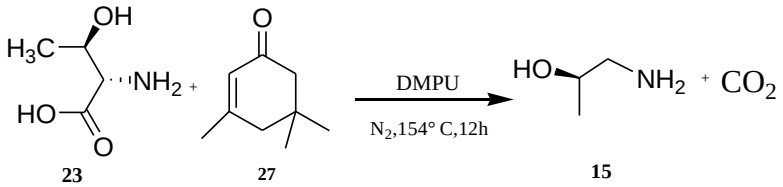

23 **27** **15**

Scheme 3.14. Improved and optimized method for synthesis of *R*-1-amino-2-propanol.

L-threonine (**23**), 1,3-dimethyl-3,4,5,6-tetrahydro-2(1*H*)-pyrimidinone (DMPU), and a catalytic amount of isophorone (**27**) were charged into a flask. The flask was heated to 154 °C under a nitrogen atmosphere. The starting material **23** was fully consumed after 12 h. The desired product **15** was collected *via* distillation from the reaction mixture to give a yield of 66% of *R*-1-amino-2-propanol as a thick clear oil. The isolated product was analysed by GC-MS and NMR spectroscopy. The NMR spectra of the distilled product is in agreement with the literature.[68] However, it also had an impurity peak observed with a chemical shift of δ 2.80 ppm (see appendix-plate 7a). These small traces of impurities observed in the NMR spectra of the isolated product were confirmed to be DMPU using GC-MS and was observed in the chromatogram with m/z of 128.

The isolated (R)-1-aminopropan-2-ol (**15**) was then condensed with EADI (**20)** following the optimized and newly developed route to produce the chiral HPI (Scheme 3.3) and HPA (Scheme 3.6); impurities were neither observed in the TLC nor in the NMR spectra.

As mentioned above, the synthesized chiral amine **15** had negligible traces of DMPU which did not affect the synthesis of the chiral HPI (**17**) since no side reactions or impurities were observed on a bench scale. This was done to fulfil the objectives of the MSc project: developing and optimizing an industrially feasible method for the first four steps in the production of the adenine core (HPA, **6**) using M4ALL technology from Scheme 2.2.

3.5 CONCLUSION

In conclusion, a new and improved practical 4-step sequence for the synthesis of HPA (a tenofovir intermediate) was developed. The new route starts with the reaction of diaminomaleonitrile (**12**) and triethyl orthoformate (**13**) in toluene at 40 ℃ containing catalytic TFA to give EADI (**20**) with 90% yield. To further process development we used the available racemic amino-2-propanol **15** and added it with imidate **20** in acetonitrile at 25 ℃, followed by the addition of basic media barium hydroxide (0.5 equiv.) at 0 ℃ to induce cyclization of the unstable **16**. To minimize side reactions such as the hydrolysis of the nitrile substituent of HPI that generates impurities like the AICA (**22**), the HPI **17** suspension was treated with aqueous HCl solution and delivered HPI with 80% yield. HPI was further condensed with FAA that was added portion-wise in DMF at 110 ℃ to generate HPA with 85% yield.

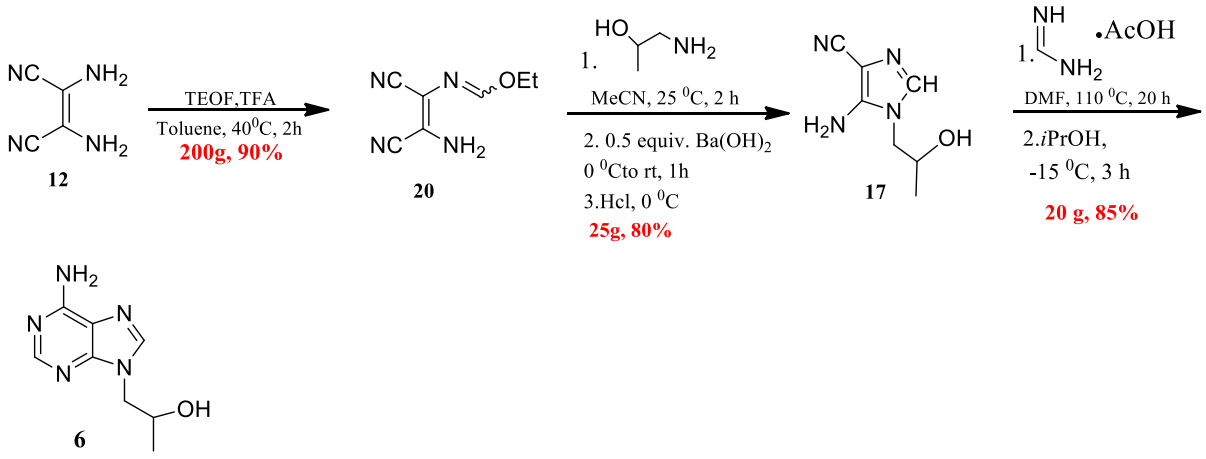

Scheme 3.15. Optimized and cost-effective process for industrial manufacturing of Tenofovir intermediates.

Part of the process development for the commercial manufacturing of tenofovir intermediate was evaluating the cost of goods or materials that are used in the synthesis of the key intermediates. The published method in Scheme 2.2 used chiral (R)-1-aminopropan-2-ol **15** which is very expensive. As part of decreasing the overall cost for tenofovir production,

improved key intermediate free base **15** processes were developed, circumventing the need to purchase the free amine base **15** from an external chemical company. *L*-threonine (**23**) was decarboxylated in DMPU in catalytic isophorone (**27**) at 154 ℃ under a nitrogen atmosphere to generate the chiral (R)-1-aminopropan-2-ol (**15)** with 66% yield. The synthesized free amine base **15** was then used to synthesize the chiral HPI (**17**) and HPA (**6**) on a small scale.

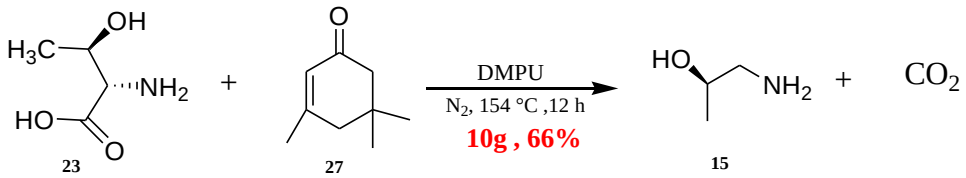

Scheme 3.16. Optimized process for the synthesis of (R)-1-aminopropan-2-ol.

The development phase of the developed routes assessed safety, the environment, economics, and throughput. With regards to safety, a route that was safe to scale up to the pilot plant was developed and as such the solvents used had to be safe for the workers to use and the environment. This is the reason hexane and dichloromethane were removed from the synthetic route developed. The incumbent two-solvent system was successfully changed to a one-solvent system which helped minimise the amount of waste produced. Control measures were put in place to minimize side reactions that generate impurities for the developed route including temperature control, reaction period, amount of TFA catalyst used, and the addition of aqueous HCl after the cyclization of **16**.

3.6 FUTURE WORK

Future work for this project will focus on reducing the number of steps and increasing the efficiency of work-up in the developed route. This can potentially be done by telescoping steps 1 and 2 to synthesize aminoimidazole derivative **17** from diaminomaleonitrile **12** in a one-pot synthesis within a short period at lower temperatures delivering high yield. Furthermore, reacting diaminomaleonitrile **12** with trimethyl orthoformate **13** in an aprotic solvent such as acetonitrile at room temperature with diluted (MeCN) catalytic TFA to generate methyl *N*(2-amino-1,2-dicyanovinyl) formimidate **13** (Scheme 3.17) is potentially an option.

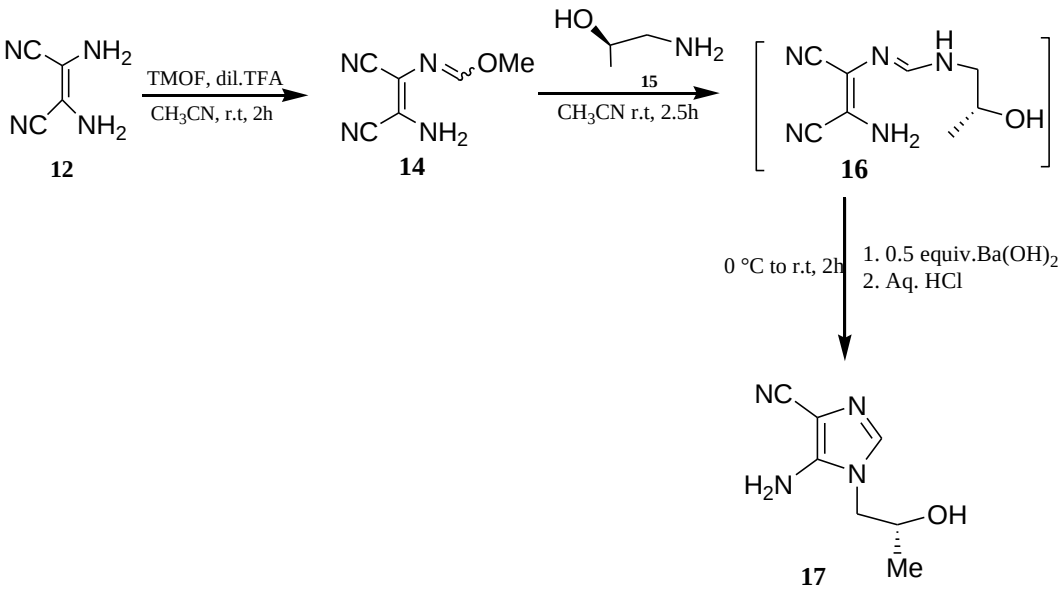

Scheme 3.17. One-pot synthesis of HPI 17.

Since both DAMN (**12**) and imidate (**14**) are decomposed easily under high temperatures, the first step of the reaction was done at room temperature rather than the published 40 °C. Instead of isolating the imidate (**14**), amidination reaction by addition of the free base (**15**) can be carried out to achieve the amino-alcohol intermediate **16** which is then subjected to a cyclization reaction in the presence of $Ba(OH)_2$ to afford **17**. This can then be isolated by filtration. The telescoped reaction was attempted at a small scale and different parameters were investigated, including selection of a suitable solvent, reaction temperature, and a reaction period. In attempts, **17** was produced as determined through TLC, see (figure 3.12) and GC-MS. The optimised process can then be applied onto the telescoped routes with observation and reporting of the results.

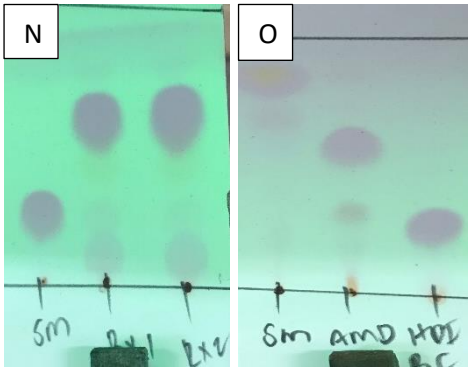

Figure 3.12. Telescoped reaction of step 1 and 2. TLC plate (N) shows synthesis of MADI in MeCN at room temperature after stirring for 1 h and 2 h. TLC plate (O) shows carry over of the imidate **14** to amidination reaction and cyclization reaction to generate HPI **17.**

There is, in addition, a need to develop a one-solvent system for the synthesis of HPA **6**. This is important because solvents are the largest source of waste in API manufacturing and thus there is a need to reduce the number of solvents used in the industrial process. In step 3 in the synthesis of HPA, DMF is used as a reaction solvent and isopropanol is used as an insolvent to help precipitate the off-white solid **6**.

Future work will also include conducting a study to quantify and characterize all the unknown impurities that form in the developed route since API manufacturers follow SAHPRA guidelines for purity, which must be updated. There is also a need to conduct a chemical stability and degradation study for each intermediate and assess possible side reactions that could occur in the developed route, including non-selective reactions that produce unwanted impurities. Furthermore, there is a need to do an HPLC on chiral column to further characterize the synthesized chiral HPI and HPA.

In step 4, the synthesis of (R)-1-aminopropan-2-ol **15**, currently generates a 66% yield of key intermediate **15** by distillation. There is a need to find an efficient method or technology to recover free base amine from the 94% amine salt since the current existing methods have not succeeded.

CHAPTER 4: EXPERIMENTAL PROCEDURES

4.1 General Information Details

All employed chemicals were obtained from commercials such as Sigma-Aldrich or Merck and were used without purification. Other solvents such as toluene, acetone, and deionized water were obtained from the CPT plant.

Thin layer chromatography was run on aluminum-backed Macherey-Nagel sheets Alugram XTRA SIL G/UV245 plates pre-coated with 0.20mm silica gel and details of the eluent are detailed in each procedure. TLC plates were analyzed under UV light (245nm) or by dipping them into $KMnO_4$ or iodine solution. Isolation of impurities by column chromatography was achieved by using Sigma-Aldrich silica (230-400 mesh) as the adsorbent. Hexane was used to pack silica with compound and mixtures of dichloromethane and ethyl acetate were used as the mobile phase.

The synthesized compounds were characterized and identified using infrared spectroscopy (IR), nuclear magnetic resonance (NMR) spectroscopy, and mass spectroscopy. IR spectrum was recorded on Agilent technologies Cary630 FT-IR spectrometer and all data were reported in wavenumber. NMR spectra were recorded at 25℃ (room temperature) on Bruker DRX 400 spectrometer (^{1}H-NMR: 400.13 MHz and ^{13}C-NMR: 100.63 MHz) or the Bruker Ultrashiled 500 Plus spectrometer at (^{1}H-NMR: 500.132 and ^{13}C-NMR: 125.757). The chemical shift was recorded in parts per million (ppm) and spin-spin coupling (*J*) in Herts (Hz). The ^{1}H and ^{13}C chemical shift for residual solvents peaks reference are δ_H 2.50, δ_C 39.52 for DMSO-d_6, δ_H 7.26 δ_C 77.0 for $CDCl_3$, and δ_H 4.79 D_2O.[60] The reported multiplicities of ^{1}H-NMR spectra was abbreviated as follows s (singlet), bs (broad singlet), d (doublet), t (triplet), q (quarter), m (mutliplet), dd (doublet of doublets).1D NMR (^{1}H, ^{13}C, and DEPT-135) and 2D NMR (COSY, HSQC, and HMBC) spectra were applied where necessary.

Reaction intermediates were monitored via GC-MS and HPLC using the published method.[42] GC used an Agilent HP-5MS ultra inert (30m x 250µm x 0.25 µm) column. Coupled to MS Agilent 5977B. The oven was maintained at 200 ℃ and the inlet at 225 for 20 min. A Split ratio (50:1) was used and the flowrate was 0.8ml/min with helium as the carrier gas.
High-pressure liquid chromatography (HPLC) was performed on a HITACHI using a Kinetex Evo C18 100 Å 150 x 4.6 mm column, at flow rates of 1.0 ml/min. A mixture of methanol:

Buffer (85%) was used as the mobile phase. The Eluted compounds were detected using a Diode Array detector. Data was interpreted with Chromster software.

Melting points were uncorrected and were taken using a digital melting point apparatus.

The high-resolution mass spectra (HRMS) were recorded using electrospray ionization in the positive or negative mode on a Waters UPLC Synapt G2 mass spectrometer.

4.2 General Experimental Procedures

4.2.1 Synthesis of Methyl *N*-(2-amino-1,2-dicyanovinyl) formimidate (MADI), 14

According to the method from Derstine *et al.*[42]: A 100 ml three-neck round bottom flask was charged with 2,3-diaminomaleonitrile (DAMN) (4.003g, 1.0 equiv.) and methanol (20ml). The reaction mixture was stirred for 5 min at room temperature (25 ℃). Trimethyl orthoformate (TMOF) (4.86ml, 1.2 equiv.) was charged to the reaction mixture in one portion. Followed by addition of trifluoracetic acid (TFA) (0.023g, 0.003 equiv.). The reaction was heated to an internal temperature of 40 ℃ and stirred for 2 h. After consumption of the starting material as determined by TLC (3:7 ethyl acetate: chloroform) and GC-MS, hexane (120 ml) was charged into the reaction. The reaction mixture was cooled down to 25 ℃ (room temperature) over 30 min. Then cooled to an internal temperature of 0 ℃ for an additional hour. The solids were isolated through vacuum filtration and dried under vacuum to afford a pale-yellow solid of **14** in 80% overall yield (4.402g).

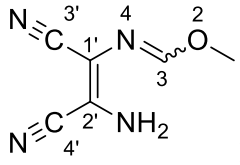

MP. =138.9-140 ^{0}C.

^{1}H NMR (400 MHz, DMSO) δ 7.99 (s, 1H, H-3); 7.04 (bs,2H, NH_2); 3.83 (s, 3H, OCH_3).

^{13}C NMR (101 MHz, DMSO) δ 157.3 (C=N, C-3); 123.5 (C=, C-2'); 115.3 (CN, C-3'); 115.1 (CN, C-4'); 98.7 (C=, C-1'); 55.1 (O<u>C</u>H_3, C-1).

IR (neat) ν_{max} 3406, 3354, 2236, 2195, 1633, 1603, 1368, 1271, 910 cm^{-1}.

HRMS-ESI m/z calculated for $C_6H_7N_4O$ $[M+H]^+$ 151.0614, found 151.08.

4.2.2 Synthesis of Ethyl *N*(2-amino-1,2-dicyanovinyl) formimidate (EADI), 20

A 2-L Reactor-ready fitted with an overhead stirrer and thermocouple was charged with 2,3-diaminomaleonitrile (DAMN) (100g, 1.0 equiv.) and toluene (400 ml). The mixture was stirred for 5 min at room temperature. Triethyl orthoformate (TEOF) (169.4 ml, 1.1 equiv.) was charged to the reaction mixture in one portion. Then added trifluoracetic acid (TFA) (0.21ml, 0.003 equiv.) into your reaction mixture in one portion. The reaction was heated to an internal temperature of 40 ℃ and stirred for 2 h. After consumption of the starting material as determined by TLC (3:7 ethyl acetate: chloroform eluent) and GC-MS, the reaction mixture was cooled down to room temperature over approximately 30 minutes. Then cooled to an internal temperature of 0 ℃ for an additional hour. The solids were isolated by vacuum filtration and dried under vacuum to afford a brown solid of **20** in a 90% yield (136g).

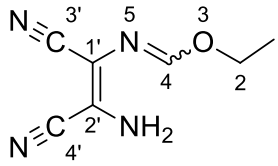

M.p = 133.9 – 135.2 ^{0}C [lit.[52], 135-137 ^{0}C]

^{1}H NMR (400 MHz, DMSO): δ 7.95 (s, 1H, CH), 7.00 (s, 2H, NH_2), 4.31-4.23 (q, 2H, *J*= 7.0 Hz, CH_2), 1.29-1.24 (t, 3H, *J*=7.1 Hz, CH_3).

^{13}C NMR (126 MHz, DMSO) δ 157.0 (C=N, C-4); 123.4 (C=, C-2'); 115.2 (CN, C-3'); 115.2 (CN, C-4'); 99.0 (C=, C-1'); 63.8 (CH_2, C-2); 14.5 (CH_3).

IR (neat) ν_{max} 3414, 3302, 3168, 2982, 2244, 2207, 1636, 1606,1472, 1379, 1256 ,954 cm^{-1}.

HRMS-ESI m/z calculated for $C_7H_8N_4O$ $[M+H]^+$ 165.0692, found 165.10.

4.2.3 Synthesis of 5-amino-1-(2-hydroxypropyl)-1H-imidazole-4-carbonitrile (HPI), 17

Into a 500 ml three-neck round bottom flask fitted with a stirrer, condenser, and thermometer. Racemic aminopropan-2-ol, (**15**) (13.33 ml, 171 mmol, 1.4 equiv.) was charged into the flask with MeCN (30 ml). The solution was stirred for 5 min at room temperature. EADI (**20**) (20g, 122mmol) was added into the reaction mixture with 130 ml of MeCN. The reaction was stirred at rt (25 ^{0}C) for 2.5 h. Consumption of the starting material was monitored by TLC. After stirring for 2 h and 30 min, TLC analysis with EtOAc: chloroform: MeOH (5:3:2) eluent shows that the starting material (EADI) was fully consumed. The reaction mixture temperature was lowered to cooler conditions (5 ℃) using an ice bath. Solid $Ba(OH)_2$ monohydrate (11.52 g, 0.5 equiv.) was charged with 35 ml of deionised water. The reaction was warmed up to rt and left to stir for 1 h and 15 min. Conversion to racemic HPI (**17**), was monitored with TLC and GC-MS, after complete cyclization of the amino-alcohol intermediate **16** the reaction temperature was lowered to 5 ℃. The reaction mixture pH was adjusted with 13.9 ml of 32%

HCl aqueous solution added dropwise, and the pH was maintained at 9.60. The reaction was stirred at cooler conditions (5 ℃) for 30 minutes. The insoluble salt $BaCl_2$ was removed by vacuum filtration using Büchner funnel with celite and the flask was rinsed with MeCN. The reaction mixture was concentrated *in vacuo* at 40 ℃. The rotavapor temperature was raised to 50 ^{0}C to remove water completely from the reaction mixture. The residue was dissolved in 150 ml of acetone and stirred at cooler conditions (10 ℃) for 40 min. The solid precipitate was removed through vacuum filtration and rinsed with cold acetone (30 ml). Then distilled off acetone using the rotavapor at 40 ^{0}C, 350 mbar. The rotavapor temperature was further increased to 50-60 ^{0}C for an entire hour to remove acetone completely. The crude product (27.1 g) was dissolved in warm water (50 ml, max 40 ℃) and transferred into a julabo flask. The flask temperature was raised to 40 ^{0}C for 20 minutes and gradually cooled down to rt then to colder conditions (3-5 ℃) for an additional hour. Upon cooling, a precipitate was observed, and the suspension was filtered using the Büchner funnel and washed with cold water (2 ℃) to afford HPI (**17**) as an off-white solid. The precipitate was dried under vacuum 30 ℃ to yield 16.69 g (82%).

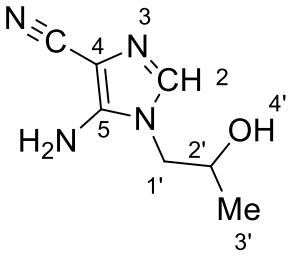

M.P =141.6-142.3 ^{0}C.

^{1}H NMR (500 MHz, DMSO) δ 7.12 (s, 1H, C2-H); 6.06 (s,2H, NH_2); 5.08- 5.07 (d,1H, *J* =4.8 Hz, OH); 3.84-3.82 (m, 1H, C2'-H);3.80-3.77 (dd,1H, *J* =14.4, 3.0 Hz, C1'-H_a) 3.65-3.61 (dd,1H, J=14.3, 7.8 Hz, C1'-H_b); 1.06-1.05 (d, 3H, *J*=6.2 Hz, CH_3) ppm.

^{13}C NMR (126 MHz, DMSO) δ 148.4 (C=C, C5); 134.0 (C=N, C2); 118.1 (CN), 90.7 (C=C, C4); 65.4 (CH, C2'); 50.6 (CH_2, C1'); 21.1 (CH_3, C3') ppm.

IR (neat) ν_{max} 3280, 3161, 2207, 1625, 1573, 1525, 950, 705 cm^{-1}.

HRMS-ESI m/z calculated for $C_7H_{10}N_4O$ $[M+H]^+$ 167.0932, found 167.11.

4.2.4 Synthesis of 5-amino-1-(2-hydroxypropyl)-1-H-imidazole-4-carboxamide (AICA), 22

A 100 ml two-neck flask fitted with a reflux condenser, thermometer, and stirrer bar was immersed into water bath. The flask was charged with HPI (**17**) (5.00g), 4ml of 25% NaOH and ethanol (15 ml). The reaction was heated to 76 ℃ and refluxed for 2 h while stirring. The reaction was monitored with TLC analysis with eluent system: EtOAc: chloroform: MeOH

(5:3:2). After refluxing and stirring for 2 h at 76 ℃, the full conversion of **17** into **22** was observed by TLC. The reaction was cooled down to room temperature with an ice bath. The reaction mixture was neutralized to pH 7 using a 32% aqueous HCl solution. After neutralization, the reaction mixture was concentrated *in vacuo* at 50 ℃ to half of the original volume. The residue was immersed in an ice bath and stirred at cooler conditions (<10 ℃) until solid product precipitated. The milky slurry suspension was filtered and washed with cold water: ethanol (1:1). The precipitate yielded a white crystalline solid (2.84 g, 51%) and was fully characterized with TLC, HRMS, IR, ^{1}H NMR, and ^{13}C NMR spectrum analysis.

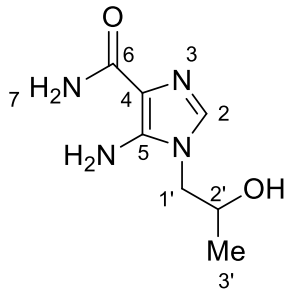

M.P =209.2-210.3 ^{0}C

^{1}H NMR (400 MHz, DMSO) δ 7.05 (s, 1H, C2-H); 6.77 (bs, 1H,H-7); 6.63 (bs,1H,H-7); 5.70 (bs, 2H, NH_2); 5.12-5.11 (d, 1H, *J*=4.8 Hz, OH); 3.90-3.84 (m, 1H, C2'-H); 3.81-3.77 (dd,1H, J = 14.3, 3.5 Hz, CH_2); 3.66-3.60 (dd, 1H, J = 14.3, 7.5 Hz,CH_2); 1.06-1.05 (d, 3H, J =6.2 Hz, CH_3) ppm.

^{13}C NMR (126 MHz, DMSO) δ 167.3 (C=O, C6); 143.7 (C=C, C5); 131.1 (C=N, C2); 112.9 (C=C, C4); 65.7 (CH, C2'), 50.3 (CH_2, C1'); 21.2 (CH_3, C3') ppm.

IR (neat) ν_{max} 3317, 3187, 3094, 1606, 1554, 1066 cm^{-1}.

HRMS-ESI m/z calculated for $C_7H_{12}N_4O_2$ $[M+H]^+$ 185.1032, found 185.12.

4.2.5 Synthesis of 9-[(RS)-2-hydroxy propyl] adenine (HPA), 6

A 250 ml three-neck bottom flask equipped with a thermometer, stirrer bar, and condenser; the flask was immersed in an oil bath. The previously synthesized 5-amino-1-(2-hydroxypropyl)-1*H*-imidazole-4-carbonitrile (**17**) (10g, 60.2 mmol, 1.0 equiv.), formamidinium acetate (8.77g, 84.24 mmol, 1.4 equiv.) and DMF (20 ml) were charged into the flask. The mixture was stirred for 5 min at room temperature then the temperature was raised to 110 ℃ using the hotplate, with the internal temperature maintained at 100 ℃. The reaction was stirred at 100 ℃ for 4 hours. After heating and stirring for 4 hours, the second portion of FAA (2.506g, 24 mmol, 0.4 equiv.) was added to the reaction mixture. The reaction was stirred overnight (18 h) at 100 ℃. The reaction progress was monitored with TLC and HPLC every 4 hours. Once the starting material **17** was consumed the reaction mixture was concentrated *in vacuo* at 50 ℃ to half the original volume. The reaction mixture was transferred into julabo flask and heated to 80 ^{0}C.

Isopropanol (60 ml) was added into the reaction mixture, and the reaction temperature was gradually decreased to rt. The reaction mixture was further cooled down to -15 ^{0}C for 3 h while stirring. As the reaction cools down, we start seeing a precipitate form at the bottom of the flask. The suspension was filtered through a Büchner funnel and was washed with cold isopropanol (30 ml, -15 ℃). The off-white solid was dried *in vacuo* at 65℃ for an hour to afford an off-white solid **6** 9.91g (85%) with 94% purity by HPLC.

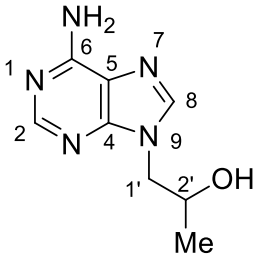

M.P=191.5 -193.4 ^{0}C

^{1}H NMR (500 MHz, DMSO) δ 8.14 (s,1H, C2-H); 8.05 (s, 1H, C8-H); 7.18 (s, 2H, NH_2); 5.03 (bs, 1H, OH); 4.13- 4.08 (m,1H, CH); 4.02- 3.98 (m, 2H, CH_2); 1.07-1.06 (d, 3H, *J* =5.8 Hz, CH_3) ppm.

^{13}C NMR (126 MHz, DMSO) δ 156.4 (C=N, C6); 152.7 (C=N, C2); 150.2 (C=C, C4); 141.9 (C=N, C8); 119.0 (C=C, C5); 65.1 (CH, C2'); 50.6 (CH_2, C1'); 21.3 (CH_3, C3') ppm.

HRMS-ESI m/z calculated for $C_8H_{11}N_5OH$ $[M+H]^+$ 194.1042, found 194.13.

4.2.6 Synthesis of (R)-1-aminopropan-2-ol, 15

A 100 ml three-neck round bottom flask was fitted with a reflux condenser, nitrogen inlet, thermometer, and stirrer bar. L-threonine (5g, 1 equiv.), 1,3-dimethyl-3,4,5,6-tetrahydro-2(1*H*)-pyrimidinone (DMPU) (20 ml) and Isophorone (0.31 ml, 0.05 equiv.) were charged into the reaction flask under nitrogen atmosphere. The reaction flask was heated from room temperature to 154^{o}C. The reaction mixture was heated under N_2 atmosphere with stirring and the reaction temperature was maintained between 150 °C and 160 ^{0}C for the duration of the reaction. After stirring and heating for 12h, the reaction mixture was a homogenous solution. A change in colour was observed as the reaction progresses from slurry mixture to clear red-brown solution. The homogenous solution was cooled down to rt and the amine product was distilled from the reaction mixture *in vacuo* at 80 ℃ to afford 2.1 g (66%) of (R*)*-1-amino-2-propanol **15** as a thick clear oil.

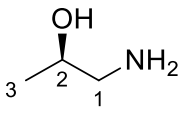

^{1}H NMR (500 MHz, D_2O) δ 3.80-3.67 (m, 1H, -C<u>H</u>-O); 2.59-2.56 (dd, *J* = 13.2, 4.5 Hz, 1H, -C<u>H</u>$_2$-); 2.53-2.49 (dd, *J* = 13.2, 7.1Hz, 1H, -C<u>H</u>$_2$-); 1.25 (d, *J* = 6.4 Hz, 3H, C<u>H</u>$_3$) ppm.

^{13}C NMR (126 MHz, D_2O) δ 68.7 (CH, C2); 45.6(CH_2, C1); 19.4 (CH_3, C3) ppm.

APPENDICES

Appendix 1. Copies of NMR Spectra

Plate 1a. ^{1}H NMR spectrum of Methyl *N*-(2-amino-1,2-dicyanovinyl) formimidate (**14**) in DMSO-*d*6

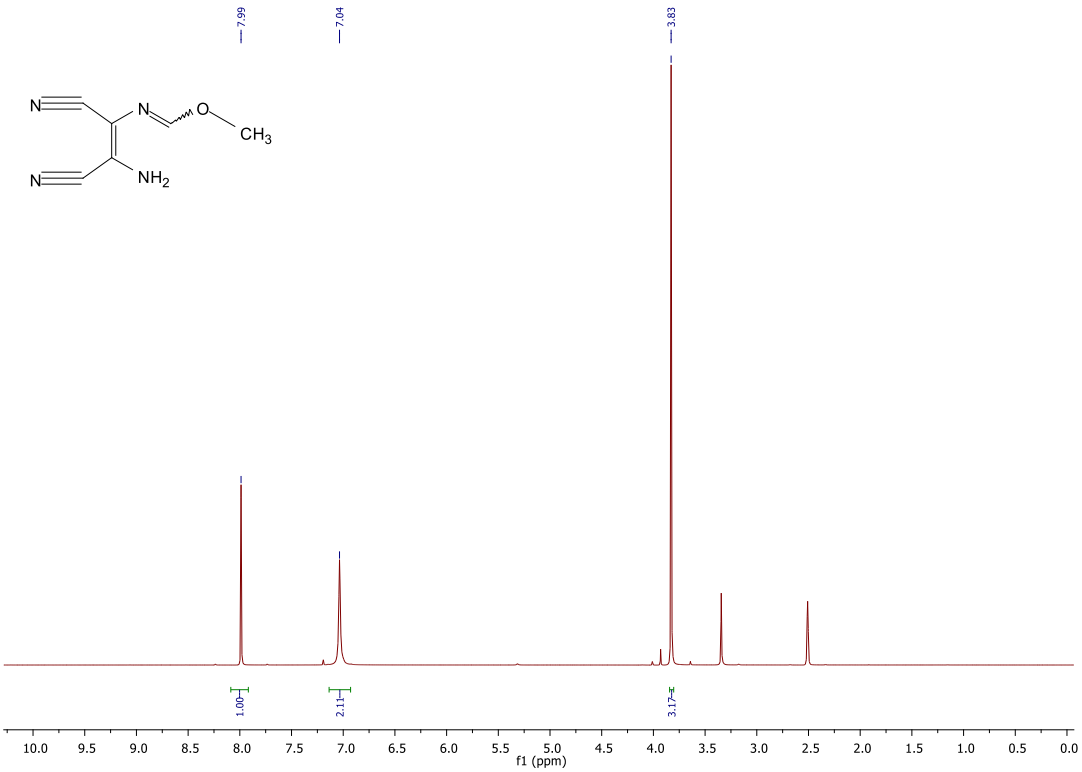

Plate 1b. ^{13}C NMR spectrum of Methyl *N*-(2-amino-1,2-dicyanovinyl) formimidate (**14**) in DMSO-*d*6

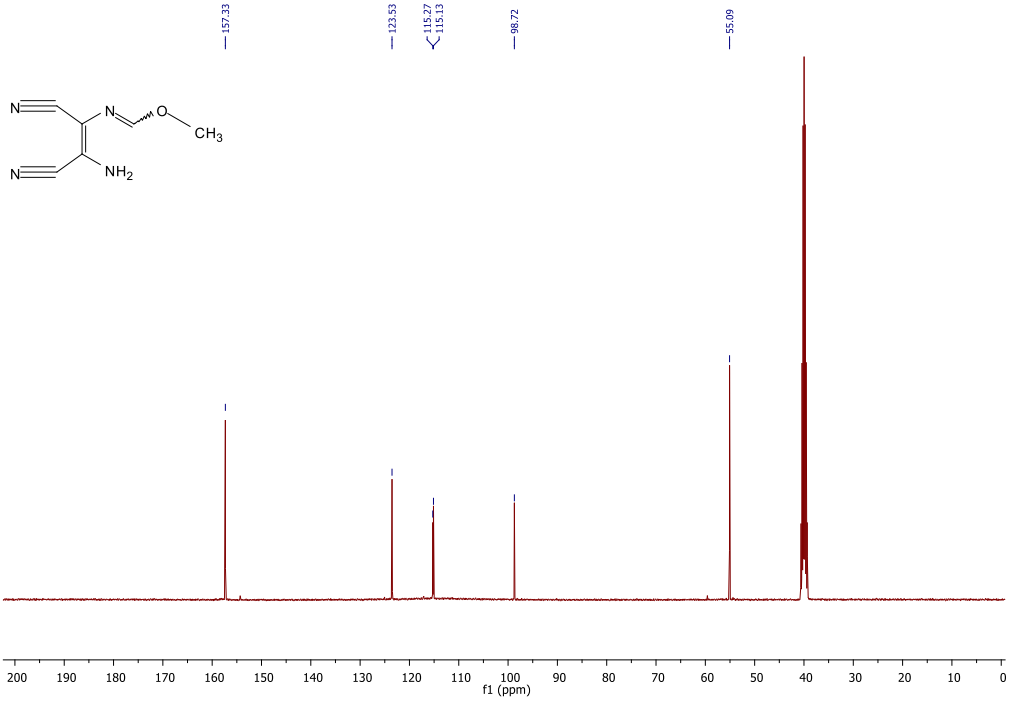

Plate 2a. ^{1}H NMR spectrum of Ethyl *N*-(2-amino-1,2-dicyanovinyl) formimidate (**20**) in DMSO-*d*6

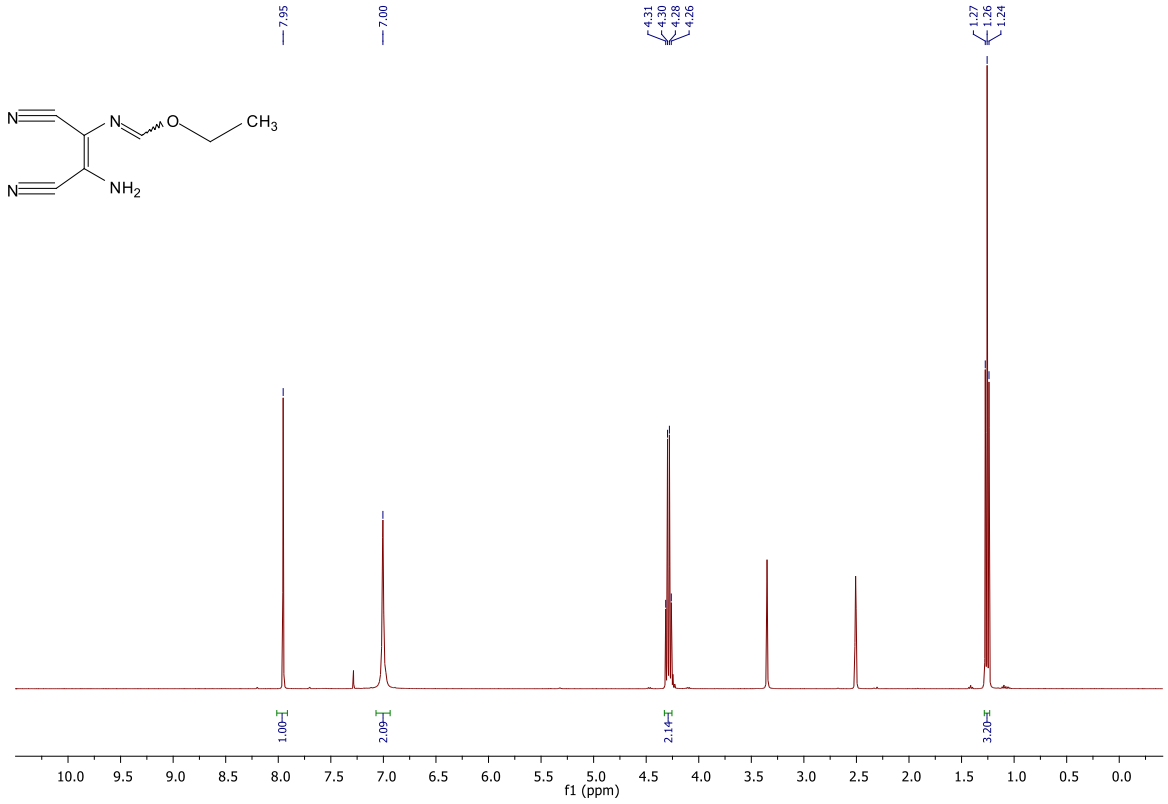

Plate 2b. ^{13}C NMR spectrum of Ethyl *N(*2-amino-1,2-dicyanovinyl) formimidate (**20**) in DMSO-*d*6

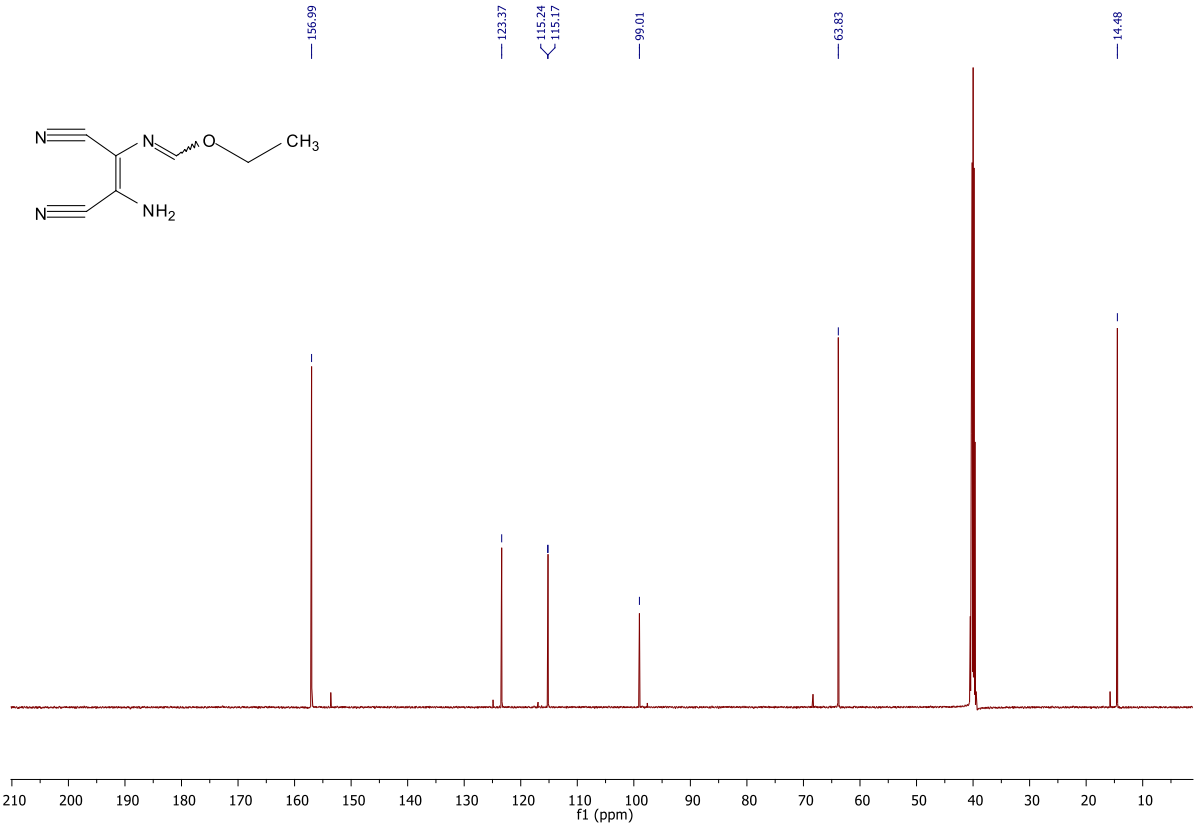

Plate 2c. DEPT 135 spectrum of Ethyl *N*(2-amino-1,2-dicyanovinyl) formimidate (**20**) in DMSO-*d*6

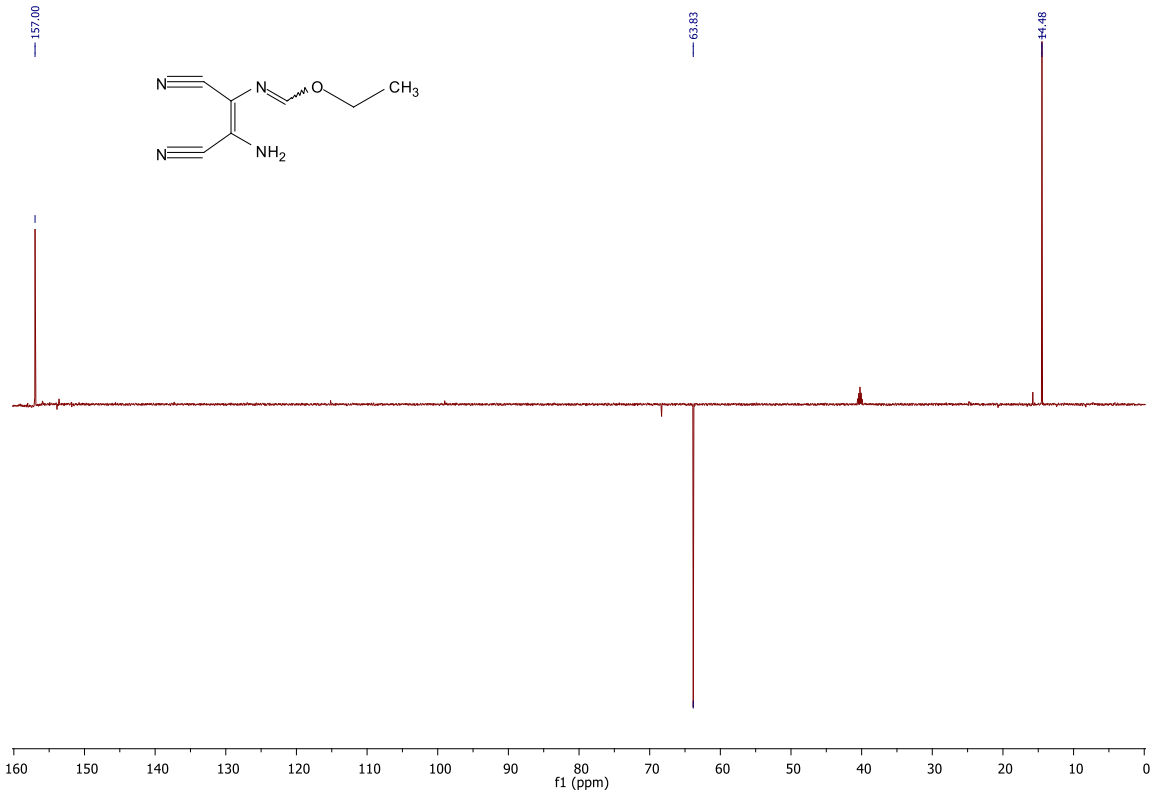

Plate 3a. ^{1}H NMR spectrum of Amino-1-(2-hydroxypropyl)-1*H*-imidazole-4-carbonitrile (**17**) in DMSO-*d*6

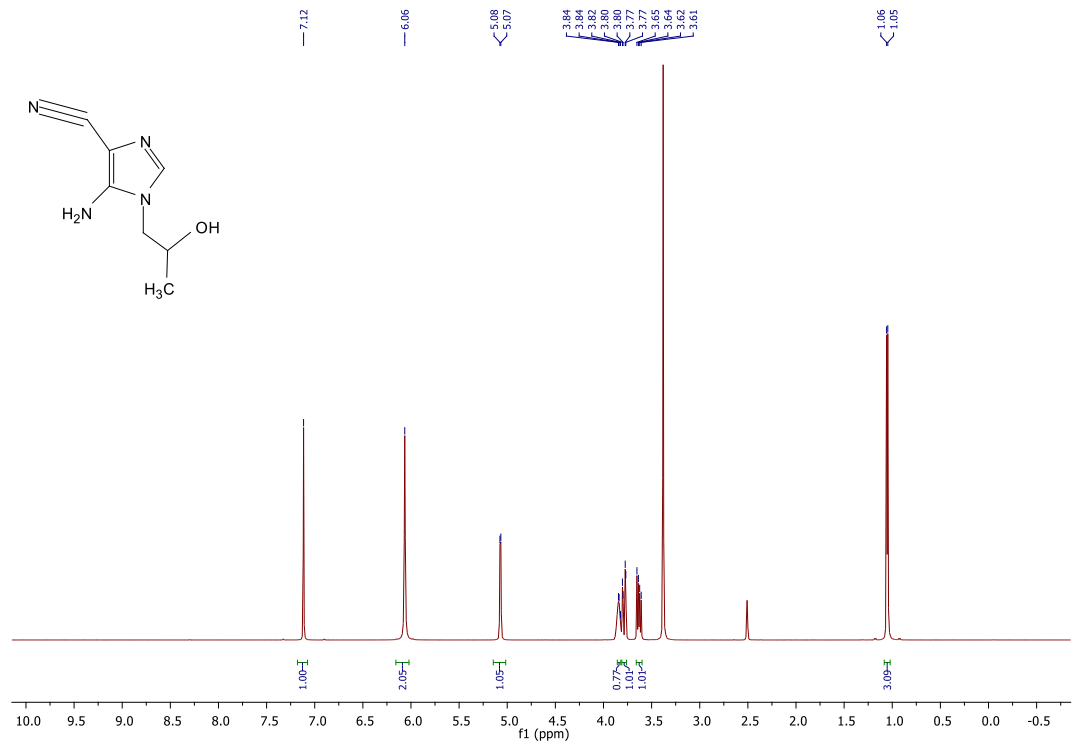

Plate 3b. ^{13}C NMR spectrum of Amino-1-(2-hydroxypropyl)-1*H*-imidazole-4-carbonitrile (**17**) in DMSO-*d*6

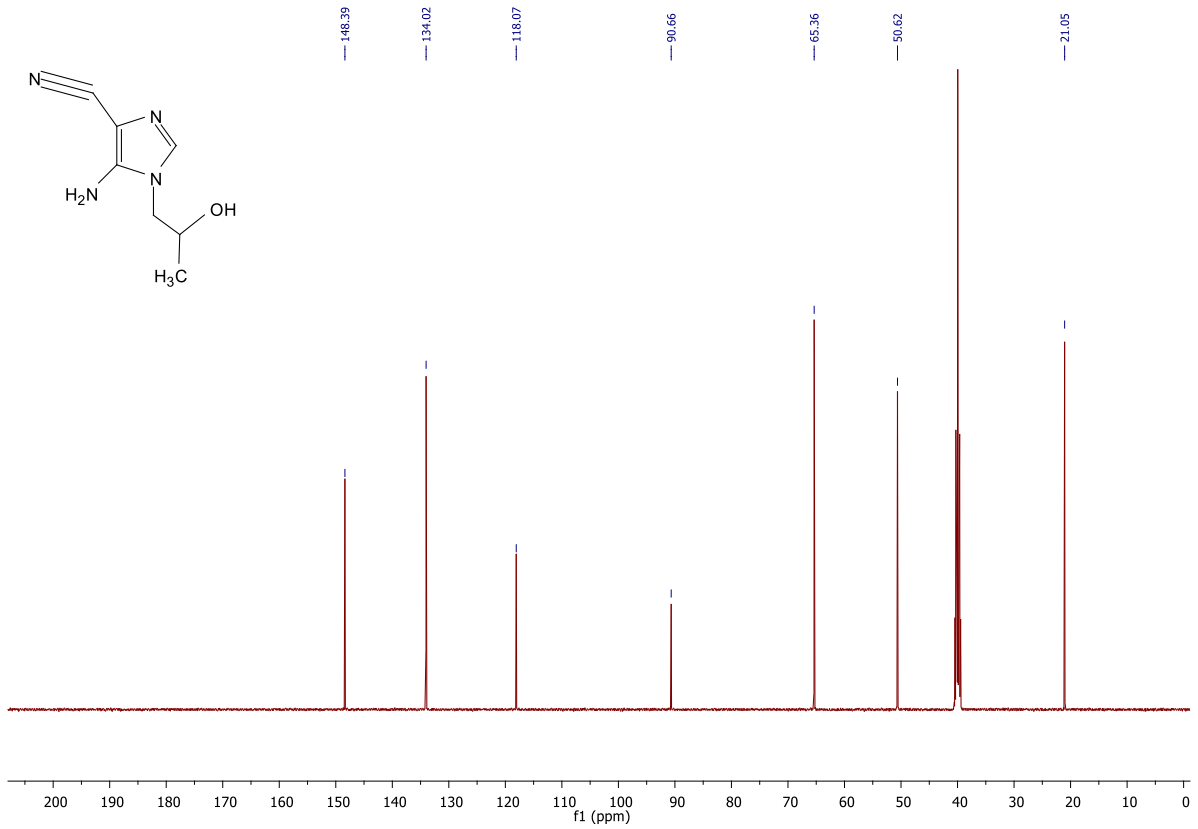

Plate 3c. HMBC (^{1}H-^{13}C correlations) of Amino-1-(2-hydroxypropyl)-1*H*-imidazole-4-carbonitrile (**17**) in DMSO-*d*6

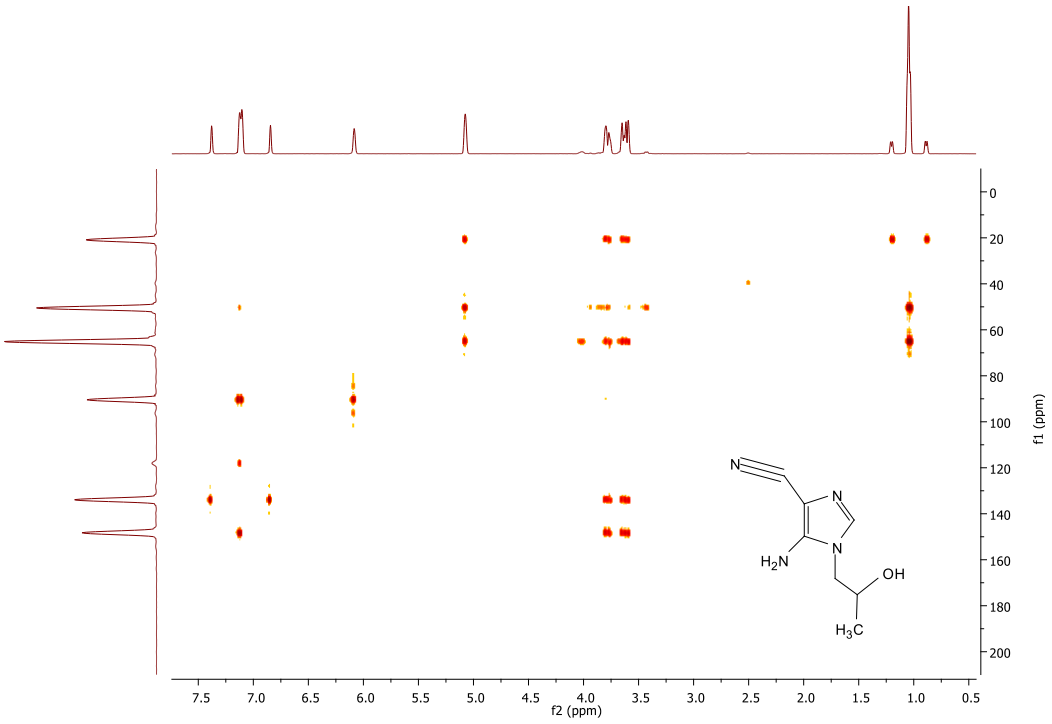

Plate 3d. COSY (^{1}H-^{1}H coupling) of Amino-1-(2-hydroxypropyl)-1*H*-imidazole-4-carbonitrile (**17**) in DMSO-*d*6

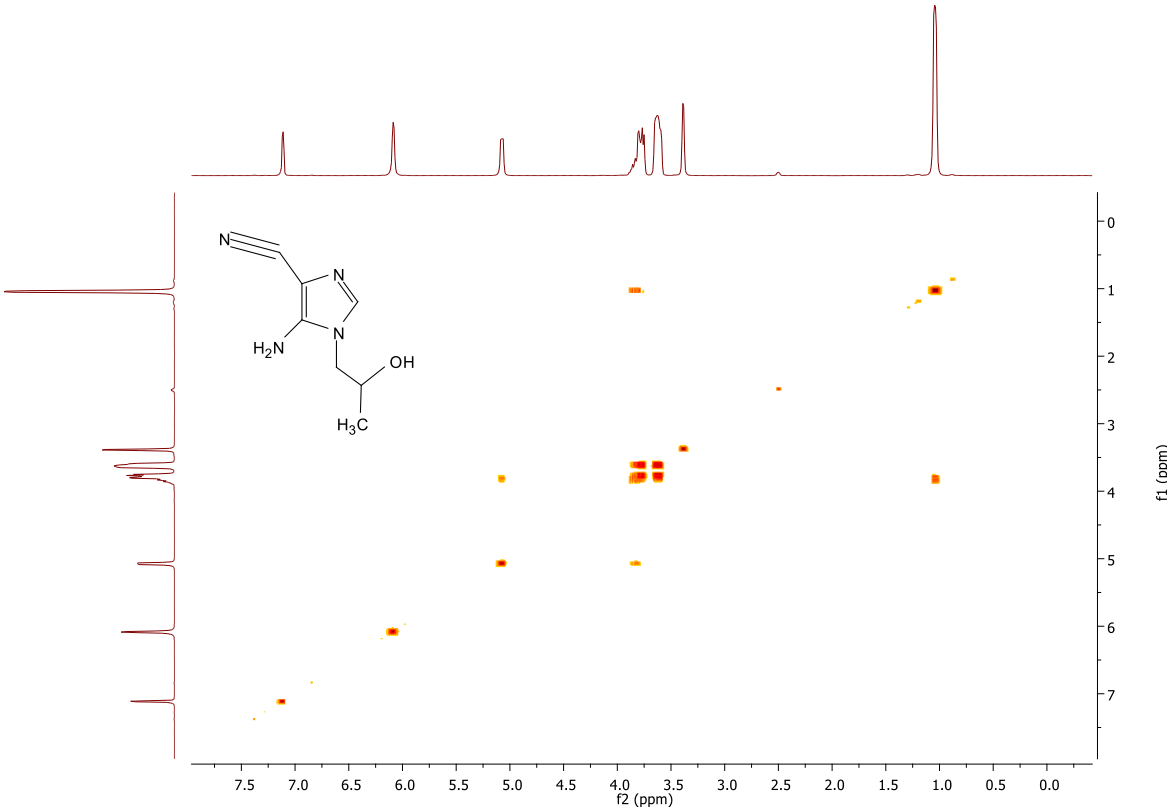

Plate 4a. ^{1}H NMR spectrum of 5-Amino-1-(2-hydroxypropyl-1-*H*-imidazole-4-carboxamide) (**22**), in DMSO-*d*6

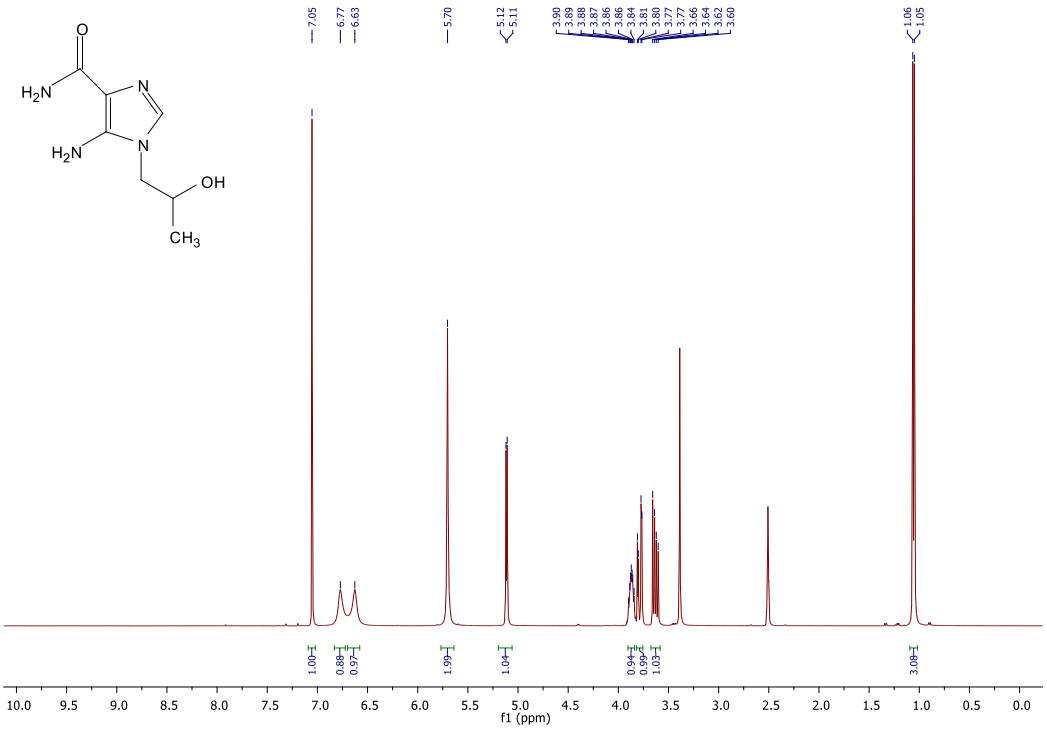

Plate 4b. ^{13}C NMR spectrum of 5-Amino-1-(2-hydroxypropyl-1-*H*-imidazole-4-carboxamide) (**22**), in DMSO-*d*6

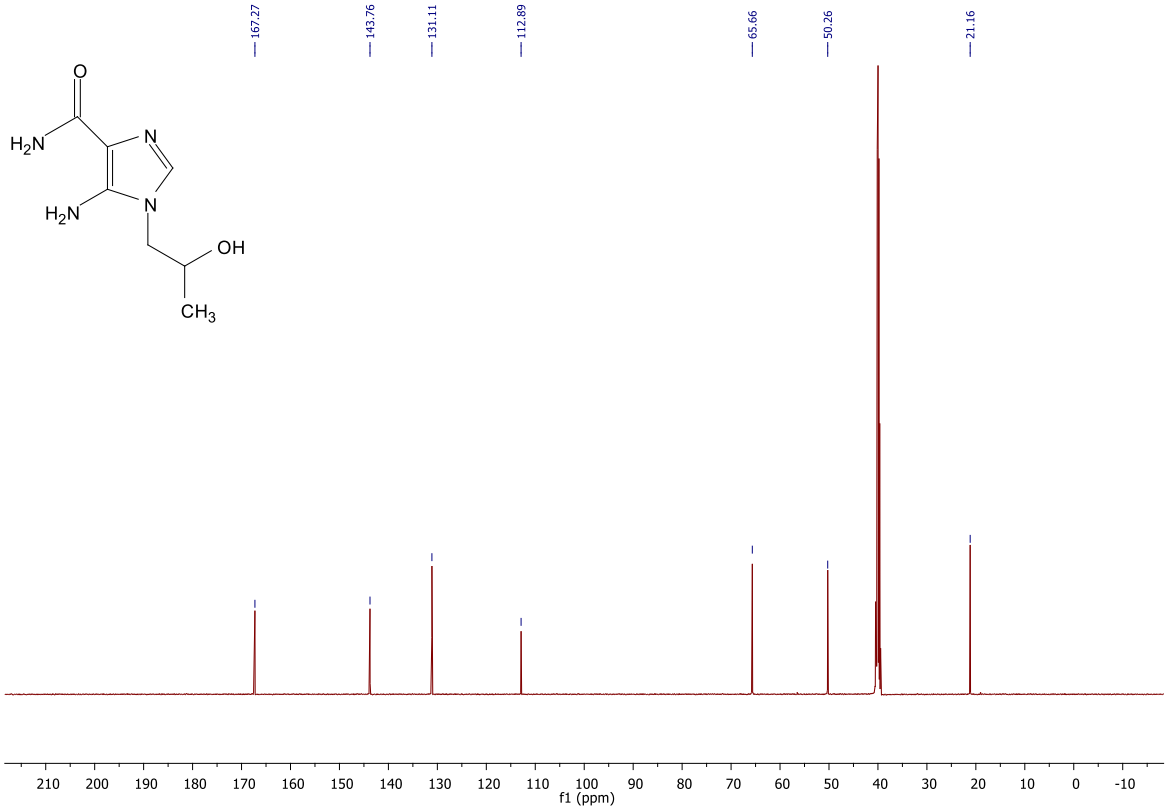

Plate 5a. ^{1}H NMR spectrum of 9-[(*RS*)-2-hydroxy propyl] adenine (**6**), in DMSO-*d*6

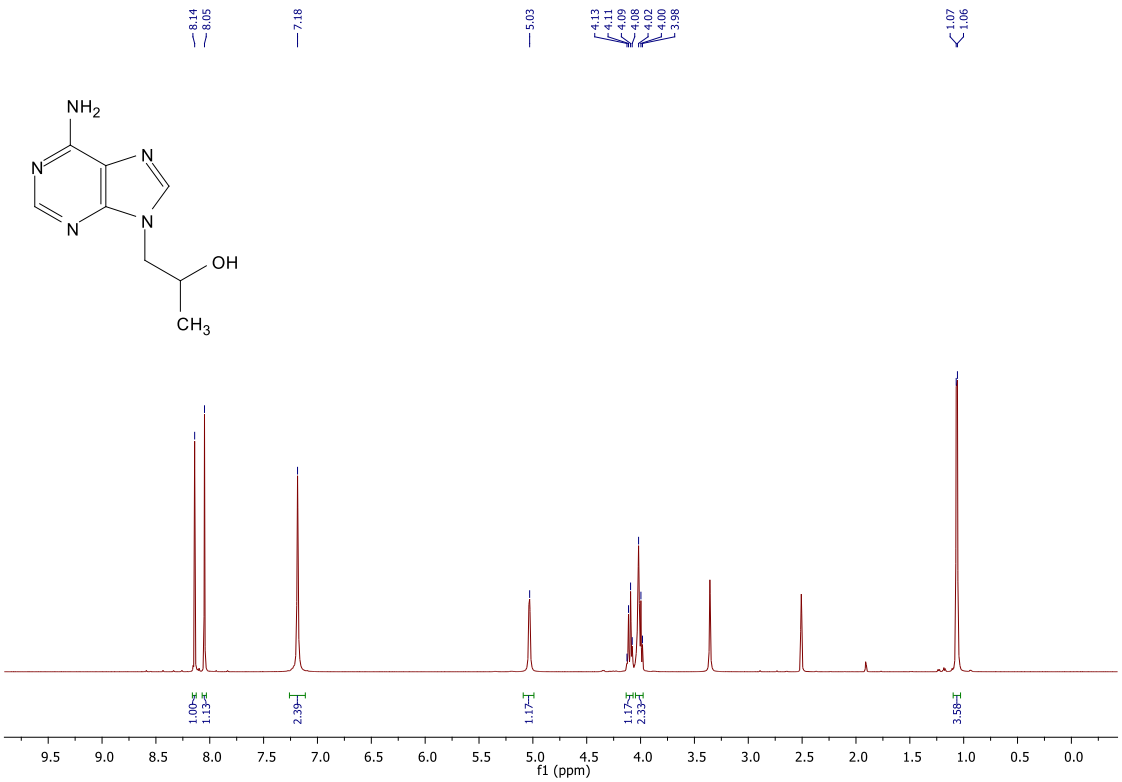

Plate 5b. ^{13}C NMR spectrum of 9-[(*RS*)-2-hydroxy propyl] adenine (**6**), in DMSO-*d*6

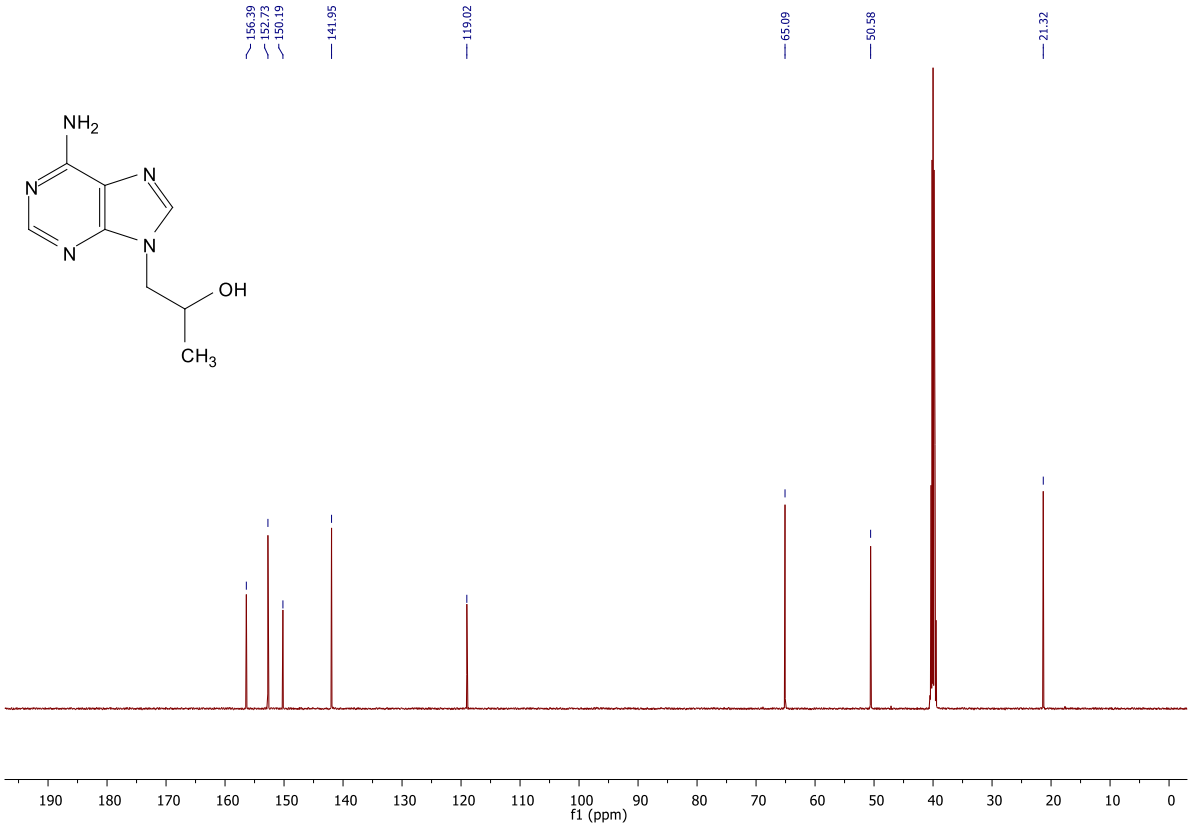

Plate 6a. ^{1}H NMR spectrum of (*R*)-1-aminopropan-2-ol. HCl (**15**) in D_2O

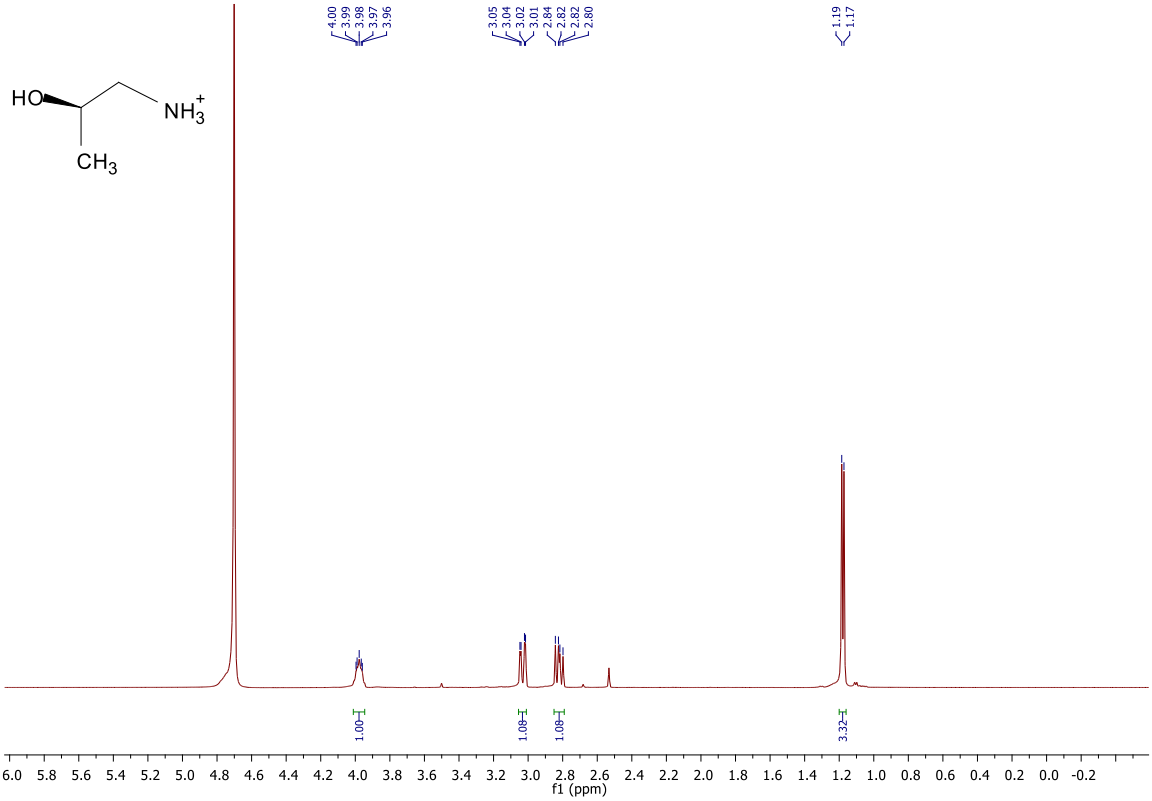

Plate 7a. ^{1}H NMR spectrum of (*R*)-1-aminopropan-2-ol (**15**) in D_2O

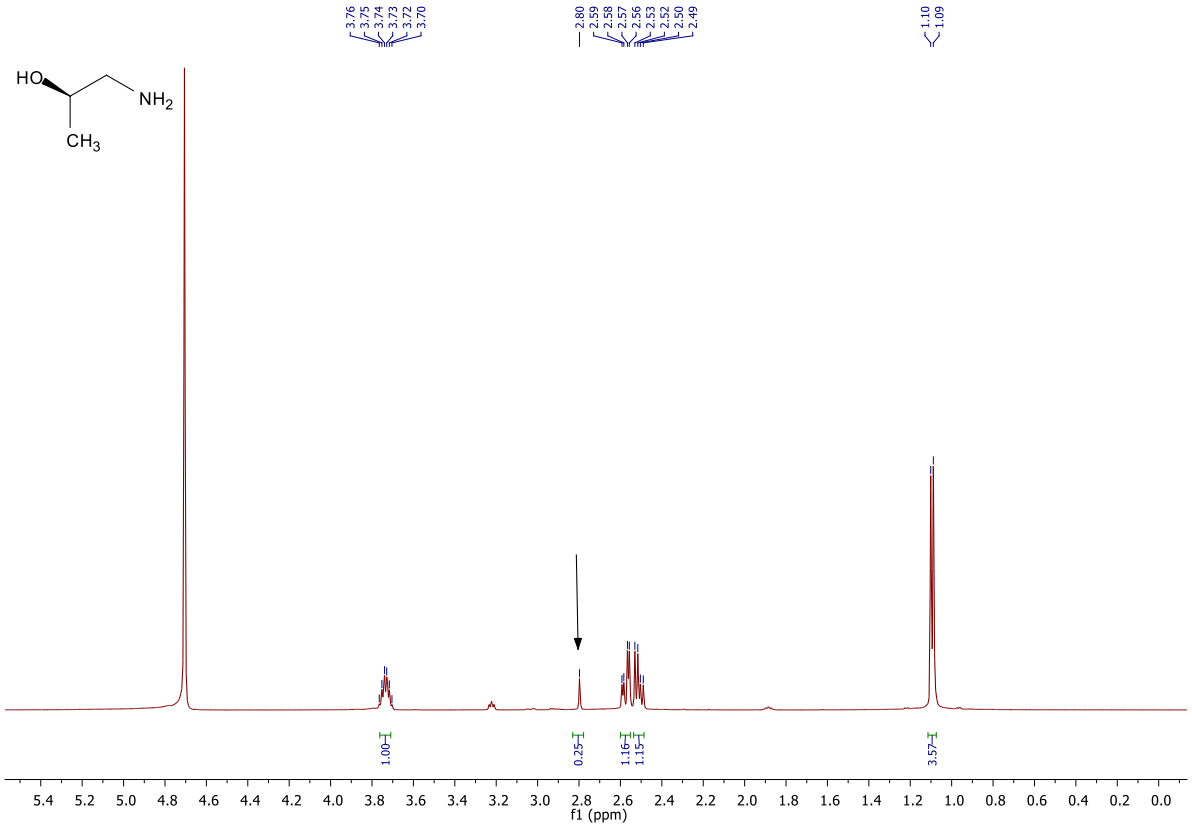

Plate 7b. ^{13}C NMR spectrum of (*R*)-1-aminopropan-2-ol (**15**) in D_2O

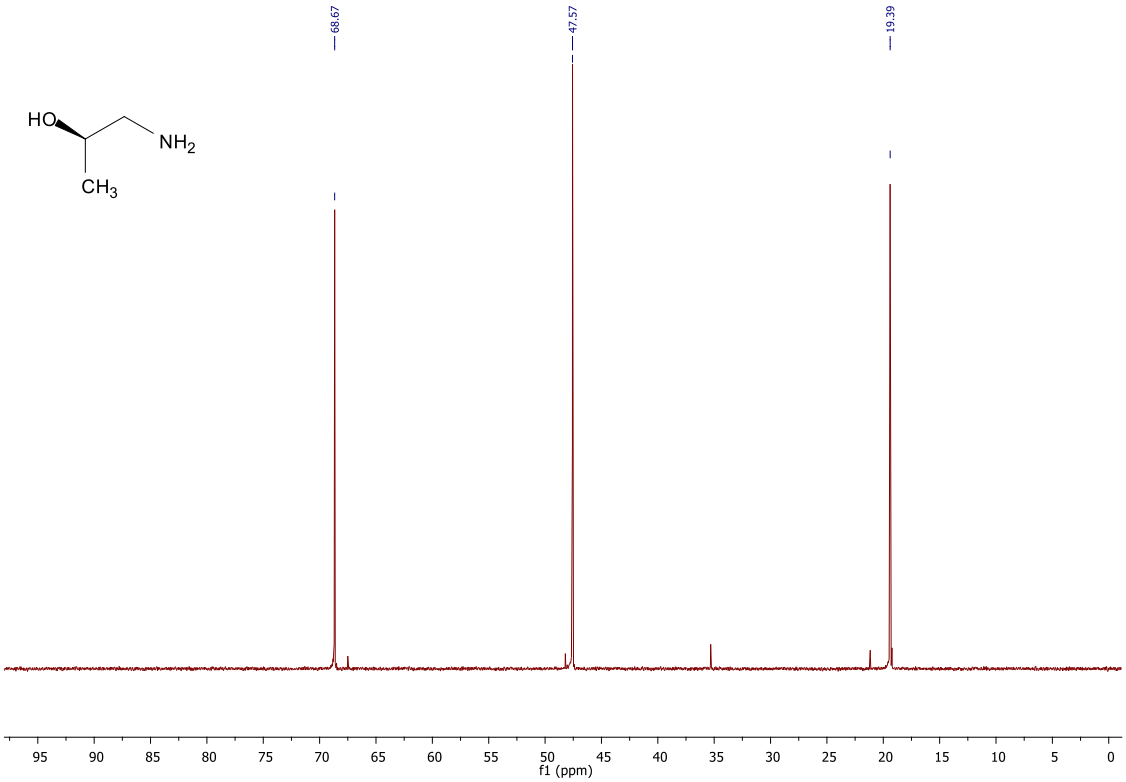

Appendix 2. Structures

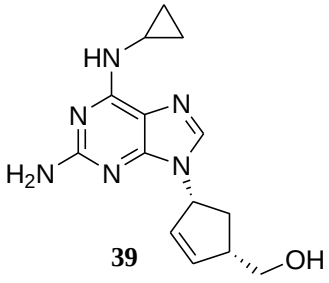

39

Abacavir

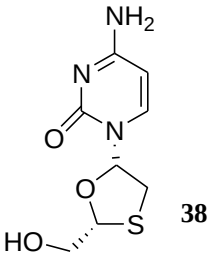

38

Lamivudine

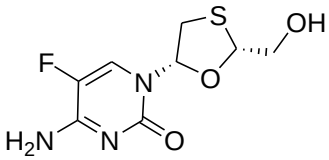

37

Emtricitabine

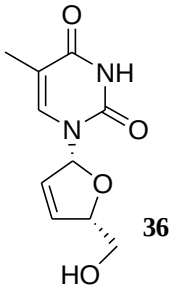

36

Stavudine

REFERENCES

(1) Naudé, C. T. W.; Luiz, J. M. An Industry Analysis of Pharmaceutical Production in South Africa. *South Afr. J. Bus. Manag.* **2013**, *44* (1), 33–46. https://doi.org/10.4102/sajbm.v44i1.146.

(2) *Making Medicines in Africa: The Political Economy of Industrializing for Local Health*; Mackintosh, M., Banda, G., Tibandebage, P., Wamae, W., Eds.; International political economy series; Palgrave Macmillan: New York, 2015.

(3) Fortunak, J. M.; Zhang, J.; Nytko, F. E.; Ellison, T. N. Green Process Chemistry in the Pharmaceutical Industry: Case Studies Update (2012-2016). In *Green Techniques for Organic Synthesis and Medicinal Chemistry*; Zhang, W., Cue, B. W., Eds.; John Wiley & Sons, Ltd: Chichester, UK, 2018; pp 621–647. https://doi.org/10.1002/9781119288152.ch23.

(4) Horner, R. Global Value Chains, Import Orientation, and the State: South Africa's Pharmaceutical Industry. *J. Int. Bus. Policy* **2022**, *5* (1), 68–87. https://doi.org/10.1057/s42214-021-00103-y.

(5) Fortunak, J. M.; de Souza, R. O.; Kulkarni, A. A.; King, C. L.; Ellison, T.; Miranda, L. S. Active Pharmaceutical Ingredients for Antiretroviral Treatment in Low- and Middle-Income Countries: A Survey. *Antivir. Ther.* **2014**, *19* (3_suppl), 15–29. https://doi.org/10.3851/IMP2897.

(6) Pinheiro, E. dos S.; Antunes, O. A. C.; Fortunak, J. M. D. A Survey of the Syntheses of Active Pharmaceutical Ingredients for Antiretroviral Drug Combinations Critical to Access in Emerging Nations. *Antiviral Res.* **2008**, *79* (3), 143–165. https://doi.org/10.1016/j.antiviral.2008.05.001.

(7) Khan, M.; Chang, Y.-C. Environmental Challenges and Current Practices in China—A Thorough Analysis. *Sustainability* **2018**, *10* (7), 2547. https://doi.org/10.3390/su10072547.

(8) Zhu, S.; He, C.; Liu, Y. Going Green or Going Away: Environmental Regulation, Economic Geography and Firms' Strategies in China's Pollution-Intensive Industries. *Geoforum* **2014**, *55*, 53–65. https://doi.org/10.1016/j.geoforum.2014.05.004.

(9) *China Policies to Promote Local Production of Pharmaceutical Products and Protect Public Health.* https://apps.who.int/iris/bitstream/handle/10665/336684/9789241512176-eng.pdf.

(10) Wu, J.; Wei, Y. D.; Chen, W.; Yuan, F. Environmental Regulations and Redistribution of Polluting Industries in Transitional China: Understanding Regional and Industrial Differences. *J. Clean. Prod.* **2019**, *206*, 142–155. https://doi.org/10.1016/j.jclepro.2018.09.042.

(11) KPMG. *INDIAN API INDUSTRY - REACHING THE FULL POTENTIAL*; 2020. https://www.globalmarketestimates.com/market-report/india-api-industry---market.

(12) Modisakeng, C.; Matlala, M.; Godman, B.; Meyer, J. C. Medicine Shortages and Challenges with the Procurement Process among Public Sector Hospitals in South Africa; Findings and Implications. *BMC Health Serv. Res.* **2020**, *20* (1), 234. https://doi.org/10.1186/s12913-020-05080-1.

(13) Palmisano, L., & Vella, S. A Brief History of Antiretroviral Therapy of HIV Infection: Success and Challenges. *Ann. Ist. Super. Sanita* **2011**, *47 1, 44–8*. https://doi.org/10.4415/ANN_11_01_10.

(14) Mandala, D.; Thompson, W. A.; Watts, P. Synthesis Routes to Anti-HIV Drugs. *Tetrahedron* **2016**, *72* (24), 3389–3420. https://doi.org/10.1016/j.tet.2016.04.075.

(15) Grim, S. A.; Romanelli, F. Tenofovir Disoproxil Fumarate. *Ann. Pharmacother.* **2003**, *37* (6), 849–859. https://doi.org/10.1345/aph.1C388.

(16) Soriano, V.; Fernandez-Montero, J. V.; Benitez-Gutierrez, L.; Mendoza, C. de; Arias, A.; Barreiro, P.; Peña, J. M.; Labarga, P. Dual Antiretroviral Therapy for HIV Infection. *Expert Opin. Drug Saf.* **2017**, *16* (8), 923–932. https://doi.org/10.1080/14740338.2017.1343300.

(17) Riley, D. L.; Strydom, I.; Chikwamba, R.; Panayides, J.-L. Landscape and Opportunities for Active Pharmaceutical Ingredient Manufacturing in Developing African Economies. *React. Chem. Eng.* **2019**, *4* (3), 457–489. https://doi.org/10.1039/C8RE00236C.

(18) Caplan, M. R.; Daar, E. S.; Corado, K. C. Next Generation Fixed Dose Combination Pharmacotherapies for Treating HIV. *Expert Opin. Pharmacother.* **2018**, *19* (6), 589–596. https://doi.org/10.1080/14656566.2018.1450866.

(19) Astuti, N.; Maggiolo, F. Single-Tablet Regimens in HIV Therapy. *Infect. Dis. Ther.* **2014**, *3* (1), 1–17. https://doi.org/10.1007/s40121-014-0024-z.

(20) Simelela, N.; Venter, W. D. F.; Pillay, Y.; Barron, P. A Political and Social History of HIV in South Africa. *Curr. HIV/AIDS Rep.* **2015**, *12* (2), 256–261. https://doi.org/10.1007/s11904-015-0259-7.

(21) Bekker, L.-G.; Venter, F.; Cohen, K.; Goemare, E.; Van Cutsem, G.; Boulle, A.; Wood, R. Provision of Antiretroviral Therapy in South Africa: The Nuts and Bolts. *Antivir. Ther.* **2014**, *19* (3_suppl), 105–116. https://doi.org/10.3851/IMP2905.

(22) Sember, R. The Social Construction of ARVs in South Africa* *This Article Is Based on a Longer Study That Was Developed in Collaboration with Sexuality Policy Watch, with Funding Provided by the Ford Foundation. For an Extended Discussion of the Issues Examined in This Article, See "Constitutional Authority and Its Limitations: The Politics of Sexuality in South Africa", Which Is Available as Part of the e-Book, *SexPolitics: Reports from the Front Lines*, Edited by Richard Parker, Rosalind Petchesky, and Robert Sember, 2007. This e-Book Includes a Series of Case Studies, as Well as a Crosscutting Analysis, Focused on the Politics of Sexual Health and Rights in Eight Countries and Two Institutional Contexts. *SexPolitics* Can Be Found Online At. *Glob. Public Health* **2008**, *3* (sup2), 58–75. https://doi.org/10.1080/17441690801981092.

(23) Hwang, B.; Shroufi, A.; Gils, T.; Steele, S. J.; Grimsrud, A.; Boulle, A.; Yawa, A.; Stevenson, S.; Jankelowitz, L.; Versteeg-Mojanaga, M.; Govender, I.; Stephens, J.; Hill, J.; Duncan, K.; van Cutsem, G. Stock-Outs of Antiretroviral and Tuberculosis Medicines in South Africa: A National

Cross-Sectional Survey. *PLOS ONE* **2019**, *14* (3), e0212405. https://doi.org/10.1371/journal.pone.0212405.

(24) Venter, W. D. F.; Fabian, J.; Feldman, C. An Overview of Tenofovir and Renal Disease for the HIV-Treating Clinician. *South. Afr. J. HIV Med.* **2018**, *19* (1). https://doi.org/10.4102/sajhivmed.v19i1.817.

(25) Wirtz, V. J.; Forsythe, S.; Valencia-Mendoza, A.; Bautista-Arredondo, S. Factors Influencing Global Antiretroviral Procurement Prices. *BMC Public Health* **2009**, *9* (S1), S6. https://doi.org/10.1186/1471-2458-9-S1-S6.

(26) Houghton, S. R.; Melton, J.; Fortunak, J.; Brown Ripin, D. H.; Boddy, C. N. Rapid, Mild Method for Phosphonate Diester Hydrolysis: Development of a One-Pot Synthesis of Tenofovir Disoproxil Fumarate from Tenofovir Diethyl Ester. *Tetrahedron* **2010**, *66* (41), 8137–8144. https://doi.org/10.1016/j.tet.2010.08.037.

(27) Southern Africa Journal of HIV Medicines. Fixed-Dose Combination for Adults Accessing Antiretroviral Therapy. **2013**. http://dx.doi.org/10.4102/hivmed.v14i1.104.

(28) Brown Ripin, D. H.; Teager, D. S.; Fortunak, J.; Basha, S. M.; Bivins, N.; Boddy, C. N.; Byrn, S.; Catlin, K. K.; Houghton, S. R.; Jagadeesh, S. T.; Kumar, K. A.; Melton, J.; Muneer, S.; Rao, L. N.; Rao, R. V.; Ray, P. C.; Reddy, N. G.; Reddy, R. M.; Shekar, K. C.; Silverton, T.; Smith, D. T.; Stringham, R. W.; Subbaraju, G. V.; Talley, F.; Williams, A. Process Improvements for the Manufacture of Tenofovir Disoproxil Fumarate at Commercial Scale. *Org. Process Res. Dev.* **2010**, *14* (5), 1194–1201. https://doi.org/10.1021/op1001337.

(29) Vella, S.; Schwartländer, B.; Sow, S. P.; Eholie, S. P.; Murphy, R. L. The History of Antiretroviral Therapy and of Its Implementation in Resource-Limited Areas of the World. *AIDS* **2012**, *26* (10), 1231–1241. https://doi.org/10.1097/QAD.0b013e32835521a3.

(30) Clososki, G.; Soldi, R.; da Silva, R.; Guaratini, T.; Lopes, J.; Pereira, P.; Lopes, J.; dos Santos, T.; Martins, R.; Costa, C.; de Carvalho, A.; daSilva, L.; Arruda, E.; Lopes, N. Tenofovir Disoproxil Fumarate: New Chemical Developments and Encouraging in Vitro Biological Results for SARS-CoV-2. *J. Braz. Chem. Soc.* **2020**. https://doi.org/10.21577/0103-5053.20200106.

(31) Kearney, B. P.; Flaherty, J. F.; Shah, J. Tenofovir Disoproxil Fumarate: Clinical Pharmacology and Pharmacokinetics. *Clin. Pharmacokinet.* **2004**, *43* (9), 595–612. https://doi.org/10.2165/00003088-200443090-00003.

(32) Chapman, T. M.; McGavin, J. K.; Noble, S. Tenofovir Disoproxil Fumarate: *Drugs* **2003**, *63* (15), 1597–1608. https://doi.org/10.2165/00003495-200363150-00006.

(33) De Clercq, E. Tenofovir Alafenamide (TAF) as the Successor of Tenofovir Disoproxil Fumarate (TDF). *Biochem. Pharmacol.* **2016**, *119*, 1–7. https://doi.org/10.1016/j.bcp.2016.04.015.

(34) De Clercq, E. Role of Tenofovir Alafenamide (TAF) in the Treatment and Prophylaxis of HIV and HBV Infections. *Biochem. Pharmacol.* **2018**, *153*, 2–11. https://doi.org/10.1016/j.bcp.2017.11.023.

(35) Riley, D. L.; Walwyn, D. R.; Edlin, C. D. An Improved Process for the Preparation of Tenofovir Disoproxil Fumarate. *Org. Process Res. Dev.* **2016**, *20* (4), 742–750. https://doi.org/10.1021/acs.oprd.5b00364.

(36) Zanella, I.; Zizioli, D.; Castelli, F.; Quiros-Roldan, E. Tenofovir, Another Inexpensive, Well-Known and Widely Available Old Drug Repurposed for SARS-COV-2 Infection. *Pharmaceuticals* **2021**, *14* (5), 454. https://doi.org/10.3390/ph14050454.

(37) Trépo, C.; Chan, H. L. Y.; Lok, A. Hepatitis B Virus Infection. *The Lancet* **2014**, *384* (9959), 2053–2063. https://doi.org/10.1016/S0140-6736(14)60220-8.

(38) Mugwanya, K. K.; Baeten, J. M. Safety of Oral Tenofovir Disoproxil Fumarate-Based Pre-Exposure Prophylaxis for HIV Prevention. *Expert Opin. Drug Saf.* **2016**, *15* (2), 265–273. https://doi.org/10.1517/14740338.2016.1128412.

(39) Pilkington, V.; Hughes, S. L.; Pepperrell, T.; McCann, K.; Gotham, D.; Pozniak, A. L.; Hill, A. Tenofovir Alafenamide vs. Tenofovir Disoproxil Fumarate: An Updated Meta-Analysis of 14 894 Patients across 14 Trials. *AIDS* **2020**, *34* (15), 2259–2268. https://doi.org/10.1097/QAD.0000000000002699.

(40) Wang, A.; Wu, S.; Tao, Z.; Li, X.; Lv, K.; Ma, C.; Li, Y.; Li, L.; Liu, M. Design, Synthesis, and Anti-HBV Activity of New Bis(L -Amino Acid) Ester Tenofovir Prodrugs. *ACS Med. Chem. Lett.* **2019**, *10* (6), 991–995. https://doi.org/10.1021/acsmedchemlett.9b00184.

(41) Ford, N.; Gray, A.; Venter, W. D. F. Tough Choices: Tenofovir, Tenders and Treatment. *South. Afr. J. HIV Med.* **2008**, *9* (1), 8. https://doi.org/10.4102/sajhivmed.v9i1.658.

(42) Derstine, B. P.; Tomlin, J. W.; Peck, C. L.; Dietz, J.-P.; Herrera, B. T.; Cardoso, F. S. P.; Paymode, D. J.; Yue, A. C.; Arduengo, A. J.; Opatz, T.; Snead, D. R.; Stringham, R. W.; McQuade, D. T.; Gupton, B. F. An Efficient Synthesis of Tenofovir (PMPA): A Key Intermediate Leading to Tenofovir-Based HIV Medicines. *Org. Process Res. Dev.* **2020**, *24* (8), 1420–1427. https://doi.org/10.1021/acs.oprd.0c00078.

(43) Yin, W.; Mao, C.; Luan, X.; Shen, D.-D.; Shen, Q.; Su, H.; Wang, X.; Zhou, F.; Zhao, W.; Gao, M.; Chang, S.; Xie, Y.-C.; Tian, G.; Jiang, H.-W.; Tao, S.-C.; Shen, J.; Jiang, Y.; Jiang, H.; Xu, Y.; Zhang, S.; Zhang, Y.; Xu, H. E. Structural Basis for Inhibition of the RNA-Dependent RNA Polymerase from SARS-CoV-2 by Remdesivir. *Science* **2020**, *368* (6498), 1499–1504. https://doi.org/10.1126/science.abc1560.

(44) Dietz, J.-P.; Ferenc, D.; Jamison, T. F.; Gupton, B. F.; Opatz, T. *The Di-Tert-Butyl Oxymethylphosphonate Route to the Antiviral Drug Tenofovir*; preprint; Chemistry, 2020. https://doi.org/10.26434/chemrxiv.12957935.v1.

(45) Thoms, H.; Epple, M.; Viebrock, H.; Reller, A. Magnesium Alcoholates as Precursors for Magnesia. *J. Mater. Chem.* **1995**, *5* (4), 589. https://doi.org/10.1039/jm9950500589.

(46) Mas, I.; Hortelano, C.; Ruiz-Bermejo, M.; de la Fuente, J. L. Highly Efficient Melt Polymerization of Diaminomaleonitrile. *Eur. Polym. J.* **2021**, *143*, 110185. https://doi.org/10.1016/j.eurpolymj.2020.110185.

(47) Dietz, J.-P.; Ferenc, D.; Jamison, T. F.; Gupton, B. F.; Opatz, T. Di- *Tert* -Butyl Phosphonate Route to the Antiviral Drug Tenofovir. *Org. Process Res. Dev.* **2021**, *25* (4), 789–798. https://doi.org/10.1021/acs.oprd.0c00473.

(48) Takase, M.; Komatsu, F. Method for Production of N-(2-Amino-1,2-Dicyanovinyl) Imidates, Method for Production of N-(2-Amino-1,2-Dicyanovinyl) Formamidine, and Method for Production of Aminoimidazole Derivatives. US8273899B2, September 25, 2012.

(49) Al-Azmi, A. ChemInform Abstract: Recent Developments in the Chemistry of Diaminomaleonitrile. *ChemInform* **2015**, *46* (28). https://doi.org/10.1002/chin.201528293.

(50) Chaudhary, A. 2,3-Diaminomaleonitrile: A Multifaceted Synthon in Organic Synthesis. *Curr. Org. Synth.* **2022**, *19* (5), 616–642. https://doi.org/10.2174/1570179419666220107155346.

(51) Cornucopia Institute. Toxic Chemicals Banned In Organics But Common in “Natural” Food Production, 2010. https://www.organicconsumers.org/sites/default/files/nvo_hexane_report.pdf.

(52) Alves, M. J.; Booth, B. L.; Proenç, M. F. J. R. P. Synthesis of 5-Amino-4-(Cyanoformimidoyl)-1H-Imidazole: A Reactive Intermediate for the Synthesis of 6-Carbamoyl-1,2-Dihydropurines and 6-Carbamoylpurines. *J Chem Soc Perkin Trans 1* **1990**, No. 6, 1705–1712. https://doi.org/10.1039/P19900001705.

(53) Lee, J.-H.; Park, D.-U.; Hong, S.-C.; Ha, K.-C. Construction of an Exposure Matrix Using a Risk Assessment of Industries and Processes Involving Dichloromethane. *Korean J. Environ. Health Sci.* **2010**, *36* (5), 391–401. https://doi.org/10.5668/JEHS.2010.36.5.391.

(54) Sruthi, P. R.; Anas, S. An Overview of Synthetic Modification of Nitrile Group in Polymers and Applications. *J. Polym. Sci.* **2020**, *58* (8), 1039–1061. https://doi.org/10.1002/pol.20190190.

(55) Abraham, R. J.; Griffiths, L.; Perez, M. ^{1}H NMR Spectra. Part 30: ^{1}H Chemical Shifts in Amides and the Magnetic Anisotropy, Electric Field and Steric Effects of the Amide Group: The Proton Spectra of 37 Amides Have Been Analysed and Recorded and the Chemical Shifts Calculated. *Magn. Reson. Chem.* **2013**, *51* (3), 143–155. https://doi.org/10.1002/mrc.3920.

(56) Taylor, E. C.; Ehrhart, W. A. A Convenient Synthesis of Formamidine and Acetamidine Acetate. *J. Am. Chem. Soc.* **1960**, *82* (12), 3138–3141. https://doi.org/10.1021/ja01497a039.

(57) Juarez-Perez, E. J.; Ono, L. K.; Qi, Y. Thermal Degradation of Formamidinium Based Lead Halide Perovskites into *Sym* -Triazine and Hydrogen Cyanide Observed by Coupled Thermogravimetry-Mass Spectrometry Analysis. *J. Mater. Chem. A* **2019**, *7* (28), 16912–16919. https://doi.org/10.1039/C9TA06058H.

(58) Sharmila Tagore, S.; Swaminathan, J.; Manikandan, D.; Gomathi, S.; Sabarinathan, N.; Ramalingam, M.; Sethuraman, V. Crystallographic Investigation, Hirshfeld Surface Analysis, NLO Characterization and Experimental Spectral (UV and NMR) Studies with DFT Probe on(R)-9-(2-HydroxyPropyl) Adenine. *Heliyon* **2021**, *7* (4), e06593. https://doi.org/10.1016/j.heliyon.2021.e06593.

(59) Lambertucci, C.; Antonini, I.; Buccioni, M.; Ben, D. D.; Kachare, D. D.; Volpini, R.; Klotz, K.-N.; Cristalli, G. 8-Bromo-9-Alkyl Adenine Derivatives as Tools for Developing New Adenosine A2A and A2B Receptors Ligands. *Bioorg. Med. Chem.* **2009**, *17* (7), 2812–2822. https://doi.org/10.1016/j.bmc.2009.02.030.

(60) Fulmer, G. R.; Miller, A. J. M.; Sherden, N. H.; Gottlieb, H. E.; Nudelman, A.; Stoltz, B. M.; Bercaw, J. E.; Goldberg, K. I. NMR Chemical Shifts of Trace Impurities: Common Laboratory Solvents, Organics, and Gases in Deuterated Solvents Relevant to the Organometallic Chemist. *Organometallics* **2010**, *29* (9), 2176–2179. https://doi.org/10.1021/om100106e.

(61) Laval, G.; Golding, B. T. One-Pot Sequence for the Decarboxylation of α-Amino Acids. *Synlett* **2003**, No. 4, 0542–0546. https://doi.org/10.1055/s-2003-37512.

(62) Dose, K. Catalytic Decarboxylation of α-Amino-Acids. *Nature* **1957**, *179* (4562), 734–735. https://doi.org/10.1038/179734b0.

(63) Gallagher, T.; Snell, E. E.; Hackert, M. L. Pyruvoyl-Dependent Histidine Decarboxylase. *J. Biol. Chem.* **1989**, *264* (21), 12737–12743. https://doi.org/10.1016/S0021-9258(18)63917-1.

(64) Hashimoto, M.; Eda, Y.; Osanai, Y.; Iwai, T.; Aoki, S. A novel decarboxylation of α-amino acids. a facile method of decarboxylation by the use of 2-cyclohexen-1-one as a catalyst. *Chem. Lett.* **1986**, *15* (6), 893–896. https://doi.org/10.1246/cl.1986.893.

(65) Claes, L.; Janssen, M.; De Vos, D. E. Organocatalytic Decarboxylation of Amino Acids as a Route to Bio-based Amines and Amides. *ChemCatChem* **2019**, *11* (17), 4297–4306. https://doi.org/10.1002/cctc.201900800.

(66) Haufa, K. Z.; Czarnecki, M. A. Molecular Structure and Hydrogen Bonding of 2-Aminoethanol, 1-Amino-2-Propanol, 3-Amino-1-Propanol, and Binary Mixtures with Water Studied by Fourier

Transform Near-Infrared Spectroscopy and Density Functional Theory Calculations. *Appl. Spectrosc.* **2010**, *64* (3), 351–359. https://doi.org/10.1366/000370210790918445.

(67) Jackson, D. M.; Ashley, R. L.; Brownfield, C. B.; Morrison, D. R.; Morrison, R. W. Rapid Conventional and Microwave-Assisted Decarboxylation of L-Histidine and Other Amino Acids via Organocatalysis with R-Carvone Under Superheated Conditions. *Synth. Commun.* **2015**, *45* (23), 2691–2700. https://doi.org/10.1080/00397911.2015.1100745.

(68) Wallbaum, S.; Mehler, T.; Martens, J. Decarboxylation of α-Amino Acids Containing Two and Three Stereogenic Centers: A Simple One-Step Procedure to Prepare Two Optically Active β-Amino Alcohols and a Bicyclic Pyrrolidine Derivative. *Synth. Commun.* **1994**, *24* (10), 1381–1387. https://doi.org/10.1080/00397919408011741.

(69) Rossen, K.; Simpson, P. M.; Wells, K. M. A Practical Synthesis of Both Enantiomers of 1-Amino-2-Propanol and Propylene Oxide. *Synth. Commun.* **1993**, *23* (8), 1071–1074. https://doi.org/10.1080/00397919308018583.